



# **Study and Characterization of Composite Materials: Biomedical Applications**

(Estudo e Caracterização de Materiais Compósitos:  
Aplicações Biomédicas)

Master in Mechanical Engineering: Industrial Production

**Miguel Fernandes Ferraz**

Leiria, março de 2022





# **Study and Characterization of Composite Materials: Biomedical Applications**

(Estudo e Caracterização de Materiais Compósitos:  
Aplicações Biomédicas)

Master in Mechanical Engineering: Industrial Production

**Miguel Fernandes Ferraz**

Master's thesis conducted under the supervision of Prof. Dr. Marcelo Rudolfo Calvete Gaspar, Professor at the School of Technology and Management of the Polytechnic Institute of Leiria, Prof. Dr. Armando Lopes Ramalho, Professor at the Polytechnic Institute of Castelo Branco, and Prof. Dr. Carlos Alexandre Bento Capela, Professor at the School of Technology and Management of the Polytechnic Institute of Leiria.

Leiria, março de 2022





# Originality and Copyright

This dissertation is original, prepared solely for this purpose, and all authors whose studies and publications have contributed to its elaboration have been duly cited.

Partial reproductions of this document will be authorized on the condition that the Author is mentioned, and reference is made to the study cycle under which it was carried out, namely the Master's Degree Course in Mechanical Engineering: Industrial Production, in the academic year 2021/2022, of the School of Technology and Management of the Polytechnic Institute of Leiria, Portugal, as well as the date of the public examinations aimed at the evaluation of this work.

# Acknowledgments

It gives me great pleasure to express my deep gratitude to all those who have supported, encouraged, and helped me in the accomplishment of this work.

I am truly grateful to my supervisors Professor Doctor Marcelo Rudolfo Calvete Gaspar, Professor Doctor Armando Lopes Ramalho and Professor Doctor Carlos Alexandre Bento Capela, since without their contribution and support the realization of this work would not have been possible.

A special thanks to my parents, and my family, who have always accompanied and supported me throughout this and all previous journeys. A heartfelt thanks to my girlfriend, for her encouragement and patience so that I could devote the limited free time I had to the development of this work.

# Abstract

In the scope of the Master's Degree in Mechanical Engineering - Industrial Production, it was sought to study the impact of sustainable materials in biomedical applications, with special focus on composite materials.

When gathering information to perform the state of the art of this work, regarding composite materials and some of their biomedical applications, it was found that there was not much evidence regarding the customized production of transfemoral prostheses using both sustainable materials and home-available low-cost manufacturing technologies.

To contribute exploring the identified research gap, numerical models were developed to carry out simulations based on finite element analysis. In turn, these have made it possible to evaluate not only the effect of friction, but also the effect that the materials and their constitutive laws have on the stress field developed in the biomechanical system, which directly affects the comfort and health of patients. Additionally, the simulations also made it possible to analyze various materials to verify their suitability for the application in question.

The results obtained made it possible to highlight sustainable materials with the potential to be used to produce sockets for transfemoral prostheses and, in turn, to demonstrate the possible suitability for customized production of these medical devices directly by patients in their homes, using low-cost additive technologies that can be easily available at home.

**Keywords:** Transfemoral amputation; Biomechanics; Finite element analysis; Customization; Additive manufacturing; Ecodesign.

# Resumo

No âmbito do Mestrado em Engenharia Mecânica – Produção Industrial, procurou-se estudar o impacto dos materiais sustentáveis em aplicações biomédicas, com especial enfoque nos materiais compósitos.

Aquando da recolha de informação para realizar o estado da arte do presente trabalho, relativamente aos materiais compósitos e a algumas das suas aplicações biomédicas, verificou-se que não havia muitas evidências no que toca à produção customizada de próteses transfemorais utilizando simultaneamente materiais sustentáveis e tecnologias de fabrico de baixo custo que possam estar disponíveis a partir de casa.

Para contribuir para a análise da lacuna de investigação identificada, foram desenvolvidos modelos numéricos com o intuito de levar a cabo simulações tendo por base a análise de elementos finitos. Por sua vez, estas possibilitaram avaliar não só o efeito do atrito, como também o efeito que os materiais e as suas leis constitutivas possuem no campo de tensões desenvolvido no sistema biomecânico, que afeta diretamente o conforto e a saúde dos pacientes. Ademais, as simulações permitiram também analisar vários materiais a fim de verificar a sua adequação à aplicação em estudo.

Os resultados obtidos permitiram evidenciar materiais sustentáveis com o potencial de serem utilizados para a produção de sockets para próteses transfemorais e, por sua vez, demonstrar a possível aptidão para a produção customizada destes dispositivos médicos diretamente pelos pacientes nas suas habitações, utilizando tecnologias aditivas de baixo custo e que possam estar facilmente disponíveis a partir de casa.

**Palavras-chave:** Amputação transfemoral; Biomecânica; Análise de elementos finitos, Customização; Fabricação aditiva; Ecodesign.

# Index

<b>Originality and Copyright .....</b>	<b>iii</b>
<b>Acknowledgments.....</b>	<b>iv</b>
<b>Abstract .....</b>	<b>v</b>
<b>Resumo .....</b>	<b>vi</b>
<b>Figure List .....</b>	<b>x</b>
<b>List of Acronyms and Abbreviations .....</b>	<b>xi</b>
<b>1. Introduction .....</b>	<b>1</b>
<b>1.1. Background and Motivation.....</b>	<b>1</b>
<b>1.2. Objectives .....</b>	<b>2</b>
<b>1.3. General Structure .....</b>	<b>2</b>
<b>1.4. Composite Materials .....</b>	<b>4</b>
1.4.1. Matrix .....	5
1.4.1.1. Polymeric Matrix .....	5
1.4.1.2. Ceramic Matrix.....	8
1.4.1.3. Metallic Matrix .....	9
1.4.2. Reinforcement .....	11
1.4.2.1. Fiber-reinforced composites .....	11
1.4.2.2. Particle-reinforced composites .....	13
1.4.2.3. Structural composites .....	14
1.4.3. Interface .....	16
1.4.4. Natural Fiber Composites (NFCs).....	17
<b>1.5. Composite Materials Applications.....</b>	<b>18</b>
1.5.1. Biomedical Applications .....	19
1.5.1.1. Dentistry .....	19
1.5.1.2. Tissue Engineering .....	21
1.5.1.3. Controlled Drug Release .....	22
1.5.1.4. Medical Imaging.....	24
1.5.1.5. Orthopedics.....	25
<b>1.6. Research Gap Identification .....</b>	<b>28</b>
<b>1.7. Research Question .....</b>	<b>30</b>
<b>1.8. Outline of the thesis .....</b>	<b>31</b>

<b>2. 1<sup>st</sup> Paper - Development of a preliminary finite element model to assess the effects of friction on the residual limb of a transfemoral amputee.....</b>	<b>36</b>
<b>2.1. Introduction .....</b>	<b>37</b>
<b>2.2. Finite Element Model.....</b>	<b>39</b>
<b>2.3. Results and Discussion .....</b>	<b>41</b>
<b>2.4. Conclusions .....</b>	<b>45</b>
<b>3. 2<sup>rd</sup> Paper - Influence of materials and their constitutive laws on the stress fields produced in the residual limb of a transfemoral amputation .....</b>	<b>48</b>
<b>3.1. Introduction .....</b>	<b>49</b>
<b>3.2. Finite Element Model.....</b>	<b>50</b>
3.2.1. Geometry .....	50
3.2.2. Mechanical Properties of the Materials – Constitutive laws .....	51
3.2.3. Friction Model.....	54
3.2.4. Finite element analysis .....	54
3.2.5. Loading.....	55
<b>3.3. Numerical Simulations Planning .....</b>	<b>55</b>
<b>3.4. Results and Discussion .....</b>	<b>57</b>
<b>3.5. Conclusions .....</b>	<b>61</b>
<b>4. 3<sup>rd</sup> Paper – Efeito do atrito no membro residual numa amputação transfemoral – Influência do modelo constitutivo dos materiais .....</b>	<b>65</b>
<b>4.1. Introdução.....</b>	<b>66</b>
<b>4.2. Descrição .....</b>	<b>66</b>
<b>4.3. Conclusões.....</b>	<b>67</b>
<b>5. 4<sup>th</sup> Paper - Recycled reinforced PLA as ecodesign solution for customized prostheses .....</b>	<b>69</b>
<b>5.1. Introduction .....</b>	<b>70</b>
5.1.1. Customization with Additive Manufacturing .....	70
5.1.2. Additive Manufacturing Environmental Sustainability through Recycling....	71
<b>5.2. Materials and Methods .....</b>	<b>72</b>
5.2.1. Recycled Reinforced PLA for Additive Manufacturing .....	72
5.2.2. Numerical Model.....	72

<b>5.3. Results and Discussion .....</b>	<b>75</b>
5.3.1. Biomechanical system simulation .....	75
5.3.2. Socket-type prostheses simulation .....	76
<b>5.4. Summary and Conclusions .....</b>	<b>91</b>
<b>6. Summary, Discussion and Conclusions .....</b>	<b>99</b>
<b>References.....</b>	<b>105</b>
<b>Attachments .....</b>	<b>111</b>
<b>Attachment 1</b> “Development of a preliminary finite element model to assess the effects of friction on the residual limb of a transfemoral amputee” .....	<b>111</b>
<b>Attachment 2</b> “Proceedings of 5th International Conference on Mechanical, System and Control Engineering: Influence of Materials and Their Constitutive Laws on the Stress Fields Produced in the Residual Limb of a Transfemoral Amputation” .....	<b>117</b>
<b>Attachment 3</b> “EFEITO DO ATRITO NO MEMBRO RESIDUAL NUMA AMPUTAÇÃO TRANSFEMORAL – INFLUÊNCIA DO MODELO CONSTITUTIVO DOS MATERIAIS” .....	<b>140</b>
<b>Attachment 4</b> “Publishing Agreement for the contribution provisionally entitled: Recycled Reinforced PLA as Ecodesign Solution for Customized Prostheses” .....	<b>142</b>
<b>Attachment 5</b> “Recycled Reinforced PLA as Ecodesign Solution for Customized Prostheses” .....	<b>152</b>

# Figure List

Figure 1 - Structural difference between thermoplastics and thermosetting polymers (Karuppiyah, 2016). .....	6
Figure 2 - Structural representation of elastomers (Sastri, 2014).....	7
Figure 3 – Ceramic matrix composite of C/SiC components on the Snecma M53-2 aircrafts’ engine (Bansal & Lamon, 2014).....	8
Figure 4 - Classification of composite materials according to the geometry of the reinforcement (Wang & Zhao, 2018).....	11
Figure 5 - Types of fiber reinforcement of composites: (a) continuous fibers; (b) discontinuous fibers; (c) hybrid (Gibson, 2016).....	13
Figure 6 - Schematic of sandwich-type composite material (Adams et al., 2001).....	15
Figure 7 – Types of composite interface bonds: (a) molecular entanglement; (b) electrostatic attraction; (c) inter-diffusion of elements; (d) chemical reaction between Group A on one surface and Group B on the other surface; (e) chemical reaction following the formation of a new compound(s), notably in metal matrix composites; (f) mechanical interlocking (Lim Goh et al., 2020).....	16
Figure 8 - Examples of applications of composite materials in several areas: a) car made of carbon fiber panels; b) military aircraft (F-16) comprising several composite materials; c) circuit made with epoxy resin reinforced with glass fibers; d) bicycle fork composed of glass and carbon fibers (Moura et al., 2009). .....	18
Figure 9 - Example of a scaffold made by SLS technology in the shape of a femoral head: (a) macroscopic view of the structure; (b) SEM image of the porous structure (Wang & Zhao, 2018). .....	21
Figure 10 - In conventional delivery systems (a.), drug levels fluctuate above the minimum toxic concentration and below the minimum effective concentrations, which can cause side effect or not be as effective as it should be. This does not happen with controlled delivery systems (b.), as the drug levels are maintained constantly within therapeutic ranges (Adepu et al., 2021).....	23
Figure 11 - Angiogram of the left internal carotid artery. The use of contrast agents makes it possible to clearly distinguish blood vessels, which are not visible in conventional examinations (Alberti et al., 2009)..	24
Figure 12 - Types of lower limb prostheses: a) trans-tibial prosthesis; b) trans-femoral prosthesis (Nurhanisah et al., 2017). .....	27
Figure 13 – Flowchart representing the steps on which the development of this work was based. ....	31
Figure 14 – Developed 2D axisymmetric model for a preliminary assessment. ....	33
Figure 15 - The 2D axisymmetric model used in the preliminary study was improved in terms of geometry definition.....	34
Figure 16 - Improved flowchart that encompasses possible steps for the development of future work.....	103



# List of Acronyms and Abbreviations

2D	Two-dimensional
3D	Three-dimensional
AM	Additive Manufacturing
CT	Computerized Tomography
E	Elastic modulus
$E_{\text{equNH}}$	Equivalent elastic modulus Neo-Hookean
$E_{\text{equO}}$	Equivalent elastic modulus Ogden
ESTG	Escola Superior de Tecnologia e Gestão
FDM	Fused Deposition Modeling
FEA	Finite Element Analysis
FEM	Finite Element Method
G	Shear modulus
H M	Hyperelastic model
IPL	Instituto Politécnico de Leiria
M-R	Mooney-Rivlin
MRI	Magnetic Resonance Imaging
NFC	Natural Fiber Composite
PA	Polyamide
PC	Polycarbonate
PCL	Polycaprolactone
PEEK	Polyetheretherketone
PET	Positron Emission Tomography
PLA	Poly(lactic acid)
PLGA	Poly (lactic-co-glycolic acid)
PMMA	Poly (methyl methacrylate)
PP	Polypropylene
rPLA	recycled Poly(lactic acid)
S C	Stiffness class
SEM	Scanning Electron Microscopy
SLS	Selective Laser Sintering

VC	Vitrous Carbon
$\mu$ / FC	Friction coefficient
$\rho$	Density / Specific mass
$\sigma$	Normal stress
$\sigma_{kk}$	Hydrostatic stress
$\sigma_{RCA}$	Raghava-Caddell-Attkins stress
$\sigma_{VM}$	Von Mises stress
$\tau$	Shear stress
$\nu$	Poisson's ratio

# 1. Introduction

## 1.1. Background and Motivation

A composite material is one that is made up by a combination of two or more distinct and insoluble materials, such as polymers, metals, and ceramics, with the aim of creating a new material with unique and/or improved properties.

An increasing effort has been made to use more sustainable and environmentally friendly materials. Several composites reinforced with natural fibers have been simulated, since fibers are degradable, reusable, recyclable, and have shown to achieve good mechanical properties and a lower production cost than synthetic fibers.

Nowadays, composite materials are being applied in a wide range of fields, from automotive and aeronautics to several biomedical areas, such as Orthopedics. The increasing number of amputations in developing countries has led to further research into the application of this type of material for the manufacture of prosthetic devices. The broad spectrum of properties that can be achieved by these materials can contribute to the development of better performing prosthetic components and allow the production of more customizable devices.

Regarding prosthetic devices for lower limb amputations, discomfort and soft tissue damage are among the main reasons why patients abandon the use of these devices, with friction being one of the main culprits.

Numerical modeling tools allow optimizing the development of complex anatomical structures, such as customized prostheses for lower limb amputees. Through finite element analysis it is possible not only to characterize the interfacial interactions that occur between the different parts of the prosthesis and the residual limb, as well as to evaluate the stress field developed in the biomechanical model.

Additive manufacturing is an efficient manufacturing method that allows the creation of better customized products, with geometries that are often not possible to achieve through traditional manufacturing processes. They allow the direct fabrication of a product from a three-dimensional model, and can make better use of material, time, and are not as labor

intensive when compared to conventional methods. Furthermore, some forms of these technologies can already be acquired at relatively low cost and can be easily implemented at home.

## **1.2. Objectives**

This exploratory study is intended to test (sustainable) composite materials that can be used in conjunction with additive manufacturing technologies, to open the possibility for patients who have suffered a transfemoral amputation to produce their own customized prostheses using low-cost methods from their homes, which would be quite innovative by today's standards. As specific objectives, the following stand out:

- Perform a literature review;
- Understand how the friction generated when wearing a prosthesis influences the comfort and health of the patient who wear it;
- Evaluate how the use of different materials and the constitutive laws that characterize them influence the stress field developed throughout the biomechanical system;
- Identify and evaluate composite materials with potential for use in the production of custom prosthetic components, with particular emphasis on materials that can be used with additive manufacturing processes.

## **1.3. General Structure**

The present study is structured in chapters that divide each stage of this work.

Firstly, in chapter 1 the literature review was developed, in which the composite materials and their matrices, reinforcements and interfaces are presented. A brief introduction to natural fiber reinforced composites is also performed, and some applications of this type of material are presented, with special focus on biomedical applications. Lastly, the research

gap is identified, followed by the definition of the research question, and the outline of the work carried out to address it.

From chapter 2 to 5, the research conducted to try to answer the outlined objectives of the study is presented, in which the effects of friction and of the defined materials and their constitutive laws in the stress field developed in the biomechanical system are also addressed. Some sustainable materials are also evaluated, to try to demonstrate their potential in the application under study.

Finally, in chapter 6, a summary of the study is presented, as well as a discussion of the most significant results. A conclusion is also made, where potential future work to be done is discussed, with the aim of deepening the development of this preliminary study.

## 1.4. Composite Materials

A composite material is said to be one that is formed by combining two or more distinct, insoluble materials, which can be polymers, metals, or ceramics, to obtain a new material with unique and/or improved properties (Barbero, 2017; Hsissou et al., 2021; Moura et al., 2009; Wang & Zhao, 2018; Yi et al., 2018).

These types of materials are not new but have been made by man for thousands of years (Gay, 2014; Krauklis et al., 2021; Pasāre et al., 2019). A simple example is clay bricks, present in many ancient constructions such as in ancient Egypt, which are essentially made of a mixture of clay and natural fiber straws. Another example widely used nowadays, is concrete. Although individually these constituents are somewhat weak structurally, when combined they achieve greatly improved mechanical properties (Krauklis et al., 2021; Reddy Nagavally, 2016).

By observing these examples, it is possible to notice that this type of material is generally composed of two phases: the **continuous phase, called "matrix"**, which comprises more than 50% of the total volume of the composite, with a lower strength and mechanical stiffness, and the **dispersed or discontinuous phase, called "reinforcement"**, which comprises less than 50% of the total volume of the composite, however presenting superior mechanical properties. Complementarily, the **"interface"** is the connection between the matrix material and the reinforcement, which will determine the mechanical behavior of the set, as well as the transmission of loads by the constituent components of the composite (Gay, 2014; Hsissou et al., 2021; Wang & Zhao, 2018).

Composites can be classified both according to the constituent material of their matrix, and by the geometry of their reinforcement, which in turn has sub-classifications. Additionally, there are also composites that use more than one type of reinforcement material, being called hybrid composites, as is the case with reinforced concrete, which allows for an even greater combination of properties (Hsissou et al., 2021; Wang & Zhao, 2018).

Composite materials thus allow a great diversity of properties to be obtained. However, due to the joining of several types of materials, these properties are not as linear as those of other materials and are therefore more difficult to predict and depend on several factors related, among others, to their manufacture (Barbero, 2017; Chawla, 2012; Hsissou et al., 2021).

### **1.4.1. Matrix**

The matrix, continuous phase of the composites, enables the maintenance of the composite shape and distribution of the reinforcement material, and provides a means of transmitting and distributing the loads imposed on the composite to the reinforcement, which generally has greater mechanical strength and stiffness. Additionally, it also provides protection to the reinforcement from external damage and environmental effects (Barbero, 2017; Gibson, 2016; Hsissou et al., 2021; Kumar, 2019).

The matrices can be classified in one of three groups, according to the type of material: **polymeric**, **ceramic**, or **metallic**. The materials are chosen according to the application and intended properties of the composite, trying to take advantage of the materials' advantages and eliminate their disadvantages, including properties such as thermal and chemical resistance, electrical conductivity, texture, appearance, among others (Barbero, 2017; Gay, 2014; Hsissou et al., 2021).

#### **1.4.1.1. Polymeric Matrix**

Polymers are a more structurally complex type of material than metals and ceramics, consisting of a large chain of repeating chemical entities, called monomers, which are bonded together via covalent bonds to form a macromolecule. Due to the abundance of these bonds, polymers are typically poor thermal and electrical conductors, which can translate into advantages or disadvantages depending on the intended application (Chawla, 2012; Hsissou et al., 2021).

Some of the advantages of this type of material is that it is relatively cheap and easy to produce, compared to other types of materials. Compared to metals, composites with a polymer matrix also allow the production of parts of complex shape. Polymers are also usually more resistant to chemicals than metals, although exposure to ultraviolet rays and some solvents can cause degradation of their properties. They also tend to have lower strength and are limited to use at lower temperatures (Chawla, 2012; Hsissou et al., 2021).

There are two main types of polymers, **plastics** and **elastomers**, which in turn can, depending on their response to heat, be classified into thermoplastics or thermosets (Chawla, 2012; Hsissou et al., 2021; McKeen, 2019).

**Thermoplastics** are polymers whose molecule structure is amorphous, i.e., the molecules are randomly arranged, with no primary connections between them. Thus, they are only kept in their positions by the action of some secondary bonds, such as van der Waals forces and hydrogen bridges. By the action of heat, these bonds can be broken, leaving the polymer softer, and it can enter a state of fusion. Upon cooling, these bonds are re-established, allowing the assignment of a new shape. Due to these properties, thermoplastics are widely used in forming and molding processes, and can be recycled. In the case of **thermosets**, the molecules have cross-links, forming a permanent network (Figure 1), making the transition to a softer state by the action of heat impossible, as it happens in thermoplastics. Because of this, recycling this type of material becomes quite difficult, whereas in thermoplastics recycling is relatively easy to accomplish (Barbero, 2017; Chawla, 2012; Hsissou et al., 2021; Karuppiyah, 2016; McKeen, 2019; Moura et al., 2009).

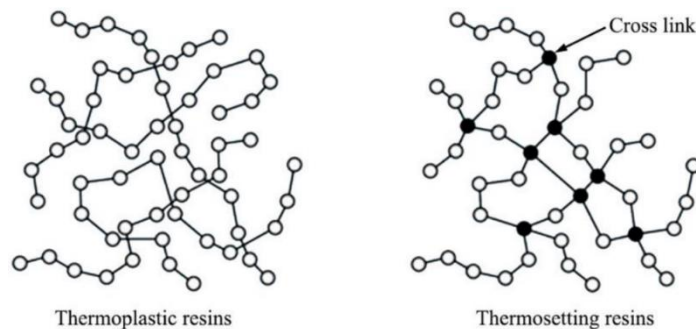


**Figure 1** - Structural difference between thermoplastics and thermosetting polymers (Karuppiyah, 2016).



**Elastomers** differ from plastics in that their structure consists of long chains of coiled molecules, which may have some cross-links between them (Figure 2). This allows these materials to be deformed and easily returned to their initial state without degradation occurring to some extent (Hsissou et al., 2021; Sastri, 2013).

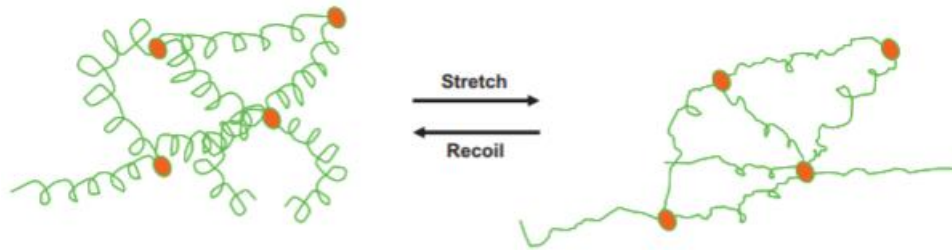


Figure 2 - Structural representation of elastomers (Sastri, 2014).

For composite materials, the most used thermoplastic matrices consist of materials such as polypropylene (PP), polyamides (PA), polycarbonates (PC), and polyether-ether-ketone (PEEK) for applications requiring high strength. The advantages of their use derive from being easily recyclable, to some extent, and can be easily molded to the desired shape. However, their somewhat significant expandability as well as their viscosity under certain conditions can bring some disadvantages in their use (Chawla, 2012; Hsissou et al., 2021; Moura et al., 2009).

Regarding **thermosetting matrices**, the most used materials are epoxy and polyester resins. Epoxy resins are generally more expensive than polyester resins, but they have higher moisture resistance, less shrinkage during curing, can be used at higher temperatures and have good adhesion with glass fibers (Chawla, 2012; Hsissou et al., 2021). They are also used in advanced composites that require high strength (Moura et al., 2009).

A relevant problem about these polymeric matrices is related to environmental effects, in which polymers may degrade at somewhat elevated temperatures and through moisture absorption, changing their initial structural properties. However, the temperature factor is not of great relevance in biomedical applications (Chawla, 2012).

It should also be noted that this type of material is being used on a large scale in the biomedical area, given its easy processing, the existence of several manufacturing processes

and the existence of several polymers that have a good biocompatibility, one of the essential requirements in biomedical applications (T. Hanawa et al., 2019). They are also the ideal type of material for applications that require a gradual and controlled degradation of the same, as used for the controlled drug delivery systems. Still, the application of these materials in this area is somewhat limited due to low strength, stiffness, and lack of bioactivity (Guo et al., 2021; Wang & Zhao, 2018).

#### 1.4.1.2. Ceramic Matrix

Ceramic materials are usually made of one or more metals combined with a non-metal, such as oxygen, carbon, or nitrogen. They are characterized by having high mechanical strength and rigidity, and are therefore a brittle material, with low toughness and low resistance to mechanical shocks. On the other hand, ceramics have low density, do not corrode, and can withstand very high temperatures, this last aspect being often decisive in the choice of this material (Figure 3) (Bansal & Lamon, 2014; Chawla, 2012; Francis et al., 2016; Freiman & Mecholsky, 2019; Rakshit & Das, 2019).



**Figure 3** – Ceramic matrix composite of C/SiC components on the Snecma M53-2 aircrafts' engine (Bansal & Lamon, 2014).

Another important aspect is the ability to achieve either an extremely smooth or porous surface, either for aesthetic or functional reasons. This one is a factor of great importance in biomedical applications (Chawla, 2012).

Structurally, although both are crystalline (except for glass), ceramic materials differ from metals due, among other things, to the type of atomic bonds they have. Whereas in metals the atoms are bonded through metal-to-metal bonds, in ceramics the atoms are mostly bonded through ionic - metal to non-metal - bonds. This results in the poor electrical conductivity of these materials (Chawla, 2012; Rakshit & Das, 2019).

In short, the great disadvantage of these materials is their great fragility. All it takes is small internal or surface flaws, such as micro cracks and scratches, for their stability to be substantially compromised. For composite materials, ceramic matrices are reinforced with fibers with the purpose of essentially increasing the fracture resistance, to try to mitigate this disadvantage. Some of the most used ceramic matrices are silicon carbide, silica-based glasses and ceramic glasses, and some oxides such as alumina. Basically, one of the main reasons for the appearance of ceramic composites was to attempt to reduce the fragility of this type of material, through the addition of reinforcing material (Freiman & Mecholsky, 2019; Rakshit & Das, 2019; Wang & Zhao, 2018).

For biomedical applications, high temperature resistance is not as relevant, but other properties are. These materials are widely used in applications that require significant load bearing, to reduce friction between surfaces, and for aesthetic reasons. The good biocompatibility and bioactivity of various bioceramics are also very important aspects for their use in this area, as well as their electromagnetic force insulating properties (Krauklis et al., 2021; Rakshit & Das, 2019; Wang & Zhao, 2018).

### **1.4.1.3. Metallic Matrix**

Metals are a particularly important type in the class of materials. They are distinguished by their phenomenal mechanical properties and the ability to undergo high levels of plastic deformation without fracture occurring - high ductility. Additionally, their properties can be vastly improved or modified through various existing processes, such as heat treatment. Metals are also distinguished by their high thermal and electrical conductivity and are therefore widely used in applications that require efficient thermal transmission or dissipation, as well as in electronic equipment and communications. Through the

development of alloys, there is also the possibility of adjusting several of these properties to specific applications, thus making these materials quite versatile. These are some of the reasons these materials are widely used in industrial applications (Chawla, 2012; Francis et al., 2016; Kareem et al., 2021).

Generally, in composites with a metal matrix, at least one component is a metal or an alloy, being the reinforcement. The other component or components are embedded in the matrix material, called the reinforcement. Additionally, to prevent chemical reactions of the reinforcement with the matrix, that can lead to corrosion and consequently failure of the composite material, a coating of the reinforcement material can be made (Bahl, 2020).

These materials can also be categorized into two distinct groups: ferrous metals (such as steel and cast iron) or non-ferrous metals (such as aluminum and copper alloys). This classification derives from the presence or absence of the element iron in their constitution, where one of the main properties exhibited by it is magnetism, which can be quite useful in various applications (Francis et al., 2016).

Metals were among the first materials to have contact with humans in medical situations, such as for cutting soft tissue. Like other materials, for biomedical applications, metals must have a good biocompatibility, mechanical and wear resistance, and resistance to corrosion. The latter is probably the main concern and disadvantage of this type of material, especially in aquatic environments, and is therefore a relevant point in biomedical applications. Nowadays, one of the main materials used in biomedical applications is titanium and its alloys. This material provides, among other properties, good mechanical strength, low density compared to other metals, high biocompatibility, and excellent corrosion resistance, and is therefore one of the materials of choice for this type of applications (T. Hanawa et al., 2019).

## 1.4.2. Reinforcement

The reinforcement, a discontinuous phase of the composites, has the main function of supporting the loads that are imposed on the composite, transmitted through the matrix, and is generally the constituent with the highest mechanical resistance and stiffness of the set (Bahl, 2020; Hsissou et al., 2021; Wang & Zhao, 2018). It can be classified into three categories according to its geometry: **fibers** (continuous and discontinuous), **particles** (large and small size), and **structural** (laminates or sandwich) (Figure 4) (Wang & Zhao, 2018).

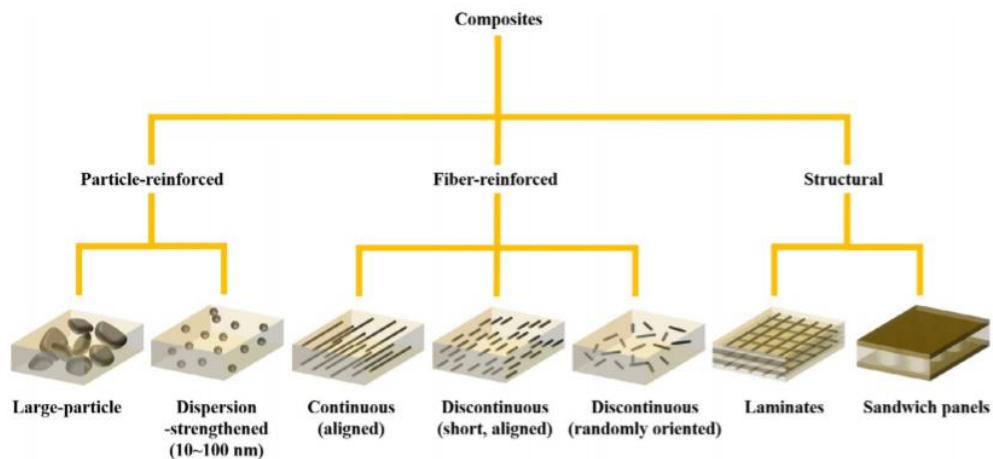


**Figure 4** - Classification of composite materials according to the geometry of the reinforcement (Wang & Zhao, 2018).

Composites that have more than one type of reinforcement material are commonly known as hybrid composites (Barbero, 2017; Chawla, 2012; Hsissou et al., 2021; Lim Goh et al., 2020).

### 1.4.2.1. Fiber-reinforced composites

Over time, composites have been used in a variety of applications. The need to obtain materials with better properties for a specific application has led to the creation of new structures, namely the addition of material in the form of fibers to the composite matrix (Bahl, 2020; Gibson, 2016; Krauklis et al., 2021).

Fiber-reinforced composites are the most predominantly used, and this is due to the vastly superior properties that most materials possess in fiber form compared to the same material in any other form, including low densities and high stiffness and mechanical strength (Chawla, 2012). This is due to the preferential orientation of molecules along the fibers and the reduced number of structural defects in this form (Barbero, 2017; Chawla, 2012). However, it should be noted that these types of composites show different properties and behaviors for different orientations of the loadings, generally presenting one in which they are optimal, depending on the orientation of the fibers. Even with the possibility of orienting the fibers in two or three directions, the composite still shows better properties only according to the fiber orientations (Chawla, 2012; Niendorf & Raeymaekers, 2021).

Based on this aspect, and to improve the performance of these materials in their various applications, several methods have been created to reinforce composites with fibers. The use of **continuous fibers** (Figure 5a) in composites is usually done in layers, where they are connected to each other, through the matrix, to form a laminated composite (Gibson, 2016; Reddy Nagavally, 2016). The fibers have well-defined orientations, according to the application in question, and are one of the most used types of reinforcements (Lim Goh et al., 2020). However, there is still a very relevant problem in this type of composites, which is related to delamination, a phenomenon in which the layers may start to separate, compromising the whole structure and properties of the composite. Thus, it is crucial that the matrix itself can withstand the efforts that it will be subject to, and that there is a strong interface (connection) between both the matrix and the reinforcement (Gibson, 2016).

Regarding the use of **discontinuous fibers** (Figure 5b), these can be oriented or randomly dispersed in the composite matrix. In this case, the delamination problem is not so significant, but the mechanical properties of the composite are generally worse than in the previous case. This type of composites is widely used in high-volume applications that require lower manufacturing costs (Gibson, 2016). The reinforcement is uniform in the case of composites containing well dispersed fibers, and there is a clear distinction between the behavior of short and long fiber composites (Lim Goh et al., 2020).

There are also composites that mix both types of fiber, or two distinct materials. These are called **hybrid** composites (Figure 5c) (Barbero, 2017; Chawla, 2012; Hsissou et al., 2021; Lim Goh et al., 2020).

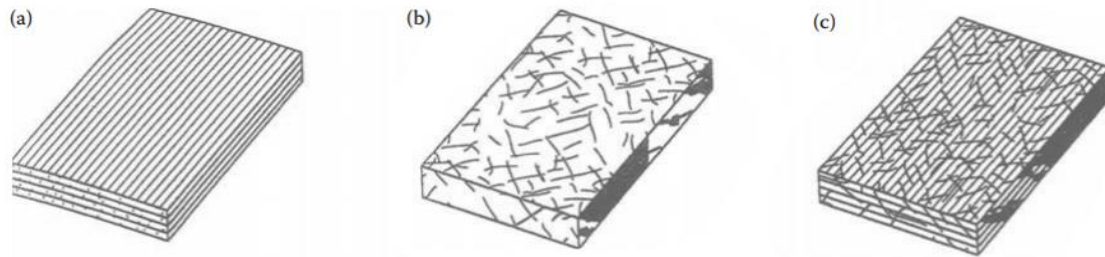


**Figure 5** - Types of fiber reinforcement of composites: (a) continuous fibers; (b) discontinuous fibers; (c) hybrid (Gibson, 2016).

The fibers used can be of two types: organic or inorganic. Organic fibers consist of polymeric fibers, such as aramid fibers, while the most used inorganic fibers are glass fibers, carbon fibers, boron fibers, ceramic fibers (such as silicon carbide and alumina) and metal fibers (such as aluminum, steel, and tungsten). Each material has its advantages and disadvantages, such as its mechanical properties, environmental characteristics, and cost, so a careful analysis must be performed to choose it correctly depending on the application and function to be performed (Barbero, 2017; Gibson, 2016; Hsissou et al., 2021).

#### 1.4.2.2. Particle-reinforced composites

According to the same objective, a method to reinforce composites with particles was also developed. Unlike fibers, a particle does not have a particular direction/orientation in which its mechanical properties are optimal, thus giving the composites a more isotropic behavior. These particles are determined by their size, that can range from micro to nanoscale (Chawla, 2012; Hsissou et al., 2021). These are used to improve several material properties depending on the application, such as increasing stiffness and mechanical strength, temperature behavior, abrasion resistance, decreasing material shrinkage, and in some cases for more aesthetic reasons (Chawla, 2012; Lim Goh et al., 2020). Often these particles are only used

as filler, to obtain materials with a lower cost, but without significantly degrading their characteristics (Berthelot & Cole, 199 C.E.).

Like fibers, the choice of matrix and particles always depends on the intended application and properties. One example is the incorporation of particles of metals with high melting points, such as tungsten and molybdenum, into more ductile metals, to improve their properties at higher temperatures while preserving their ductility at room temperature (Berthelot, 2008; Kareem et al., 2021).

### 1.4.2.3. Structural composites

There are two main types of structural composites: **laminates** and **sandwich**. **Laminates** consist of composites formed by stacking several layers (laminas), which can be made of different materials or even layers of other composite materials (Adams et al., 2001; Krauklis et al., 2021).

This type of structure is widely used in composites, due in large part to the numerous possible combinations of materials, orientations and sequences of layers used to manufacture them. This allows for more customized properties for various specific applications (Gibson, 2016; Lim Goh et al., 2020; Saeedifar & Zarouchas, 2020). Another advantage is that if the layers are made of fibrous composites, they can have different fiber orientations for each layer, making it possible to obtain a final composite with very adjustable properties (Adams et al., 2001).

Moreover, this type of composite can be found at the macro, micro, or even nano scale, in both natural and man-made composites. As an example, fiberglass and aluminum composites can be found in structures for aviation, while nanocomposites consisting of layers of ceramic and polymer materials are present, for example, in the shells of the mollusk abalone (Chawla, 2012).

Because they are made up of the connection of several layers, it is again especially important to have a good interface between them, to avoid delamination phenomena, which is one of the main problems that these types of composites can have (Saeedifar & Zarouchas, 2020).



**Sandwich** composites generally consist of a core of some thickness and low density, situated between two thinner plates of material with high mechanical strength. The connection between the core and these plates is made either by means of a sheet of appropriate adhesive material, or through the resin that surrounds the fibers of the plates, if applicable (Gay, 2014). Most composites in sandwich structure have a honeycomb core. This shape is one of the most optimized patterns in relation to the space occupied and properties obtained and allows to design strong and rigid structures with the least possible weight, and with a high bending strength (Adams et al., 2001). In Figure 6 is a representation of the structure of this type of composite.

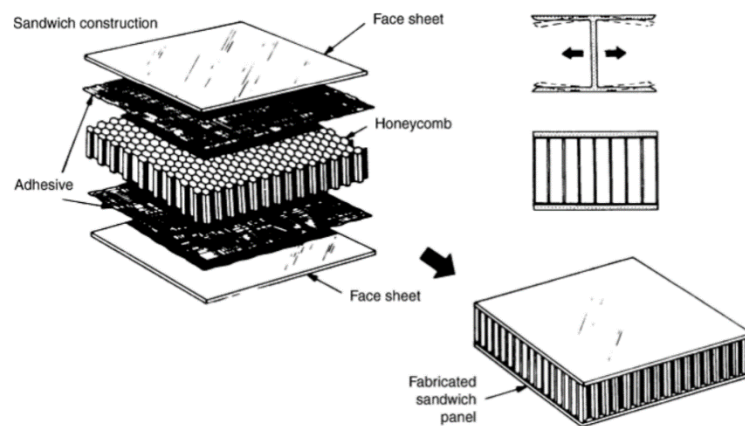


**Figure 6** - Schematic of sandwich-type composite material (Adams et al., 2001).

Each component on its own is relatively weak mechanically, however when combined they produce a strong, rigid, and lightweight structure (Adams et al., 2001). The plates on the surface of the composite are intended to support bending loads, while the core supports shear loads. Also, like what happens with the various types of composites, it is essential to have a good interface between the plates and the core to have an effective and uniform transfer of efforts between the various components, thus improving the performance of the composite, and to avoid the delamination phenomena (Adams et al., 2001; Saeedifar & Zarouchas, 2020).

### 1.4.3. Interface

Since composites are made of distinct materials, it is necessary to have an interface that connects them. This consists of a layer of material that performs the union between the different materials, allowing a uniform transmission of stresses between the various components of the composite, and has a very significant impact on the properties and behavior of the assembly over time (Lim Goh et al., 2020). Generally, a strong interface results in a composite with high strength but low hardness (Wang & Zhao, 2018).

The interface between the matrix and the reinforcement may be essentially of two types: physical or chemical. However, in most cases, physical bonds are made, such as molecular entanglement, electrostatic attraction, and mechanical interlocking (Figure 7).

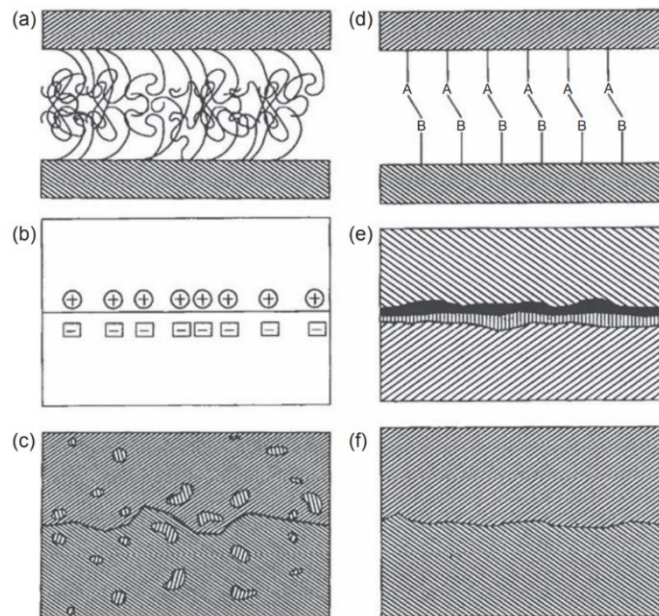


**Figure 7** – Types of composite interface bonds: (a) molecular entanglement; (b) electrostatic attraction; (c) inter-diffusion of elements; (d) chemical reaction between Group A on one surface and Group B on the other surface; (e) chemical reaction following the formation of a new compound(s), notably in metal matrix composites; (f) mechanical interlocking (Lim Goh et al., 2020).

Therefore, the surface characteristics of both the matrix and the composite reinforcement, such as their morphology and electrical charges, are crucial for the choice and formation of the most appropriate interface (Lim Goh et al., 2020; Wang & Zhao, 2018).

#### **1.4.4. Natural Fiber Composites (NFCs)**

Lately, and increasingly, an effort has been made to use more sustainable and environmentally friendly materials (Jayamani et al., 2021). Thus, composites reinforced with natural fibers have been increasingly gaining more attention among researchers and industries, due to the fibers being degradable, reusable, can be recycled, and have shown to achieve good mechanical properties and a lower cost of production than synthetic fibers (Jayamani et al., 2021; Nurhanisah et al., 2018). However, they also present some issues, like poor interfacial adhesion between the matrix and the natural fibers due to the hydrophilic nature of natural fibers, moisture absorption and sometimes low durability, that can be attenuated for example by making physical and chemical modifications of the natural fibers (Gholampour & Ozbakkaloglu, 2020).

Some of the most common used natural fibers are jute, kenaf, sisal and flax fibers, being jute and flax fibers the most popular ones (Jayamani et al., 2021; Nurhanisah et al., 2018).

There are already some applications in the biomedical area with some good results, namely the production of prosthetic sockets, by using a ramie fiber reinforced epoxy composite (Soemardi et al., 2011) and a kenaf woven fabric composite (Nurhanisah et al., 2018).

Still, there is a lot of room for development and improvement in this area, so there may be several other options to explore.

## 1.5. Composite Materials Applications

Composite materials are currently applied in numerous areas, such as in electronic components, buildings, roads, land, sea and air transport, aerospace engineering, sports, and many other application areas (Figure 8) (Gay, 2014; Pasăre et al., 2019; Reddy Nagavally, 2016).

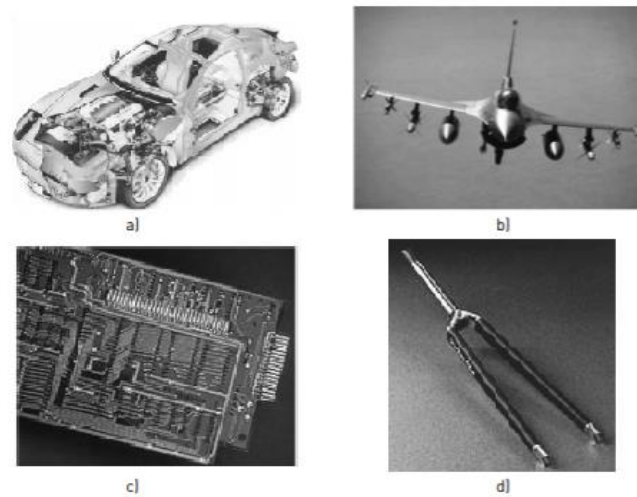


**Figure 8** - Examples of applications of composite materials in several areas: a) car made of carbon fiber panels; b) military aircraft (F-16) comprising several composite materials; c) circuit made with epoxy resin reinforced with glass fibers; d) bicycle fork composed of glass and carbon fibers (Moura et al., 2009).

A widely used practical example that demonstrates in a simple way some of the advantages from the use of composite materials is related to air transport. Two crucial factors in the production of these air means are performance and cost/savings. The use of composite materials makes it possible to obtain materials with better mechanical properties, including better fatigue and corrosion resistance, all with a lower density when compared to conventional materials. In turn, these improved properties will increase the life of the material, reducing the need for maintenance and replacement. Also, the weight reduction provided by composites will in the long run translate into fuel savings. In short, the use of composite materials enables two very important factors to be addressed in the production of this equipment, which would not be as efficient with the use of conventional materials (Gay, 2014; Gibson, 2016; Pasăre et al., 2019; Reddy Nagavally, 2016).

More recently, one of the areas where composites have a great potential for evolution is related to applications in medicine, namely in the Biomedical area. With the recent technological developments, it is increasingly possible to obtain more complex materials and structures, as well as composites in very small scales (micro and nano), which makes it viable to open a wide area of exploration in medicine (Ambrosio, 2017).

### **1.5.1. Biomedical Applications**

Various anatomical structures of the human body consist of natural composites, composed of both soft and hard tissues which, although they differ greatly in their composition, structure, and properties, perform their function as a whole (Ambrosio, 2017).

In nature, there are numerous examples of natural composites, such as bones, teeth, mollusk shells, wood, among many others. These structures are extremely optimized, which is the result of a long period of refinement. Humans have been trying to mimic these various structures to apply them in various areas, including Biomedics. Some of the biomedical areas where composites are being used nowadays are dentistry, tissue engineering, controlled drug release, medical imaging, and orthopedics (Liu et al., 2020; Maghsoudi-Ganjeh et al., 2019; Pasăre et al., 2019; Scholz et al., 2011).

#### **1.5.1.1. Dentistry**

Currently, most people suffer from at least some kind of dental problem throughout their lives. Thus, there have been several advances in dentistry, particularly in the research of different biomaterials to address the numerous problems, from filling dental cavities to tooth replacement (Wang & Zhao, 2018). Some of the materials traditionally used in dental applications are amalgam, alumina, zirconia, and gold, but they all have been almost fully replaced by composite resins (Scholz et al., 2011).

For restorative materials, they must have a low viscosity to fully fill cavities, a thermal expansion coefficient like dentin, resistance to fatigue, wear and water absorption, and good

biocompatibility. Since the commonly used restorative materials have limitations in their biocompatibility and mechanical properties, the application of composite materials has been studied in these situations (Wang & Zhao, 2018).

In cases where it is necessary to insert a dental post into the root canal, composites have proven to be less time consuming, thus making surgical procedures less traumatic for the patient (Scholz et al., 2011). Usually, these structures are made from cobalt-chromium or titanium alloys, but equally composite materials are being studied to promote better performance, such as epoxy matrix composites reinforced with carbon or glass fibers (Ambrosio, 2017; Krishnakumar & Senthilvelan, 2021; Wang & Zhao, 2018). Composite materials of polymethylmethacrylate (PMMA) with vitreous carbon (VC) have also already been used. These allowed to obtain some advantages, such as fast healing with minimal discomfort in patients, and the lower modulus of elasticity of the material when compared to that of bone provided a better transfer of loads from the implant to the bone supporting it, minimizing the bone loss that is sometimes observed in these applications (Ambrosio, 2017). Additionally, finite element analyses have shown that these dental posts ideally should have varied stiffness along their length for best performance, which is not possible using homogeneous materials (Wang & Zhao, 2018).

Some other important factors that influence the use of composite materials in this area of study are: aesthetics – for example, by using a ceramic reinforcement with a transparent matrix almost all dental shades can be obtained; corrosion – composites with a polymeric matrix are less susceptible to corrosion, when compared to metal alloys; toughness – polymer matrix composites are not brittle, hence the problem of abrasion and fracture is reduced; metal allergy – many people exhibit an allergic reactions to the presence of metallic devices in their body, therefore devices made of polymer and ceramic composites eliminate such allergic reactions (Fujihara et al., 2004; Krishnakumar & Senthilvelan, 2021).

Furthermore, it is also possible to apply coatings of a layer of a bioactive ceramic material, such as hydroxyapatite, which will favor cell growth, and in turn improve osseointegration (Mazumder et al., 2019; Nasar, 2019).

### 1.5.1.2. Tissue Engineering

Tissue engineering applications aims to repair and/or regenerate living tissues that have similar compositions, structures, and functions to the original tissue, by combining techniques from multiple areas and disciplines, and has shown great potential when compared to conventional techniques of prosthesis implantation, and tissue and organ replacement/transplantation (Ambrosio, 2017; Wang & Zhao, 2018).

Currently, the techniques used in this area are increasingly focused on the application of a porous matrix, called *scaffold* (Ambrosio, 2017; Scholz et al., 2011). This consists of a porous and biodegradable structure that promotes cell adhesion, proliferation, and differentiation (Figure 9). Being biodegradable, these structures enable cell proliferation in a certain controlled pattern and have the great advantage that they can be introduced into the human body without the need for a second intervention to remove them, since after the structure is degraded, only the intended new tissue will be left in its place (Wang & Zhao, 2018). Also, the amount of donor tissue required over a given period would be reduced, since cells may be engineered in vitro (Scholz et al., 2011).

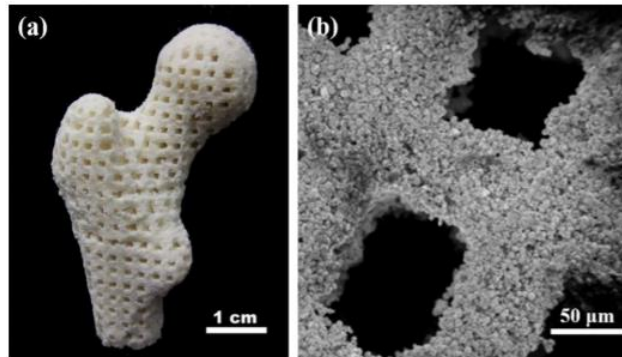


**Figure 9** - Example of a scaffold made by SLS technology in the shape of a femoral head: (a) macroscopic view of the structure; (b) SEM image of the porous structure (Wang & Zhao, 2018).

Moreover, the properties of these scaffolds, such as degradation rate, biocompatibility, and overall mechanical and biochemical properties are dependent on the types of materials that constitute them. Most *scaffolds* currently used are made from relatively simple biodegradable polymers such as PLA, PLGA and PCL, however these have some limitations (Wang & Zhao, 2018). As an example, PLA has the great advantage of biodegradability,

however it has a low cell adhesion and degradation rate, due to some of its properties like hydrophobicity. This can lead to inflammation and necrosis of the cells (Liu et al., 2020).

To address some of these problems, composite development is being increasingly investigated. By combining different materials, it is possible to modify and improve currently existing scaffolds by maintaining the materials' advantages while eliminating or attenuating their disadvantages (Liu et al., 2020; Wang & Zhao, 2018). By using the right materials, it will be possible to obtain structures that can achieve good performance, such as good biocompatibility and bioactivity, vascular support, non-immunogenicity, and a well-defined degradation rate. Moreover, it is also possible to add particles of certain materials to the structure, such as graphene particles to provide greater electrical conductivity, potentially useful for nerve tissue regeneration, and bioceramics to promote greater bioactivity and osseointegration in bone tissue regeneration (Liu et al., 2020; Wang & Zhao, 2018).

### **1.5.1.3. Controlled Drug Release**

A drug is a substance that is intended for use in the diagnosis, cure, mitigation, treatment, or prevention of diseases (Adepu et al., 2021). Controlled drug release systems were developed with the purpose of allowing a greater control of the exposure to drugs over time, helping them to cross physiological barriers and protect them from being prematurely eliminated, as well as to direct them to the required site of action, thus minimizing their exposure to the rest of the body (Adepu et al., 2021; Rathbone et al., 2012). These still have some limitations, namely the lack of materials suitable for their application (Wang & Zhao, 2018).

The simplest systems are based on the degradation of a polymeric material, which encompasses the drug in its composition, and then the drug is released as the system degrades (Rathbone et al., 2012). However, the need for a more precise control has arisen. Composite materials can be extremely flexible in terms of their physical and chemical properties, which makes them excellent candidates in the search for new materials for this biomedical application (Wang & Zhao, 2018). Therefore, some controlled drug release systems have already been created using this type of materials, which can release drugs over time or in response to different induced stimuli, such as temperature, light, magnetic and electrical



forces, ultrasound, pH variations, among others. This allows the concentration of the respective drug to always be within therapeutic limits, thus being more effective (Figure 10) (Wang & Zhao, 2018).

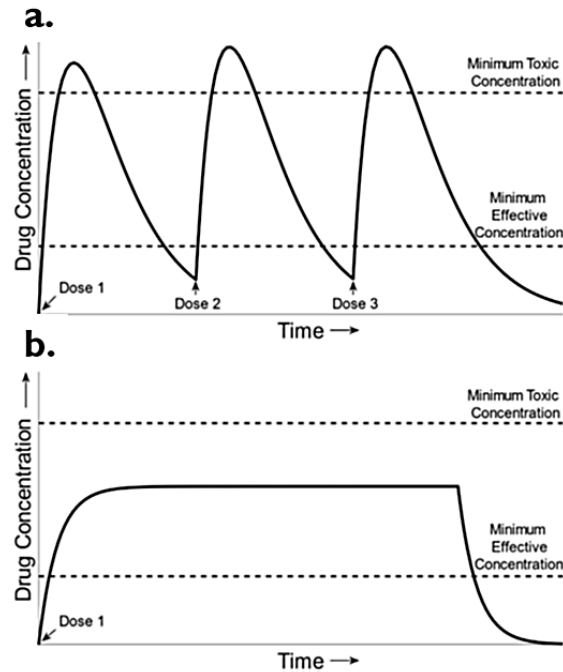


**Figure 10** - In conventional delivery systems (a.), drug levels fluctuate above the minimum toxic concentration and below the minimum effective concentrations, which can cause side effect or not be as effective as it should be. This does not happen with controlled delivery systems (b.), as the drug levels are maintained constantly within therapeutic ranges (Adepu et al., 2021).

A widely used drug delivery system is hydrogel nanocomposites. These composites consist of encapsulating functional nanoparticles, such as metallic and/or ceramic, in a hydrogel matrix that also holds the drugs. The change of structure of this hydrogel, such as its expansion or shrinkage, will enable the release of the drug, and this change will be regulated by certain stimuli, stimuli that will be defined according to the type of polymer and nanoparticles present in the composite, hence the versatility of this type of material being a great asset in this matter (Wang & Zhao, 2018).

Another example are polymersomes, which are small synthetic vesicles that enclose liquid drugs, and are usually made of polymer-lipid composites. Compared to liposomes, these structures possess some enhancements such as improved colloidal stability, encapsulation efficiency (they can encapsulate both hydrophobic and hydrophilic drugs), and they are also more stable and have lesser toxicity in the body (Adepu et al., 2021).

### 1.5.1.4. Medical Imaging

Medical imaging stands for the use of imaging technologies, such as computed tomography (CT) and magnetic resonance imaging (MRI), to non-invasively obtain *in vivo* information of living subjects, as opposed to *ex vivo* invasive procedures such as biopsy. The diagnosis of various diseases, such as cancer, relies heavily on these modern medical imaging techniques. The information that can be obtained is directly related to the contrast agents that are used, that consist of substances that are administered to the patient, which in turn will promote the enhancement of specific body tissues in the exam results, thereby facilitating their analysis (Figure 11) **Erro! A origem da referência não foi encontrada.** (Huang, 2020; Pellico et al., 2021; Wang & Zhao, 2018).



**Figure 11** - Angiogram of the left internal carotid artery. The use of contrast agents makes it possible to clearly distinguish blood vessels, which are not visible in conventional examinations (Alberti et al., 2009).

However, being substances that will be introduced into the body, they must meet several requirements and ensure good efficacy. It is crucial to have an excellent biocompatibility, to avoid causing any adverse effect to the body, and to provide a good stability, contrast intensity, and cellular absorption. It is also relevant to mention that the most used contrast agents currently have usually some kind of weakness, from poor contrast intensity to biocompatibility problems which cause the body to capture and expel these substances (through the reticuloendothelial system) (Wang & Zhao, 2018).

Multimodal imaging, a relatively recent technology, combines different techniques and materials, namely the use of specific nanocomposites, to provide more reliable and accurate detection of disease sites. Each imaging technique on its own has significant intrinsic strong

and weak points, that are difficult to overcome just by the improvement of the technique alone (Lee et al., 2012; Pellico et al., 2021). As an example, PET images provide functional information about the disease with high sensitivity, whereas CT and MRI provide high-resolution images for anatomical information. By combining different techniques, it is possible to get a more precise and detailed information that can be crucial to the diagnosis (Lee et al., 2012).

The use of nanocomposites allows the development of advanced contrast agents, which effectively mitigate or even eliminate some of the disadvantages present in the various techniques. It is possible to integrate different nanoparticles to improve or add certain properties to them. For example, metallic particles can be integrated to improve the magnetic response of the contrast agents, as well as increase the biocompatibility of its particles by creating a polymeric coating (micelles) around them, thus decreasing toxicity, and prolonging their effectiveness due to non-exclusion by the body (Wang & Zhao, 2018).

### **1.5.1.5. Orthopedics**

#### **Bone Fractures**

Regarding the field of orthopedics, composite materials have already been investigated for different applications, such as bone fracture repair and internal and external prostheses. When it comes to the treatment of bone fractures, there are usually two types that are clinically used: **external fixation** and **internal fixation** (Akbari Aghdam et al., 2019; Scholz et al., 2011; Wang & Zhao, 2018).

**External fixation** does not require opening the fracture site. It keeps the bone fragments aligned by means of casts, splints, braces, or similar fixation devices. Traditional materials are usually made of calcium sulfate plaster reinforced with woven cotton fabrics, or glass and polyester fibers providing the necessary reinforcement of the material (Scholz et al., 2011). Other external fixation systems made from carbon fiber composites and epoxy resins have also attracted a lot of attention. These materials allow obtaining devices with low weight and mechanical properties comparable to those of metallic devices. In addition, since they have no metallic components, the use of these materials does not cause artefacts in

radiographs, facilitating the process of monitoring the healing process using medical imaging techniques (Scholz et al., 2011; Wang & Zhao, 2018).

On the other hand, **internal fixation** requires opening the fracture site for subsequent implantation of fixation devices such as screws, plates, pins, and wires to hold the bone fragments in place. These devices are usually made of metallic materials, but composites with properties close to those of bone are now being developed, allowing for greater biocompatibility and better results in the healing processes. In addition, these kinds of composites can either be non-resorbable, partially resorbable or fully resorbable. Regarding the latter ones, these possess the advantage of avoiding a second surgery for removing them, however it is generally difficult to achieve a fully non-toxic degradation (Scholz et al., 2011; Wang & Zhao, 2018).

### **Amputations**

Amputation is one of the oldest surgical procedures, with an history of over 2500 years. It consists of a surgical procedure that is made as a last resort, when the recovery of a limb is impossible, or when it is dead or nonfunctional, risking the patients' life (Gebreslassie et al., 2018). In developing countries, the number of amputations has been increasing, mainly related to the lower limbs. In general, the main causes of amputations are related to peripheral vascular disease, diabetes, traffic accidents (particularly motorcycle accidents), but there are many other causes including diseases such as cancer, congenital deformities, work accidents, and war-related causes (Day et al., 2019; Gebreslassie et al., 2018; Junqueira et al., 2019; Nurhanisah et al., 2017).

Amputation can indeed be a lifesaving procedure; however, the resulting impact can be life changing to the patient, thus needing individual adjustments in almost every way of his/her life. Along with physical changes, such as compromised mobility, pain, and discomfort, these patients also deal with several social and psychological challenges (Day et al., 2019). To improve the quality of life of patients, there have been several advances in treatments and in the used medical devices that replace, supplement, or restore a certain function, such as prostheses (Nurhanisah et al., 2017).

As for lower limb prostheses, there are two main types: trans-tibial (for below the knee amputations) and trans-femoral (for above the knee amputations) (Figure 12) (Nurhanisah et al., 2018). These prostheses usually have three main components, which are the artificial foot, the connector tube (also known as pylon), and the socket, which is where the contact with the residual limb takes place, by means of the liner. In the case of trans-femoral prostheses, a component for articulation of the knee area is also indispensable (Nurhanisah et al., 2017, 2018).

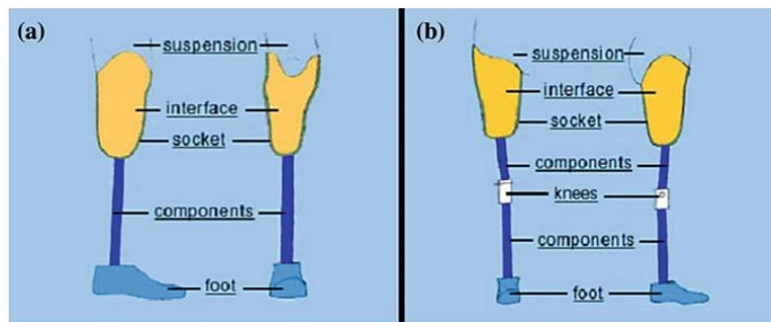


**Figure 12** - Types of lower limb prostheses: a) trans-tibial prosthesis; b) trans-femoral prosthesis (Nurhanisah et al., 2017).

The socket is a very important component of a prosthesis, as it does the connection between the stump and the other prosthetic components. It is also responsible for a major part of the patient's comfort, due to the force distribution and pressure on the stump. Even currently it is difficult to meet the exact needs of patients, being the main reason of abandoning the use of these devices (Nurhanisah et al., 2017; Wang et al., 2021). Some of the most observed problems are related with soft tissue damage, such as blisters and ulcers, and poor blood circulation (Wang et al., 2021). The need for high level of customization on these kinds of devices lead to further investigation on better manufacturing procedures. Prosthesis should be fully customizable devices, to provide patients the best comfort and quality of life possible (Maji et al., 2014; Stenvall et al., 2020; Vitali et al., 2017). Regarding sockets for lower limb prostheses, orthopedic laboratories around the world share a standard procedure with minimal variations for creating them, which consists of creating a negative cast model. It is also crucial that the model must copy the residual limb in a compressed state, which is the real shape the limb will have during normal activities, due to the body weight and compression forces. To do this, the orthopedic technicians squeeze the plaster cast by hand to simulate the load, while it dries off. However, being a manual procedure, which relies

mainly on the technicians' skills and experience, it is susceptible to errors, which can impact patients' comfort. Moreover, this procedure takes a few days to complete, in which patients must go multiple times to the lab to complete it. (Vitali et al., 2017) That said, the transition from conventional manufacturing methods to additive manufacturing can bring numerous advantages in the customization of the types of medical devices (Maji et al., 2014; Silva et al., 2017; Stenvall et al., 2020; Vitali et al., 2017).

Currently, several fiber-reinforced polymeric materials are used in orthopedics, particularly in upper and lower limb prostheses. Furthermore, some composites reinforced with natural fibers, such as kenaf fibers, have already been studied, especially in the production of the liner, which have demonstrated a good weight/strength ratio, high impact strength, and greater biocompatibility, being natural products. However, the results are often subjective, especially in terms of prosthesis comfort, and may vary from patient to patient (Jayamani et al., 2021; Nurhanisah et al., 2018; Soemardi et al., 2011).

## **1.6. Research Gap Identification**

When gathering information to perform the state of the art of this work regarding composite materials and some of their biomedical applications, some pertinent information was obtained.

It was found that there are already some studies regarding the use of natural fibers in the production of composites, the natural fiber composites (NFCs), as an approach to more sustainable and eco-friendly materials. Additionally, some studies that successfully used these types of composites on the development of prosthetic sockets have already been carried out.

Another important acquired information is that the customization of prosthesis is crucial when it comes to the patients comfort on using the medical device, which is very often the reason why patients stop using it. To improve this customization, some studies about using additive manufacturing technologies in orthopedic applications were acquired.

At this point, after elaborating the state of art of this work, it was found that at present there are several studies and advances being made. Composite materials made with more sustainable materials are being developed, and the integration of newer manufacturing techniques like additive manufacturing are being implemented around biomedical devices, namely the production of prostheses' sockets.

Nonetheless, it was noted that there is no specific study that contemplates simultaneously sustainable composite materials, customization through additive manufacturing, and above all the possibility of being the user (patient) doing the upgrades at the comfort of his/her home. This would be truly groundbreaking in which it could improve considerably their quality of life.

For this purpose, firstly a model of a patient's stump must be acquired, to create a model for numerical simulation analysis.

Then, a study to understand the main causes of discomfort in patients must be carried out. By gathering information for the state of art of this work, it is already known that friction is one of the main causes of discomfort, causing soft tissue damage, such as blisters and pressure ulcers.

After getting this problem studied, some composite materials compositions, including with more sustainable materials, must be analyzed. It is crucial to consider several options to check if they can meet the mechanical requirements for this kind of application.

After gathering some materials that meet the necessary conditions, the focus must go to the composite materials made with more sustainable materials, and that subsequently can be transformed in a filament liable to be used with additive manufacturing processes, such as fused deposition modeling (FDM).

The possibility of a patient being able to produce a fully customized prosthesis' socket at his/her home by using a 3D printer would be groundbreaking, as it would increase its comfort and be less energy and time-consuming comparing with conventional processes.

## 1.7. Research Question

Based on the research gap above defined, we derive the following research question:

**“How can an amputee design and manufacture his/her own custom-made prosthetic sockets using low cost home available devices?”**

To further contribute to answer this research question, some partial goals were defined:

1. Friction being one of the main causes that influence the comfort of wearing prosthetic devices, what is the best way to develop a model that makes it possible to assess its effects?
2. How to correctly define the properties of the different materials (biological and non-biological) that will make up the biomechanical model, to obtain simulations that are reliable?
3. How to select potential sustainable materials for the development of a prosthetic socket?
4. How can low-cost home-available scanning and manufacturing processes be used for the patient to build his/her own prosthetic device?



## 1.8. Outline of the thesis

Usually, the development of new products follows a dedicated sequence of steps, from the identification of the potential user's needs and wants, to the final prototype and validation, that will allow for the manufacturing of the desired product. Therefore, the definition of some essential steps to carry out this work was performed (Figure 13).

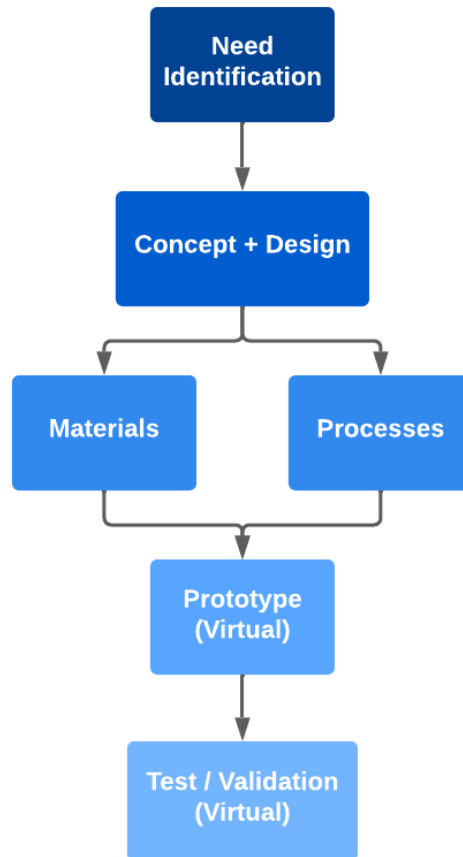


**Figure 13** – Flowchart representing the steps on which the development of this work was based.

Firstly, the need to contribute to improving the quality of life of amputees was identified, since this is increasingly the case, both due to traffic accidents, diseases, and even war. By reviewing existing studies, a market need was identified, leading to the formulation of the above-mentioned research question. Then, based on those identified market gaps, it was necessary to carry out a formulation of ideas about the best way to develop the study in question. Research was conducted to obtain some information needed to define a concept and to learn more about the design to be applied later in the creation of a prototype. At this

point, to further develop that concept and design, some potential materials and manufacturing processes that could prove useful in answering the identified research question were explored. Additionally, some optional requirements regarding materials were imposed. Lastly, and once all the necessary data was obtained, some prototypes were developed and further improved, with which several numerical simulations were carried out. These made it possible to test and validate the model and give a better understanding of whether the customized production of prosthetic devices using low-cost home-available devices could be achievable.

To tackle each of the four envisaged goals of the current research, four dedicated exploratory research-studies were performed.

### **1<sup>st</sup> Study – Preliminary Biomechanical Model Development**

#### **(Need Identification/Concept & Design/Early Prototype/Early Test)**

After analyzing the market and having defined the research question, the first study was performed. This study was developed to assess the effects of friction on the residual limb (stump) of a transfemoral amputee, by developing a preliminary finite element model. Customization is a key point in the development of this work, since a good one will provide better comfort to patients that use this kind of prosthetic devices. Additionally, to optimize function, it was not only important to customize the geometry, but also to ensure that the assembly performs a correct accommodation of stresses, to avoid soft tissue injuries, one of the main reasons for the abandonment of this type of devices.

Since the geometry of the stump can be considered as approximately symmetrical, throughout this whole exploratory study the biomechanical model was developed as a 2D axisymmetric model. At this stage, for the creation of the preliminary model, a simplified geometry for the anatomical shapes of the patient's stump was considered, leading to the formulation of the first 2D axisymmetric model (Figure 14).

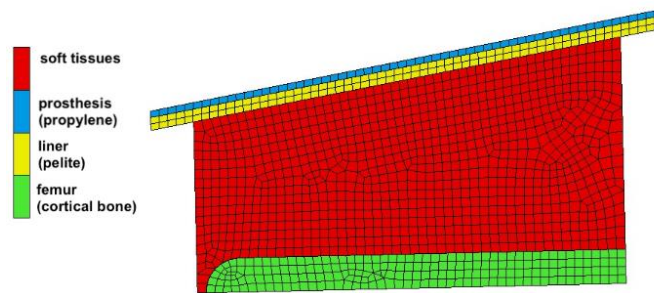


**Figure 14** – Developed 2D axisymmetric model for a preliminary assessment.

The initial properties of the preliminary model's constituent materials as well as boundary conditions were defined, based in some literature. This allowed the development of a preliminary finite element analysis to help evaluate the effects of friction coefficient on the contacts of the various parts of the biomechanical model – socket, liner, stump, and femoral bone – information that will be crucial to further progress with this research.

## **2<sup>nd</sup>/3<sup>rd</sup> Study – Improvement and Validation of the Biomechanical Model**

### **(Materials/Final Prototype/Test and Validation of the Model)**

The need to conduct a more in-depth and realistic study led to this second article. To achieve a correct design, besides having a more realistic geometry, it should be understood how the materials and their constitutive laws affect the stress field produced in the biomechanical system.

To better evaluate the stress field at the prosthesis interfaces with the defined material properties and constitutive laws using the finite element method numerical simulation, the previously developed model was improved, both in terms of its geometry and the characterization of the materials. Though, its 2D axisymmetric formulation was maintained.

To create this improved model, a 2D profile of a patient's stump was obtained by segmenting a medical imaging of a patient's stump (Figure 15).

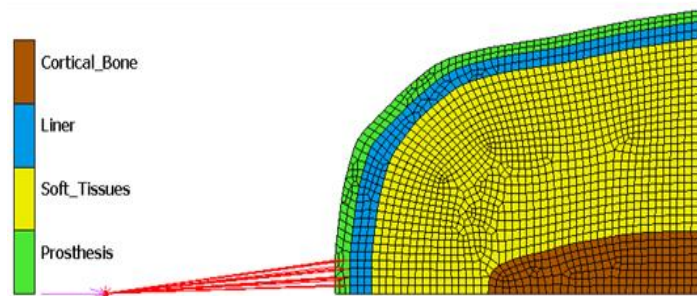


**Figure 15** - The 2D axisymmetric model used in the preliminary study was improved in terms of geometry definition.

Regarding the material characterization, one important aspect was the fact that soft tissues were not considered homogeneous and isotropic materials. In fact, the anisotropic properties of their main components – skin, fat, muscle, blood vessels, and fascia – were considered. Furthermore, in most finite element analysis of biomechanical systems, soft tissues are characterized by a linear elastic model. However, this is not adequate, since they are subject to large deformations. Therefore, some hyperelastic models were also considered.

As an additional goal, some sustainable materials were also considered, to also attempt to contribute to a greener environment. For the composition of the prosthesis (socket), three materials were analyzed: the thermoplastic polymer propylene; an epoxy resin with a mostly vegetal molecular structure (SR GreenPoxy 56); and a composite material in which the matrix consisting of the previous referred epoxy resin is reinforced with natural jute fibers. It was the latter that was considered for most of the simulations performed, to study the influence of friction and the constitutive laws of materials on the stress fields produced in the biological tissues of a patient with a transfemoral amputation. These simulations were also useful in that it allowed the potential of these materials in the manufacture of a prosthetic socket to be assessed.

#### **4<sup>th</sup> study – Customized Prosthetic Device Production by Patients (Materials/Processes/Final Test and Validation)**

At this point, there was still the goal of studying how it might be possible to integrate low-cost manufacturing processes into the production of customized prosthetic sockets, using more sustainable materials. To try to achieve this, it was necessary to consider manufacturing processes that could meet these conditions, as well as materials that could satisfy the necessary requirements. Some more sustainable materials were also considered, and some further numerical simulations were performed, to assess whether they met the necessary requirements for the type of application in question.

Additive manufacturing was the selected manufacturing process that best suits the needs to achieve this goal. In addition to being effective in producing customizable products, it is also not as material-wasting, time-consuming, or labor-intensive when compared with conventional manufacturing processes. These processing technologies also have the great advantage that one can directly use 3D models of the anatomical profile of the patient's stump, obtained for example by medical imaging, or even by using a home-available device such as a flatbed scanner.

Based on the positive results obtained for some of the tested materials, the possibility of using them to produce the medical device under consideration using additive manufacturing technologies has become quite plausible, having indeed the potential for patients to be able to produce these devices using low-cost methods from their homes.

Based on these exploratory research-studies, four publications were developed.

## **2. 1<sup>st</sup> Paper - Development of a preliminary finite element model to assess the effects of friction on the residual limb of a transfemoral amputee**

### **Abstract**

The use of numerical modelling tools allows optimizing the development of complex anatomical artefacts, such as customized prostheses for lower limb amputees. These numerical tools make it possible to characterize the interfacial interactions taking place between different parts of the prosthesis and the residual limb. This allows for understanding which rectifications and fittings having to be made on the custom design of the artificial body part without the need for manufacturing and donning prostheses. To such end, current research focused on the development of a preliminary Finite Element Model to assess the effects of friction on the residual limb of a transfemoral amputee, as the friction on the contact between the soft tissues, the liner and the prosthesis of the amputee is of major importance for his/her health and comfort.

Keywords: Finite Element Analysis; Prosthetic liner; Interfacial stresses; Amputee; Patient comfort and health; Customized medical devices.

## **2.1. Introduction**

In the current paper, a preliminary study was carried out as part of a broader project that intends to use numerical modelling tools in order to optimize the development of customized prostheses for lower limbs of transfemoral amputees. The main goals of using the Finite Element Method (FEA) as a numerical modelling tool in the development of this prosthesis are the following: 1. Facilitate the understanding of the interfacial interaction between the different parts of the prosthesis and the residual limb; further, the field of stresses in the soft tissues is assessed to enable the evaluation of the stresses in areas not available in vivo studies. 2. Facilitate the prosthesis rectifications and fitting that enable the custom design without the need to build and donning prostheses; this process allows reducing the physical and psychological impact on the life of the patient. To help in the distribution and cushioning of the loads transferred between the socket and the soft tissues in the residual limb, soft prosthetic liners are usually interposed between both parts [1].

The aim of the FEA in this project is to assess the effect of the prosthetic liner material properties in the interfacial stresses between the parts of the prosthesis and the residual limb. The load distribution effect on the stresses generated inside the residual soft tissues will be also assessed.

The finite element model will be validated in specific geometries and through the clinical study of amputated patients. At this stage of the project, a patient with a transfemoral amputation was selected, and the necessary approvals are still being analyzed by the local ethics committees.

To generate the Finite Element Model (FEM) the following tasks will be carried-out:

### **1. Geometric modelling of the stump and the socket**

The patient morphology acquired by medical images will be segmented using the software Matlab and Rhinoceros 3D, in order to obtain the stump and bones surfaces. The inner socket surface will be furnished by the cad manufacture software. The geometry of the liner will be inputted and parametrized.

## **2. Meshes**

The surfaces will be imported to software MSC Patran where the solid model will be prepared, meshed, and parameterized.

## **3. Material properties**

The material properties obtained in the literature [2-4] will be adapted to the model considering the experimental results.

## **4. Boundary conditions – slip model**

The contact-slip models in the literature [5] will be adapted to the model considering the experimental results.

## **5. Boundary conditions – loading**

The loading will be done in two steps. In a first step will be simulated the donning and fitting of prosthesis [6]. In a second step were superimposed a loading considering the experimentally measured three-dimensional ground reaction forces and moments using a force platform while the patient walked – the forces and moments were transferred to the top surface of the bones [7, 8].

## **6. Procedures**

The FEM will be run in the MSC Marc software.

## **7. Validation of the FEM**

The model will be validated with the experimental results published in the literature [5, 7-10] and with the obtained experimental results.

In the current stage of this project, the anatomical characteristics of the patient cannot be used. Therefore, a preliminary study related to the above-mentioned task 4 was carried out. In this study, a preliminary FEA was developed to assess the effects of the friction coefficient on the contacts of the parts of the biomechanical model – socket, liner, stump and residual femoral bone – in the stress field at the stump. In fact, the friction coefficient on the contact between the soft tissues, the liner and the prosthesis of the amputee is of major importance for patient health and comfort. The effect of the friction coefficient on the positioning of the prosthesis was studied by W.C.C. Lee and M. Zhang [11]. The effect of the friction coefficient between the femur and soft tissues was studied by J.F. Ramirez and J.A. Vélez



[10]. The importance of the liner in the patient's health and comfort drove many investigations [6, 12, 13]. Accurate assessment of stress distribution between the skin and prosthetic devices is also very important in robotics [14, 15]. In the current preliminary study, the effect of friction on the contact of all these parts of the biomechanical model will be assessed.

## **2.2. Finite Element Model**

The Finite Element Model used in this research was based on the one by M.B. Silver-Thorn and D.S. Childress [8], with a simplified and adapted geometry to the anatomical shapes of the patient, as well as to the scope of this preliminary study.

### **Geometry**

In this exploratory research, the simplified geometry of the model (Fig.1.a) approximates the patient's residual limb anthropometry, being the femur approximated to a spherical-end cylinder. Considering muscle atrophy, the simplified shape of the stump was considered as a conical trunk with its base on the distal end, a diameter of 160 mm and a 10-degree slope. The liner was modelled as a 6 mm thick conical surface fitted to the stump. Finally, the socket type prosthesis was also modelled as a conical surface fitted to the liner, with an overall thickness of 3 mm.

### **Mechanical Properties of Materials**

The materials of current research - soft tissues, liner (pelite [3]), cortical bone [4] and prosthesis (propylene) - are all defined as an isotropic, homogeneous, and linear elastic material, that have an elastic modulus (E) and Poisson's ratio ( $\nu$ ) as follows: Soft tissues -  $E=0.06$  MPa,  $\nu=0.45$  (approximately incompressible); Liner -  $E=0.38$  MPa,  $\nu=0.49$  (approximately incompressible); Cortical bone -  $E=11.5$  GPa,  $\nu=0.31$ ; Prosthesis -  $E=1$  GPa,  $\nu=0.30$ .

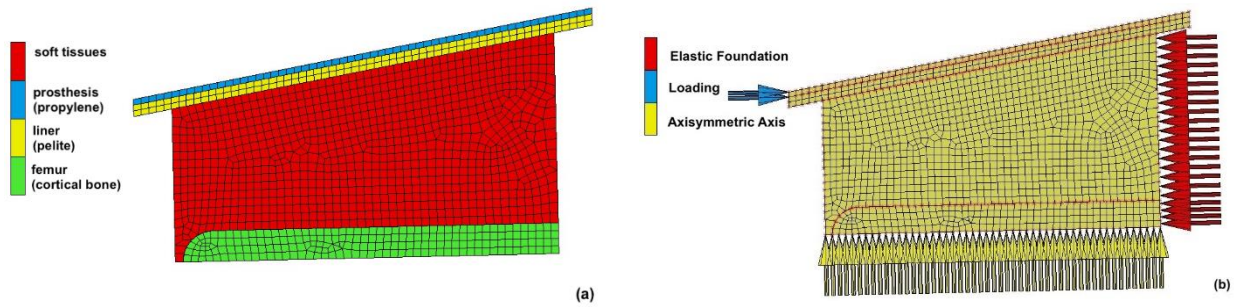


Fig. 1. (a) Numerical model geometry and materials; (b) Boundary conditions of the model.

### Boundary conditions

An elastic foundation, with a stiffness value of  $E=0.06$  MPa, was considered for the proximal part of the model. This condition was intended to approximate the interaction of the stump with the rest of the body. To make contact modelling less dependent on the finite element mesh, the interaction between bodies was modelled using the segment-to-segment algorithm [16], which uses the Augmented Lagrangian constraint method that allows the contact between organic surfaces to be more efficiently approximated. Three numerical models were developed in order to assess the effect of the friction coefficients on the stresses developed at the biomechanical model's soft tissues:

- **Model 1** was based on a Coulomb's bilinear friction model, with an average friction coefficient between the cortical bone and the soft tissues of  $\mu=0.415$  [4]. A friction coefficient of  $\mu=0.6$  was also considered on the contact between the prosthesis and the liner [11], whilst for the contact between the liner and the soft tissues, the friction coefficient was of  $\mu=0.8$  [12].
- **Model 2** is similar to Model 1 and was created to validate the numerical model, allowing comparing the results with those of different authors [8, 10]. In this model, the contact between soft tissues and femur was modelled as glued.
- **Model 3** was based on Model 1 with a prestress in the liner, with both horizontal and vertical ring loads of 40 N. Distributing compressive stresses over the residual limb, particularly in sensitive regions with bony prominences, is desirable [6]. Some manufacturers customize their liner to impose these compressions in the donning process.

The preload imposed in model 3 generates an initial pressure similar to that considered by that author.

### **Loading**

The prosthesis is considered to support the patient's total weight (70 kgf), during the static stance. Loading is imposed quasi-static conditions [17], as illustrated in Fig.1.b.

### **Finite element analysis**

Given the symmetry of the model, a 2D axisymmetric analysis was performed. This simplification allowed for a more efficient analysis with reduced computational cost. The simulations with this model were made using the implicit module of MSC Marc Mentat 2018. This method, when applied to models that suffer large deformations, can cause several convergence problems related to kinematic nonlinearities, mesh distortion, shear locking, etc. However, the implicit method allows for efficient use of contact models for materials with nonlinear constitutive relationships.

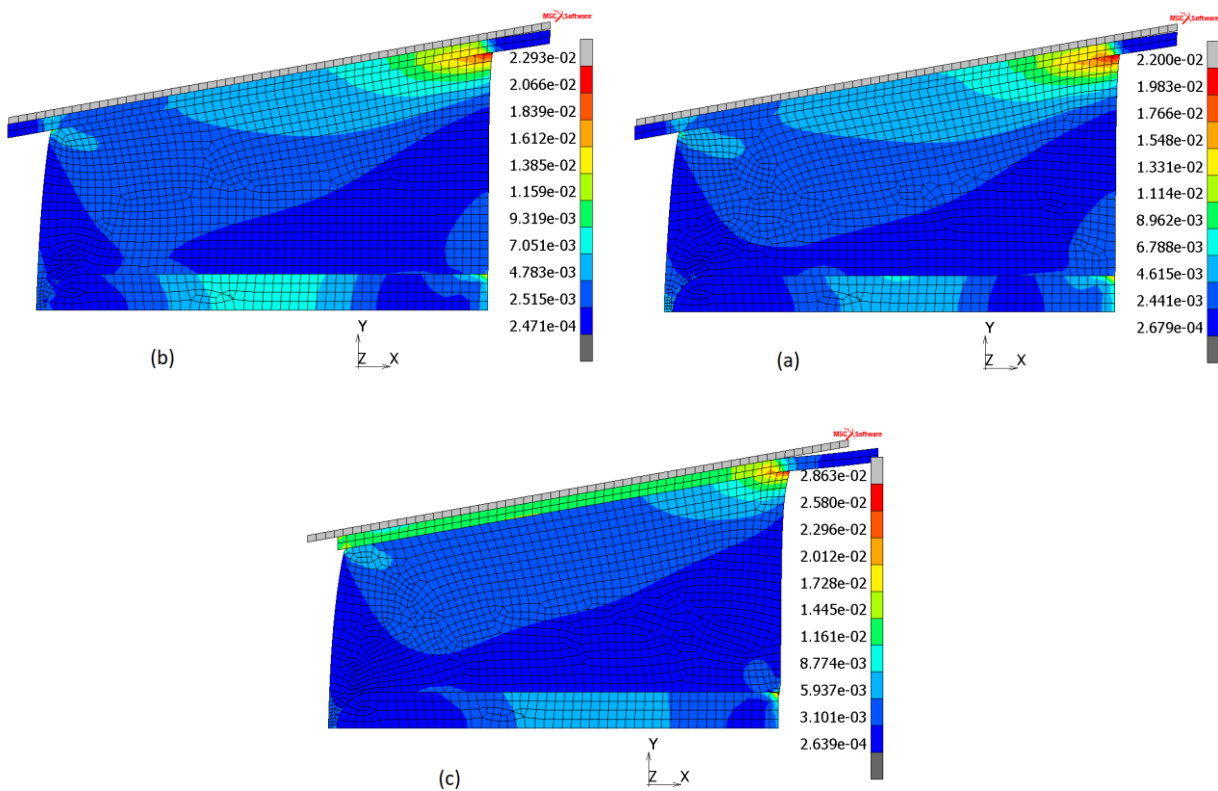
Current exploratory research is the preliminary foundation of a broader project that aims at developing dedicated FEA models of customized anatomic geometries and characterize the mechanical behavior of constitutive materials. The numerical constrictions associated with the implicit method were overcome using mesh adaptivity algorithms. Due to the geometric complexity of the models at which this work aims being applied to, an automatic algorithm was used for meshing, and linear quadrilateral axisymmetric solid elements with four nodes (Quad 10) were used. The initial mesh dimensions of the elements were of 4 mm. This value was established in a previous iterative process and is considered as an objective in the adaptive mesh algorithm. In this process, the mesh size may be reduced to a quarter of its initial value, depending on the strain change and the distortion that may occur in each element.

## **2.3. Results and Discussion**

The von Mises stress distribution (in MPa), for Models 1, 2 and 3 are shown on Fig.2. It can be observed that for Model 1 (Fig.2.a) and Model 2 (Fig.2.b), in the biological parts, the highest stresses occur in the proximal part, for the soft tissues near the liner. When compared

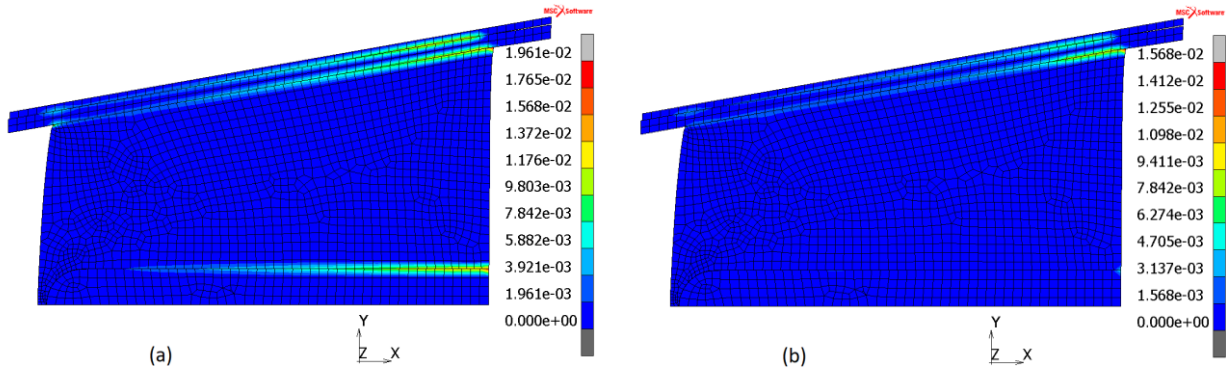
with the results by other authors [8, 10] the numerical model can be validated. Whereas the geometry and loading are different, von Mises stresses have the same orders of magnitude and similar distributions, although in the present study the effect of friction between the prosthesis, liner and soft tissues is visible. The obtained results allow assessing the influence of the friction coefficient between the prosthesis, the liner and the soft tissues on the stress distribution of the whole biomechanical system.

In Model 3 (Fig.2.c), at the soft tissues, the highest stresses occur in the proximal part, near the liner. When compared with previous Model 1 and 2, in Model 3 one can observe that the von Mises stress is higher. From the analysis of the von Mises stress distribution, we cannot conclude about the influence of friction between the bodies in the biomechanical model.



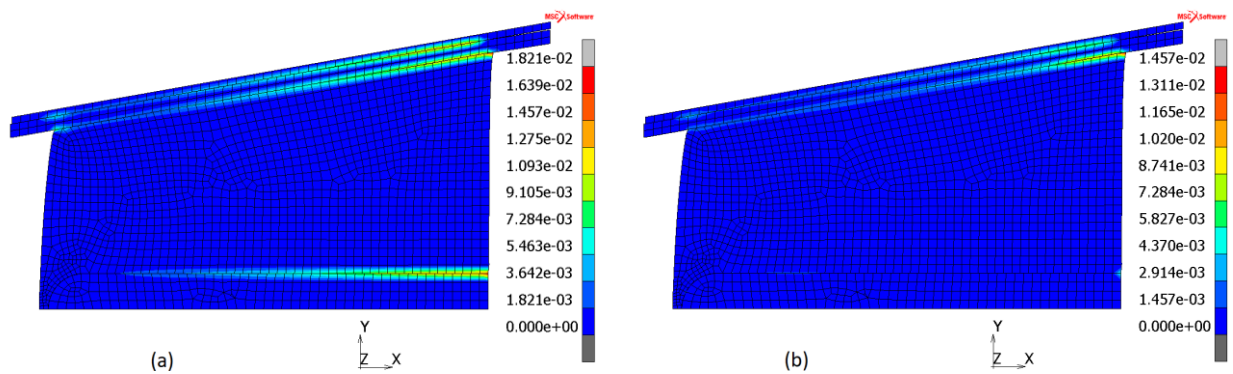
**Fig. 2.** (a) Von Mises stress distribution (MPa) for Model 1; (b) for Model 2; (c) and for Model 3.

Fig.3 shows the normal and shear contact stresses, between all the solids, for Model 1. Both images plot the contact stresses between the prosthesis and the liner, between the soft tissues and the liner, as well as between the soft tissues and the patients' femur. Fig.3.a presents the normal stresses for Model 1, whereas Fig.3.b show the tangential stresses for the same Model.



**Fig. 3.** (a) Normal contact stresses for Model 1; (b) Shear contact stresses of Model 1.

Fig.4 presents the normal and shear contact stresses, between all the solids, for Model 2. In Fig.4.a, normal stresses between the prosthesis and the liner, between the soft tissues and the liner, as well as between the soft tissues and the patients' femur can be observed. Fig.4.b shows the shear stresses that occur between the same biological solids of the patient.



**Fig. 4.** (a) Normal contact stresses for Model 2; (b) Shear contact stresses of Model 2.

When compared, at the biological solids' interfaces, the normal and shear contact stress distribution for both Model 1 (Fig.3) and Model 2 (Fig.4) show to be similar. However, for Model 2 (Fig.4), the stress distribution in the soft tissues near the femur and the liner is more homogeneous than for Model 1 (Fig.3), and the influence of stress has a less superficial effect, extending to deeper layers.

For Model 3, the normal and shear contact stresses, between all the solids, are presented in Fig.5. As for previous Model 1 (Fig.3) and Model 2 (Fig.4), both images plot the contact stresses between the prosthesis and the liner, between the soft tissues and the liner, as well as between the soft tissues and the patients' femur. Fig.5.a presents the normal stresses for Model 3, whereas Fig.5.b show the shear stresses for the same Model.

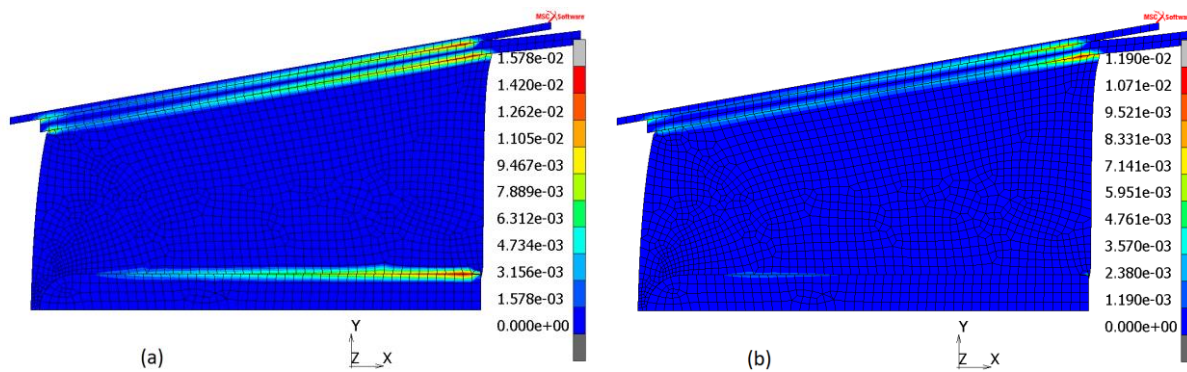


**Fig. 5.** (a) Normal contact stresses for Model 3; (b) Shear contact stresses of Model 3.

When observing Fig.5.a, on Model 3, the normal stresses are evenly distributed over the entire surface of the liner and much of the surface of the femur, than those of Model 1 (Fig.3.a) and Model 2 (Fig.4.a). When analyzing the shear stresses that take place between contacting bodies on Model 3 (Fig.5.b), these show to be significantly lower than those of Model 1 (Fig.3.b) and Model 2 (Fig.5.b). This 24% shear contact stress reduction is due to the effect of the prestress on the liner that affects the stress distribution inside the soft tissues. This positively affects the patient's comfort and health, as shear stresses are one of the main cause of injuries on this type of prosthetic devices [18].

## 2.4. Conclusions

The developed Finite Element Model reveals to be effective when assessing the effects of friction on the residual limb of a transfemoral amputee.

The results obtained allow evaluating the influence of the friction coefficient between the prosthesis, the liner and the soft tissues on the stress distribution of the whole biomechanical system.

The friction between the bodies of the biomechanical model has a great influence on the stress distribution that takes place in the soft tissues, thus enhancing or compromising the patient's comfort and health.

The FEA Model 3, with a prestress on the liner, improves the effect of friction on the biomechanical model. The uniform pressure in the contact between the liner and the soft tissues due to the prestress lowers the contact shear stresses, which is one of the main causes of injuries on patients using this type of prosthetic devices.

## References

- [1] Klute, Glenn K., Brian C. Glaister and Jocelyn S. Berge. "Prosthetic liners for lower limb amputees: A review of the literature." *Prosthetics and Orthotics International* 34(2) (2010) 146-153.
- [2] Sanders, Joan E., Brian S. Nicholson, Santosh G. Zachariah, Damon V. Cassisi, Ari Karchin and John R. Ferguson. "Testing of elastomeric liners used in limb prosthetics: Classification of 15 products by mechanical performance." *Journal of Rehabilitation Research & Development* 41(2) (2004) 175-186.
- [3] Steege, J. W. and D.S. Schnur. "Prediction of pressure in the below knee socket interface by finite element analysis." *ASME Symposium on Biomechanics of Normal and Pathological Gait* 1987.
- [4] Ivarsson, B. J., J. R. Crandall, G. W. Hall and W. D. Pilkey. "Biomechanics", in: F. Kreith (Ed.) *Handbook of Mechanical Engineering* (2004) CRC Press, Boca Raton.
- [5] Lee, Winson C. C., Ming Zhang, David A. Boone and Bill Contoyannis. "Finite element analysis to determine the effect of monolimb flexibility on structural strength and

interaction between residual limb and prosthetic socket.” *Journal of Rehabilitation Research & Development* 41(6A) (2004) 775-786.

[6] Boutwell, Erin, Rebecca Stine, Andrew Hansen, Kerice Tucker and Steven Gard. “Effect of prosthetic gel liner thickness on gait biomechanics and pressure distribution within the transtibial socket.” *Journal of Rehabilitation Research & Development* 49(2) (2012) 227-240.

[7] Jiaa, Xiaohong, Ming Zhanga and Winson C. C. Lee. “Load transfer mechanics between trans-tibial prosthetic socket and residual limb – dynamic effects.” *Journal of Biomechanics* 37 (2004) 1371-1377.

[8] Silver-Thorn, M. Barbara and Dudley S. Childress. “Parametric Analysis Using the Finite Element Method to Investigate Prosthetic Interface Stresses for Persons with Trans-tibial Amputation.” *Journal of Rehabilitation Research and Development* 33(3) (1996) 227-238.

[9] Sanders, Joan E. and Colin H. Daly. “Normal and shear stresses on a residual limb in a prosthetic socket during ambulation: Comparison of finite element results with experimental measurements.” *Journal of Rehabilitation Research & Development* 30(2) (1993) 191-204.

[10] Ramirez, Juan Fernando and Jaime Andrés Vélez. “Incidence of the boundary condition between bone and soft tissue in a finite element model of a transfemoral amputee.” *Prosthetics and Orthotics International* 36(4) (2012) 405-414.

[11] Lee, Winson C. C. and Ming Zhang. “Using computational simulation to aid in the prediction of socket fit: a preliminary study.” *Med Eng Phys* 29(8) (2007) 923-929.

[12] Cavaco, A., A. Ramalho, S. Pais and L. Durães. “Mechanical and structural characterization of tibial prosthetic interfaces before and after aging under simulated service conditions.” *Journal of the Mechanical Behavior of Biomedical Materials* 43C (2014) 78-90.

[13] Derler, S., G. U. Schrade and L.-C. Gerhardt. “Tribology of human skin and mechanical skin equivalents in contact with textiles.” *Wear* 263(7-12) (2007) 1112-1116.



- [14] Misra, S., K. B. Reed, B. W. Schafer, K. T. Ramesh and A. M. Okamura. "Mechanics of Flexible Needles Robotically Steered through Soft Tissue." *Int J Rob Res.* 29(13) (2010) 1640-1660.
- [15] Pacchierotti, C., L. Meli, F. Chinello, M. Malvezzi and D. Prattichizzo. "Cutaneous haptic feedback to ensure the stability of robotic teleoperation systems." *Int J Rob Res.* 34(14) (2015) 1773-1787.
- [16] Laursen, T. A. and J. C. Simo. "Algorithmic symmetrization of Coulomb frictional problems using augmented Lagrangians." *Computer Methods in Applied Mechanics and Engineering*, 108 (1993) 133-146.
- [17] Lin, Chih-Chieh, Chih-Han Chang, Chu-Lung Wu, Kao-Chi Chung and I-Chen Liao. "Effects of liner stiffness for trans-tibial prosthesis: a finite element contact model." *Med Eng Phys* 26(1) (2004) 1-9.
- [18] Sanders, Joan E., Colin H. Daly and Ernest M. Burgess. "Interface shear stresses during ambulation with a below-knee prosthetic limb." *Journal of Rehabilitation Research & Development* 29(4) (1992) 1-8.

### **3. 2<sup>rd</sup> Paper - Influence of materials and their constitutive laws on the stress fields produced in the residual limb of a transfemoral amputation**

#### **Abstract**

Current research uses a finite element analysis to characterize the effect of the materials mechanical and tribological properties on the interaction between the biological tissues of a transfemoral amputation and the combined prosthesis. Considering that both friction and mechanical properties influence the stress distribution between different interfaces, these were analyzed on the contacts of the prosthesis and the liner, the liner and the soft tissues and, finally, the soft tissues and the cortical bone. This is of significant importance, as it has been acknowledged that the shear stress distribution at these interfaces significantly impacts the patients' comfort. These shear stresses have also been reported as one of the leading causes of pressure ulcers in osteotomized patients. Finally, this research discusses the influence of the soft tissues and the liner constitutive law in the stress field generated at the biological tissues. For the liner, the results using a linear elastic model are compared with those using the Mooney-Rivlin hyperelastic model. The results using a linear elastic model are compared with the Neo-Hookean and Ogden models' results for the soft tissues.

Keywords: Finite Element Analysis, Interfacial stresses, Transfemoral Amputation, Constitutive law, Friction

### 3.1. Introduction

The friction coefficient between the various components of a prosthesis and the contacting biological tissues has a significant influence on the intensity of the shear stresses generated at the interfaces of the biological materials of lower limb osteotomized patients [1, 2]. Furthermore, the distribution of shear stresses at the interface between the liner and the soft tissues is referred to as one of the leading causes of pressure ulcers in patients with transfemoral amputation [3].

Even though it is widely recognized that the materials' constitutive laws have a significant influence on the stress fields generated at the residual limb (when interacting with the combined socket prosthesis), most simulations of these biomechanical systems using the finite element method (FEM) still use linear elastic models [4–7]. Thus, such linear elastic models are mostly suitable for simulating most rigid materials, e.g., cortical bone and most of the hard sockets prosthesis. However, this model is not suitable for more flexible materials when subjected to large deformations, namely the liners and the soft tissues [8–10].

In most simulations using FEM, the soft tissues are generally approached as homogeneous and isotropic materials. Nonetheless, the use of software that allows generating geometries with various components collected from medical images (e.g., Materialize) provide for the simulation of these materials in a more realistic way, thus separating the soft tissues into their main components – skin, fat, muscle, blood vessels, fascia – and allowing for considering the anisotropy of their properties [9].

The mechanical characterization of biomaterials that allows the definition of its constitutive law is widely available in the current literature [8, 10]. However, this characterization is limited when considering biological materials. This is mainly since these materials' characterization is strongly endogenous. In most simulations using the FEM of biomechanical systems, soft tissues are characterized by a linear elastic model. Nonetheless, this approach does not seem adequate when these biological materials are subject to large deformations. Thus, according to the literature, hyperelastic models are the most used for nonlinear soft tissue mechanical characterization [9, 11, 12]. The main hyperelastic models used in the simulation of soft tissues' constitutive law are the Mooney-Rivlin model (in their Mooney second and third-order variants) and the Neo-Hookean model, the Yeoh model and the Ogden model.

In this study, the stress field at the prosthesis interfaces (of a patient with transfemoral amputation) is assessed using FEM numerical simulation. The influence of the constitutive law applied in modelling the mechanical behavior of the liner material, and the soft tissues, are analyzed and discussed. Additionally, the friction coefficient between the prosthesis and the liner, the liner and the skin and between the soft tissues and the femur are also analyzed and discussed. The model previously presented by the authors in [1] is improved in terms of the geometry and the materials characterization. For the manufacturing of the prosthesis, propylene thermoplastic is compared with the use of an epoxy resin in which most of the molecular structure is of vegetable origin (SR GreenPoxy 56) produced by Sicomin. In most of the simulations presented, a composite material is used for prosthesis manufacturing in which the GreenPoxy resin is reinforced with natural jute fibers. This composite is modelled as a linear elastic material with anisotropic behavior.

## **3.2. Finite Element Model**

### **3.2.1. Geometry**

The two-dimensional finite element model previously presented by the authors in [1] has been improved in terms of geometry definition. Several points were collected from the femur and limb profiles presented in [13]. These points allowed for modelling the profiles of these organic components using cubic spline interpolation. The previous 2D axisymmetric formulation was maintained. An elastic foundation is used to support the patient's limb. To increase the damping effect, the liner's thickness was reinforced in the distal part of the stem [4, 7]. The connection between the socket and the pylon, considering its rigidity, is modelled through a REB2 type connection [14].

Three materials were considered to build the socket type prosthesis model: the thermoplastic previously used in [1], propylene, the SR GreenPoxy 56 resin produced by Sicomin and a composite in which the SR GreenPoxy 56 is reinforced with natural jute fibers. Considering the mechanical properties of these materials, the prosthesis's thickness was increased in the distal part of the stump, where the stresses in the prosthesis are higher.

The geometry, finite element mesh, and the model's various components are presented in Figure 1.

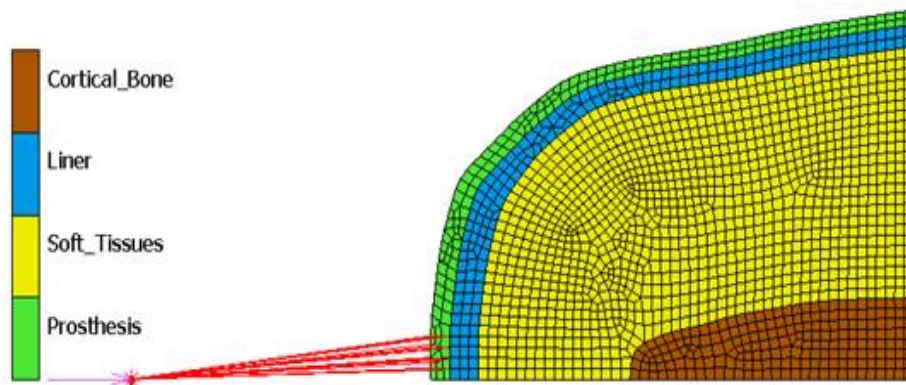


**Fig. 1.** Geometry, mesh and deformable bodies of the numerical model.

### 3.2.2. Mechanical Properties of the Materials – Constitutive laws

#### Biologic Materials

The femur is modelled as an isotropic, homogeneous, and linear elastic material. The cortical bone properties are considered along the longitudinal direction [15], with an elastic modulus,  $E = 11.5$  GPa, and Poisson's ratio,  $\nu = 0.31$ .

For the soft tissues, two different models were used: the Neo-Hookean model (presented in [12]) for the muscle, with  $C_{10} = 4.25$  kPa and the volumetric behavior obtained only with the first term of the series,  $D1 = 24.34$  MPa<sup>-1</sup>; the first order Ogden model (presented in [9]) for the muscle, with the ground state shear modulus  $\mu = 1,907$  kPa, strain hardening  $\alpha = 4.6$  and volumetric behavior obtained only with the first term of the series,  $D1 = 10.5$  MPa<sup>-1</sup>.

To compare the results using the hyperelastic model with those of the linear elastic model (after acquiring the stress field in the soft tissues), the properties of an equivalent elastic material were computed. The volume deformation energy was equivalent to that absorbed in both simulated hyperelastic models for the equivalent elastic material. In this process, the Poisson's ratio was fixed at  $\nu = 0.45$ , corresponding to an approximately incompressible situation. The equivalent elasticity coefficients' values were  $E_{\text{equNH}} = 0.0534$  MPa (Neo-Hookean model) and  $E_{\text{equO}} = 0.0196$  MPa (Ogden model).

## Liner

When modelling the liner, the experimental results presented in [10] were used. Four different liners were chosen from each presented stiffness classes, ordered from C1 to C4 by increasing stiffness value. For the more rigid class, C1, an elastomer was selected, the Fillauer Silicone liner, produced by Fillauer, Inc., Chattanooga, Tennessee; for the next class, C2 a polyurethane, TEC Pro 18, produced by TEC Interface Systems, Waite Park, Minnesota; for class C3 an elastomer, Icross Comfort, produced by Ossur USA, Inc., Columbia, Maryland was chosen; for the most flexible class, a gel was selected, the Super Stretch, made by ALPS, St. Petersburg, Florida. The selection of these materials was based not only on their stiffness value but also considering the corresponding friction coefficient between that material and human skin. These friction coefficient values were also ordered in different classes (F1 to F4), from the highest to the lowest.

The experimental results were approximated fitting time-independent data by differential evolution, using the finite element software MSC Marc 2018 [14]. In the approximation, the results available in [10], corresponding to the tensile, compression and pure shear tests, were considered. Among the hyperelastic models (H M) available, the best approximations for the selected liners corresponded to the second-order Mooney-Rivlin (M-R) and Yeoh models, shown in Table 1. The friction coefficient (FC) shown in the table refers to the friction between the liner and the skin. Also is defined a stiffness class (S C) and a friction class (FrC) for the liners.

On an initial exploratory study, the constitutive equations presented in [16] were used on the liner, for a Neo-Hookean model, with  $C_{10} = 23$  kPa and the bulk modulus of 230 MPa.

**Table 1.** Hyperelastic models used for various liners.

Liner	S C	FC/FrC	H M	Parameters and coefficients
Fillauer Silicone	C1	$\mu_f = 0.6$ F3	Yeoh	$C_{10} = 0.923252 \text{ kPa}$ $C_{20} = 2.18386 \times 10^{-5} \text{ kPa}$ $C_{30} = 44.9592 \text{ kPa}$
TEC Pro 18	C2	$\mu_f = 1$ F1	M-R	$C_{10} = 1.5152 \times 10^{-6} \text{ kPa}$ $C_{01} = 41.365 \text{ kPa}$
TEC Pro 18 L	C2	$\mu_f = 0.65$ F1		$C_{11} = 9.4846 \times 10^{-7} \text{ kPa}$ Bulk Modulus = 413650 kPa
Iceross Comfort	C3	$\mu_f = 0.4$ F4	M-R	$C_{10} = 2.19397 \times 10^{-5} \text{ kPa}$ $C_{01} = 20.775 \text{ kPa}$ $C_{11} = 1.28457 \times 10^{-5} \text{ kPa}$ Bulk Modulus = 207750 kPa
Super Stretch Gel	C4	$\mu_f = 0.65$ F2	M-R	$C_{10} = 1.23146 \times 10^{-4} \text{ kPa}$ $C_{01} = 10.5949 \text{ kPa}$ $C_{11} = 2.89243 \times 10^{-9} \text{ kPa}$ Bulk Modulus = 105905 kPa

## Prosthesis

For the socket type prosthesis composition, three different materials were analyzed: propylene thermoplastic; an epoxy resin in which most of the molecular structure is of vegetable origin (SR GreenPoxy 56 produced by Sicomin) and a composite material in which an SR GreenPoxy 56 resin matrix is reinforced with jute fibers.

The propylene thermoplastic is modelled as homogeneous, isotropic, and linear elastic, based on the mechanical properties presented in [17], with an elastic modulus (E) of 1000 MPa and the Poisson's ratio  $\nu = 0.30$ .

SR GreenPoxy 56 resin is also modelled as homogeneous, isotropic, and linear elastic, based on the properties presented in [18] with an elastic modulus (E) of 3000 MPa, a Poisson's ratio  $\nu = 0.39$  and the specific mass  $\rho = 1180 \text{ kg/m}^3$ .

The jute fiber is modeled as homogeneous, 2D orthotropic and linear elastic, based on the properties presented in [19], with elastic modulus  $E_1 = 23949 \text{ MPa}$  and  $E_2 = 978 \text{ MPa}$ , the Poisson's ratio  $\nu_{12} = 0.374$  and  $\nu_{21} = 0.014$ , the shear modulus  $G_{12} = 411 \text{ MPa}$  and the specific mass  $\rho = 1440 \text{ kg/m}^3$ .

Based on the Halpin-Tsai model for discontinuous fibers, the composite material's elastic properties (SR GreenPoxy 56 resin matrix reinforced with jute fibers) were computed in the

MSC Patran 2019 software [20] considering a 60/40% for the resin/fiber volume ratio. A 10 to 1 ratio was considered for the fibers' length vs diameter.

The fiber of this composite was later dispersed using a 2D short fiber model implemented in the MSC Patran 2019 software [20], with angles  $\alpha = 0^\circ$  and  $\phi = 45^\circ$ , a standard deviation of  $10^\circ$  through a random process, with zero correlation, using 1000 Monte Carlo iterations. The elasticity matrix of this composite is represented in equation (1). The composite was oriented so that axis 1 has, at each point, the direction of the tangent to the prosthesis profile shown in Figure 1. Axis 2 has the direction of thickness and axis 3, the radial direction [14].

$$[C_{ij}] = \begin{bmatrix} 1.30 \times 10^5 & 1.39 \times 10^5 & 1.26 \times 10^5 & 3.07 \times 10^1 \\ 1.39 \times 10^5 & 1.59 \times 10^5 & 1.40 \times 10^5 & 5.04 \times 10^1 \\ 1.26 \times 10^5 & 1.40 \times 10^5 & 1.31 \times 10^5 & 5.32 \times 10^1 \\ 3.07 \times 10^1 & 5.04 \times 10^1 & 5.32 \times 10^1 & 2.10 \times 10^3 \end{bmatrix} (MPa) \quad (1)$$

### 3.2.3. Friction Model

In the contact between the system's various components, a Coulomb's bilinear friction model was used, with an average friction coefficient between the cortical bone and the soft tissues of  $\mu = 0.3$  [21]. A friction coefficient of  $\mu = 0.5$  was considered for the contact between the socket type prosthesis made of SR GreenPoxy 56 and the liner [22]. When the prosthesis is made of propylene, a friction coefficient of  $\mu = 0.6$  between the prosthesis and the liner was kept [1]. On the contact between the liner and the soft tissues, the friction coefficient varies, considering each of the liners, the values shown in Table 1. In the numerical model, the contact between deformable bodies is modelled by the finite sliding segment-to-segment contact algorithm. The separation criteria are based upon stresses (Lagrange multipliers): separation threshold is treated as residual stress of negligible magnitude ( $0.9 \times 10^{-06}$  MPa).

### 3.2.4. Finite element analysis

Given the symmetry of the model, a 2D axisymmetric analysis was performed. The simulations with this model were made using the implicit module of MSC Marc Mentat 2018 [14]. A multifrontal direct sparse solver, the Paradiso solver, is used with a Newton-Raphson



iterative procedure. For convergence testing, a relative force tolerance of 10% is used. An adaptive multicriteria stepping procedure is used for load increment – was used the initial time step (load increment) of  $1e-06$ . The numerical constrictions associated with the implicit method were overcome using a mesh adaptivity algorithm, the advancing front quadrilateral. An automatic algorithm was used for meshing, and linear quadrilateral axisymmetric solid elements with four nodes (Quad 10) were used. The initial mesh dimensions of the elements were 3 mm. This value was established in a previous iterative process and is considered an objective in the adaptive mesh algorithm. In this process, the mesh size may be reduced to a quarter of its initial value, depending on the strain change and the distortion that may take place in each element [1]. In the structural analysis, large strain nonlinear procedures were used. Based on an automatic algorithm depending on the constitutive law, the Multiplicative Updated Lagrange procedure is preferential for hyperelastic materials.

### **3.2.5. Loading**

The prosthesis is considered to support the patient's total weight (70 kgf) during the static stance. Loading is imposed in quasi-static conditions [1], as illustrated in Figure 1.

## **3.3. Numerical Simulations Planning**

A preliminary simulation was carried out to compare the effect of the constitutive law on the stress field produced at the prosthesis's different components. Model 3, presented in [1], was simulated varying only the liner and soft tissues' constitutive law. The geometry and all the remaining parameters were maintained. For the soft tissues, the Neo-Hookean model presented in [12] was used, whereas, for the liner, a Neo-Hookean behavior with the parameters of in [16] was considered. The constitutive law used for soft tissues has a much less rigid behavior than that of the previously used linear elastic model. In addition, the volumetric compressibility is also much lower in the constitutive law. Thus, much higher deformation and normal (80%) and shear stresses (40%) were observed for the same loading. However, it appears that this variation is much smaller in terms of biological tissues. The resulting normal and shear stress fields (MPa) are shown in Figure 2.

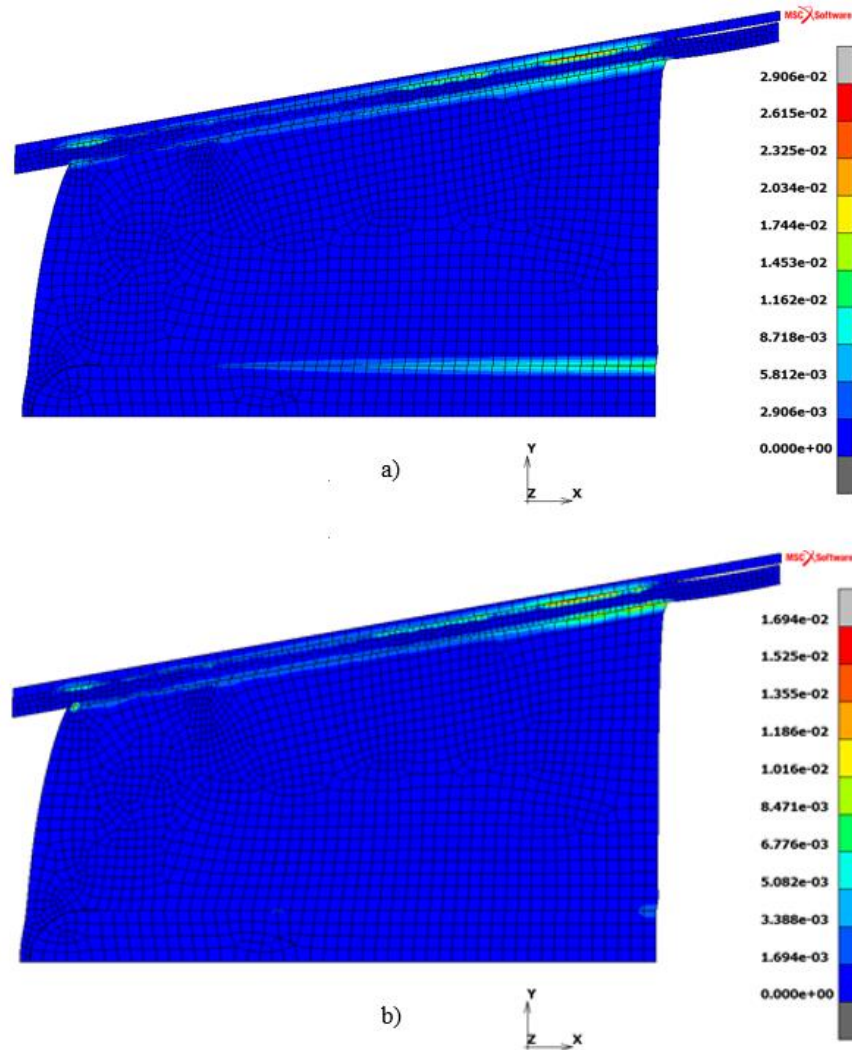


Fig. 2. Preliminary study: a) Normal contact stresses. b) Shear contact stresses.

This pilot simulation allowed outlining a set of simulations to be carried out with the geometry presented in Figure 1. In addition to the influence of the constitutive law, the simulations focused on the effect of friction. When comparing models, it was essential to consider the stiffness and the volumetric compressiveness. Considering that the study presented in [10] provides the required data for the range of liners available on the market, it was decided to use that data for the parameters of current work, according to Table 1.

The first simulations led to the rupture of the propylene-based prosthesis. Thus, considering the more sustainable nature of the bio epoxy and the improved mechanical properties, the GreenPoxy 56 resin was selected for current research with and without the reinforcement of

natural jute fibers. Thus, to study the influence of friction and the constitutive law of materials in the stress fields produced in the biological tissues of a patient with a transfemoral amputation, the simulations presented in Table 2 were carried out.

**Table 2.** Characterization of the performed simulations.

Simulation	Soft tissues constitutive law	Prosthesis Material	Liner
A1	Neo-Hookean	Propylene	TEC Pro 18
A2	Neo-Hookean	GreenPoxy 56	TEC Pro 18
A3	Neo-Hookean	GreenPoxy 56	TEC Pro 18L
A4	Neo-Hookean	Composite	Fillauer Silicone
A5	Neo-Hookean	Composite	TEC Pro 18
A6	Neo-Hookean	Composite	Iceross Comfort
A7	Neo-Hookean	Composite	Super Stretch Gel
A8	Ogden	Composite	TEC Pro 18
A9	Elastic equivalent Neo-Hookean	Composite	ElasEqTEC Pro 18
A10	Elastic equivalent Ogden	Composite	ElasEqTEC Pro 18
A11	Neo-Hookean	Composite	TEC Pro 18L
A12	Elastic equivalent Neo-Hookean	Composite	TEC Pro 18L

### 3.4. Results and Discussion

The biological tissues use most of the volume of the numerical model. This verifies that the constitutive law used in its modelling has a significant effect on the results.

Figure 3 shows the stress distribution (MPa) in the biological tissues of the A5 model, which is considered representative of the generic distribution that occurred in the various simulations in which the soft tissues were characterized with the Neo-Hookean model.

On what concerns the normal stresses, it can be observed that at the biological tissues level, the highest stresses take place at the interface between the femur and the soft tissues (on the distal part of the femur at the osteotomized section).

On what refers to the shear stresses, it can also be observed that the higher stresses occur either at the interface between the liner and the soft tissues (in the proximal part of the liner), or close to the femur (in the region adjacent to that in which the maximum normal tensions take place). This distribution varies significantly in intensity for the various simulations.

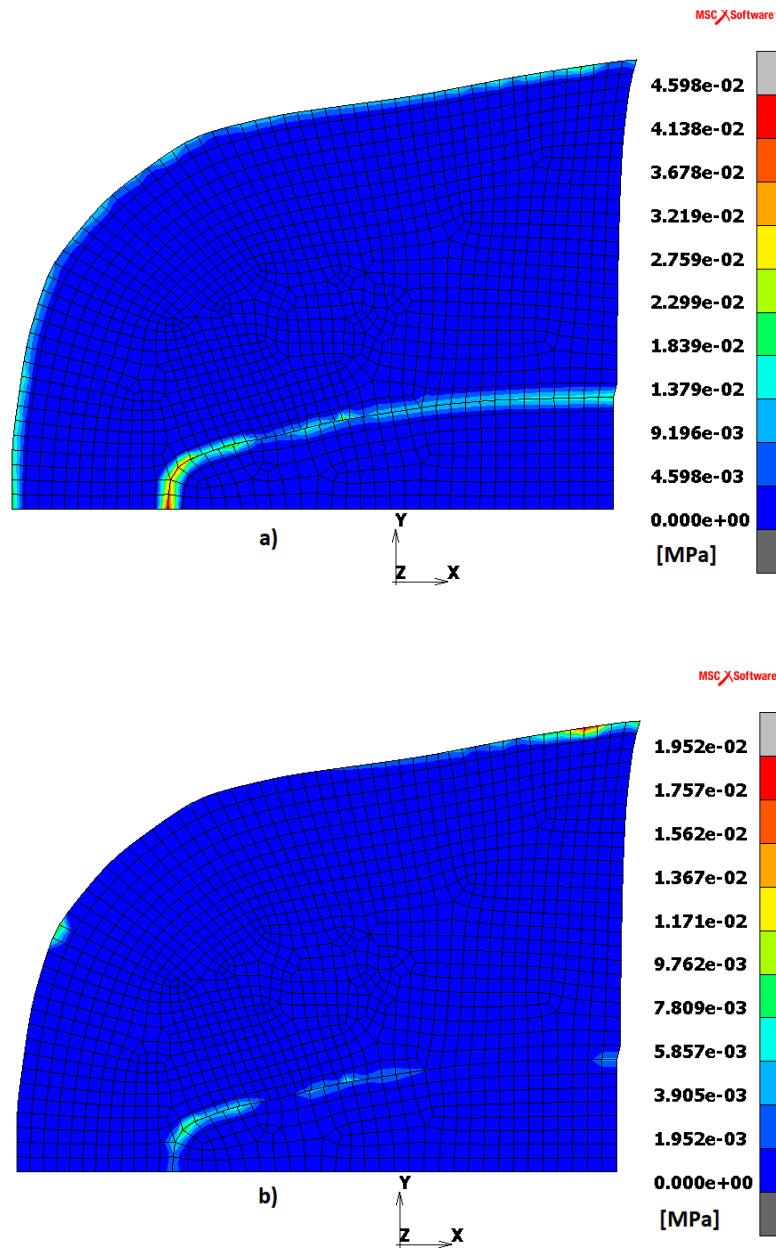


**Fig. 3.** Contact stresses at biological tissues, A5 model: a) Normal stresses; b) Shear stresses.

Figure 4 shows the stress distribution (MPa) in the biological tissues of the A8 simulation, which is considered representative of the generic distribution that occurred in the various models in which the soft tissues were characterized with the Ogden model.

This figure shows that at the biological tissues' level, the maximum normal stress occurs at the interface between the liner and the soft tissues (on the distal part of the stump).

On what concerns the shear stresses, the highest stresses occur at the interface between the liner and the soft tissues (in the proximal part of the liner). This distribution varies significantly in intensity for the various simulations.

Finally, it can be observed that in the area where the normal contact stresses are highest, the shear stresses are neglectable, as there is no slip.

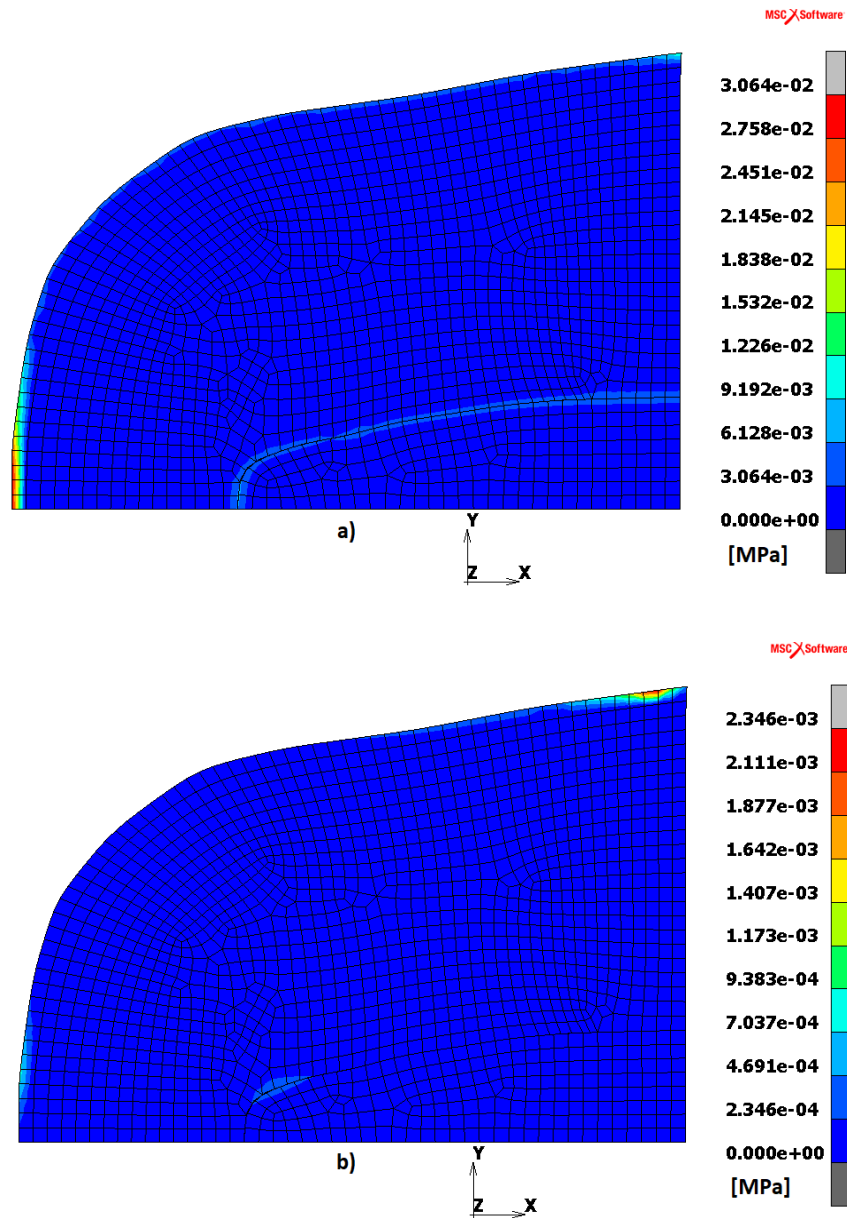


Fig. 4. Contact stresses at biological tissues, A8 model: a) Normal stresses; b) Shear stresses.

The highest values of normal and shear contact stresses that take place at the interfaces of the various components of the prosthesis ( $\sigma$  and  $\tau$ ) and the biological tissues ( $\sigma_B$  and  $\tau_B$ ) are shown in Table 3, as well as the equivalent Von Mises ( $\sigma_{VM}$ ) stress that occurs in the prosthesis (hard socket).

**Table 3.** Summary of the simulation results.

Simulation	$\sigma$ [kPa]	$\tau$ [kPa]	$\sigma_B$ [kPa]	$\tau_B$ [kPa]	$\sigma_{VM}$ [MPa]
A1	68.24	17.94	68.24	17.94	63.84
A2	56.27	14.43	56.27	14.43	55.45
A3	44.86	3.09	14.53	3.09	54.81
A4	46.45	13.67	46.45	13.37	14.78
A5	67.84	19.52	45.98	19.52	13.77
A6	51.57	9.40	51.57	7.38	14.87
A7	68.57	19.50	36.29	10.37	13.59
A8	21.86	4.04	30.64	2.35	10.16
A9	60.47	18.88	60.47	17.93	14.99
A10	33.17	5.58	11.35	5.58	13.10
A11	50.06	14.52	50.06	14.52	14.34
A12	45.12	18.11	45.12	16.52	14.98

In the initial simulations (A1-A3), it can be observed that the stiffness increase of the prosthesis material leads to a slight decrease in contact stresses, as well as in the equivalent Von Mises stress that occurs in the prosthesis. The significant material stiffness increase does not lead to a very substantial change in the maximum stresses due to the influence of the prosthesis's small thickness on the overall stiffness of the structure. In the case of A3 simulation, reducing the friction coefficient between the liner and the soft tissues leads to a significant decrease in the normal and shear stresses at the interfaces. It is observed that the stresses that take place in the prosthesis exceed the resistance stresses of the materials [16, 20]. The use of a short fiber composite has the particularity of increasing the stiffness of the material and of the whole prosthesis. According to Equation (1), this occurs by decreasing the membrane effect with the significant increase in stiffness in the direction of thickness, resulting from the short fibers' orientation. The substantial increase in normal stresses observed along direction 2 (alongside the thickness) leads to a significant decrease in the equivalent Von Mises stress that occurs in the prosthesis, also leading to some changes in the distribution in the contact stress field (A2 and A5).

The decrease in friction between the liner and the soft tissues seems to lower, with some consistency, the shear stresses. When comparing the evolution of these shear stresses in simulations A5, A7, A4 and A6, the inconsistency between the results of A7 and A4 can be explained due to the Yoeh model used in A4. This effect is more evident when comparing the results of simulations A5 and A11, in which the only change observed is for the friction coefficient between the liner and the soft tissues, which changes from 1 to 0.65. The friction decrease leads to an increase in the normal contact stress and a reduction in the shear contact stress. These results, focusing on the friction coefficient variation, are consistent with those presented in [23].

The effect of the constitutive law used in the characterization of soft tissues, and the liner, can be observed when comparing the use of hyperelastic models in simulations A11, A5 and A8 with the equivalent linear elastic simulations A12, A9 and A10. Thus, at the biological tissues level, one can observe a significant decrease in the normal contact stresses and a slight increase in the shear contact stresses.

### **3.5. Conclusions**

The developed Finite Element Model reveals to be effective when assessing the effects of friction on the residual limb of a transfemoral amputee.

The results obtained allow evaluating the influence of the friction coefficient between the prosthesis, the liner, and the soft tissues on the whole biomechanical system's stress distribution.

The stiffness and the anisotropy of the prosthesis material effectively influence the contact stresses field developed in the residual limb of a transfemoral amputation.

The friction between the liner and the soft tissues has an effective influence on the field of contact stresses developed in the residual limb of a transfemoral amputation.

The constitutive laws used to characterize liner and soft-tissue materials effectively influences the fields of contact stresses developed in the residual limb of a transfemoral amputation.

## **Acknowledgements**

This research is sponsored by national funds through FCT – Fundação para a Ciência e a Tecnologia, under the project UIDB/00285/2020.

## **References**

- [1] A. Ramalho, M. Ferraz, M. Gaspar, and C. Capela: Development of a preliminary finite element model to assess the effects of friction on the residual limb of a transfemoral amputee. *Mater. Today Proc.*, 33, 1859–1863 (2020).
- [2] J. F. Ramírez and J. A. Vélez: Incidence of the boundary condition between bone and soft tissue in a finite element model of a transfemoral amputee. *Prosthet. Orthot. Int.* 36(4), 405–414 (2012).
- [3] J. E. Sanders, C. H. Daly, and E. M. Burgess: Interface shear stresses during ambulation with a below-knee prosthetic limb. *J. Rehabil. Res. Dev.* 29(4), 1–8 (1992).
- [4] M. Zhang, A. F. T. Mak, and V. C. Roberts: Finite element modelling of a residual lower-limb in a prosthetic socket: A survey of the development in the first decade. *Med. Eng. Phys.* 20(5), 360–373 (1998).
- [5] S. Misra, K. T. Ramesh, and A. M. Okamura: Modeling of Tool-Tissue Interactions for Computer-Based Surgical Simulation: A Literature Review. *Presence (Camb)*. 17(5), p. 463 (2008).
- [6] J. Mackerle: Finite element modeling and simulations in orthopedics: A bibliography 1998-2005. *Comput. Methods Biomech. Biomed. Engin.* 9(3), 149–199 (2006).
- [7] H. Gholizadeh, N. A. Abu Osman, A. Eshraghi, S. Ali, and N. A. Razak: Transtibial prosthesis suspension systems: Systematic review of literature. *Clin. Biomech.* 29(1), 87–97 (2014).
- [8] J. C. Cagle, B. J. Hafner, N. Taflin, and J. E. Sanders: Characterization of prosthetic liner products for people with transtibial amputation. *J. Prosthetics Orthot.* 30(4), 187–199 (2018).



- [9] S. Kallin, A. Rashid, K. Salomonsson, and P. Hansbo: Comparison of mechanical conditions in a lower leg model with 5 or 6 tissue types while exposed to prosthetic sockets applying finite element analysis. *ArXiv*, 1–27 (2019).
- [10] J. E. Sanders, B. S. Nicholson, S. G. Zachariah, D. V. Cassisi, A. Karchin, and J. R. Fergason: Testing of elastomeric liners used in limb prosthetics: Classification of 15 products by mechanical performance. *J. Rehabil. Res. Dev.* 41(2), 175–185 (2004).
- [11] S. Misra, K. B. Reed, B. W. Schafer, K. T. Ramesh, and A. M. Okamura: Mechanics of flexible needles robotically steered through soft tissue. *Int. J. Rob. Res.* 29(13), 1640–1660 (2010).
- [12] S. Portnoy, I. Siev-Ner, N. Shabshin, and A. Gefen: Effects of sitting postures on risks for deep tissue injury in the residuum of a transtibial prosthetic-user: A biomechanical case study. *Comput. Methods Biomech. Biomed. Engin.* 14(11), 1009–1019 (2011).
- [13] J. S. Hoellwarth, M. Al Muderis, and S. R. Rozbruch: Cementing Osseointegration Im-plants Results in Loosening: Case Report and Review of Literature. *Cureus* 12(2), (2020).
- [14] MSC Software Corporation: *Marc 2018.0 Theory and User Information*. Newport Beach, CA 92660 USA (2018).
- [15] B. J. Ivarsson, J. R. Crandall, G. W. Hall, and W. D. Pilkey: *Biomechanics*. In: F. Kreith (ed.) *Handbook of Mechanical Engineering*, 2nd edn. CRC Press, Boca Raton (2004).
- [16] S. Łagan and A. Liber-Kneć: The determination of mechanical properties of prosthetic liners through experimental and constitutive modelling approaches. *Czas. Tech.* 3, 197–209 (2018).
- [17] D. S. Silver-Thorn, M. B. Childress: Parametric analysis using the finite element method to investigate prosthetic interface stresses for persons with trans-tibial amputation. *J Rehabil Res Dev.* 33(3), 227–238 (1996).
- [18] A. Perrier: *Influence du Vieillissement Hydrique Sur le Comportement Mécanique de l'Interface Fil/Matrice Dans des Composites Chanvre/Époxy*. L'École Nationale Supérieure de Mécanique et D'Aérotechnique (2016).

- [19] V. Suthenthiraveerappa and V. Gopalan: Elastic constants of tapered laminated woven jute/epoxy and woven aloe/epoxy composites under the influence of porosity. *J. Reinf. Plast. Compos.* 36(19), 1453–1469 (2017).
- [20] MSC.Software Corporation: Materials Application - Theory - Composite Materials, in Patran 2008 r1, Reference Manual Part 4: Functional Assignments, 88–160, Santa Ana, CA 92707 USA (2008).
- [21] S. Shacham, D. Castel, and A. Gefen: Measurements of the static friction coefficient between bone and muscle tissues. *J. Biomech. Eng.* 132(8), 1–4 (2010).
- [22] B. N. J. Persson: Silicone Rubber Adhesion and Sliding Friction. *Tribol. Lett.* 62(2), 1–5 (2016).
- [23] M. Zhang, M. Lord, A. R. Turner-Smith, and V. C. Roberts: Development of a non-linear finite element modelling of the below-knee prosthetic socket interface. *Med. Eng. Phys.* 17(8), 559–566 (1995).

## **4. 3<sup>nd</sup> Paper – Efeito do atrito no membro residual numa amputação transfemoral – Influência do modelo constitutivo dos materiais**

### **Resumo**

Neste artigo é avaliado o efeito das propriedades mecânicas e tribológicas dos materiais na interação entre os diversos componentes da prótese numa amputação transfemoral, através de uma análise por elementos finitos. O modelo numérico é desenvolvido sobre o software MSC.marc. O atrito vai influenciar a distribuição de tensões entre as diversas interfaces – prótese/liner, liner/tecidos moles e tecidos moles/osso cortical. A distribuição das tensões de corte junto às interfaces, influencia o conforto do paciente, sendo uma das principais causas da geração de úlceras de pressão nos pacientes amputados que usam este tipo de próteses.

É analisada a influência dos modelos constitutivos utilizados na modelação dos tecidos moles e do liner, na distribuição de tensão. Em concreto são comparados os resultados obtidos com a utilização de um modelo linear elástico com os obtidos com modelos hiperelásticos.

Palavras-chave: Método dos elementos finitos; Tensões de contacto; Amputação transfemoral; Modelos constitutivos; Atrito.

## **4.1. Introdução**

A distribuição das tensões de corte na interface entre o liner e os tecidos moles é uma das principais causas do desenvolvimento de úlceras de pressão nos pacientes com amputação transfemoral, Sanders et al. (1992).

O coeficiente de atrito tem grande influência na intensidade das tensões de corte que se desenvolvem ao nível das interfaces das próteses nos pacientes amputados nos membros inferiores, Ramalho et al. (2020).

No presente artigo é avaliado o campo de tensões nas interfaces de uma prótese de um paciente com amputação transfemoral, através de simulação numérica por elementos finitos sendo analisada a influência dos modelos reológicos utilizados na modelação do comportamento mecânico do material do liner e dos tecidos moles. O modelo anteriormente apresentado pelos autores em Ramalho et al. (2020), é melhorado ao nível da geometria e da caracterização dos materiais. Na definição dos modelos hiperelásticos, são utilizados os parâmetros e caracterização mecânica apresentados em Kallin et al. (2019) e Sanders et al. (2004).

## **4.2. Descrição**

O modelo bidimensional de elementos finitos anteriormente apresentado pelos autores em Ramalho et al. (2020), foi melhorado ao nível da definição da geometria. Foram obtidos diversos pontos nos perfis do fémur e do coto apresentados em Hoellwaarth (2020). Estes pontos permitiram a obtenção dos perfis através de interpolação por splines cúbicas. Manteve-se a formulação 2D axi-simétrica anteriormente utilizada. No suporte do coto é utilizado uma fundação elástica.

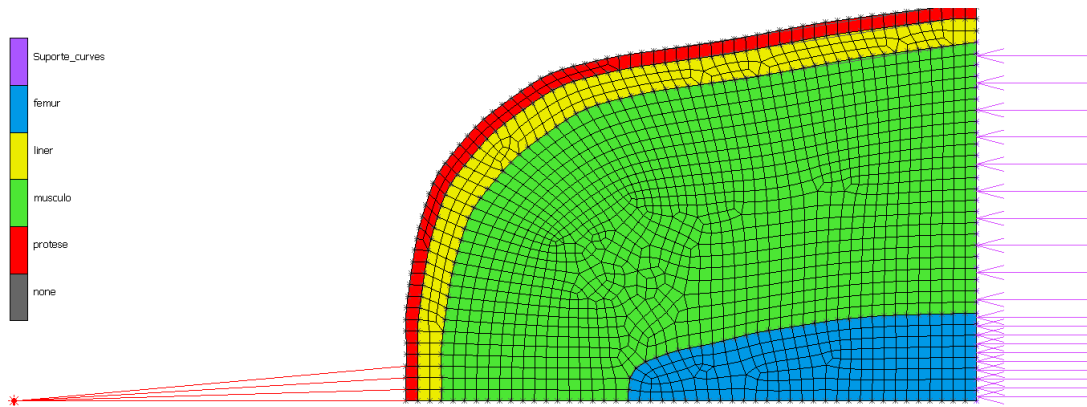


**Fig. 1.** – Modelo numérico

O modelo de escorregamento foi adaptado para permitir a caracterização hiperelástica do liner e dos tecidos moles. Para suportar as grandes deformações, manteve-se o algoritmo de refinamento automático da malha, baseado na deformação ao nível dos elementos.

### 4.3. Conclusões

O modelo numérico desenvolvido produz resultados coerentes com os apresentados por outros autores. A rigidez e a anisotropia do material da prótese influenciam o campo de tensões de contato desenvolvido no membro residual de uma amputação transfemoral. Os modelos constitutivos usados para caracterizar os materiais do liner e dos tecidos moles influenciam os campos de tensões de contato desenvolvidos no membro residual.

### **References**

- Hoellwarth, J.S., Al Muderis, M., Rozbruch, R.S. (2020). Cementing Osseointegration Implants Results in Loosening: Case Report and Review of Literature. *Cureus* 12(2): e7066. DOI10.7759/cureus.7066.
- Kallin, S., Rashid, A., Salomonsson, K. and Hansbo, P..Comparison of mechanical conditions in a lower leg model with 5 or 6 tissue types while exposed to prosthetic sockets applying finite element analysis. *ArXiv*, pp. 1–27, 2019.

Ramalho, A., Ferraz, M., Gaspar, M., Capela, C. (2020). Development of a preliminary finite element model to assess the effects of friction on the residual limb of a transfemoral amputee. *Mater. Today Proc.*, vol. 33, pp. 1859–1863, doi: 10.1016/j.matpr.2020.05.199.

Sanders, J.E., Daly, C.H., Burgess, E.M. (1992). Interface shear stresses during ambulation with a below-knee prosthetic limb, *Journal of Rehabilitation Research & Development*, 29(4): 1-8.

Sanders, J.E., Nicholson, B.S., Zachariah, S.G., Cassisi, D.V., Karchin, A., Ferguson, J.R. (2004). Testing of elastomeric liners used in limb prosthetics: Classification of 15 products by mechanical performance, *Journal of Rehabilitation Research & Development*, Vol. 41, No. 2, 175-186.

## 5. **4<sup>th</sup> Paper - Recycled reinforced PLA as ecodesign solution for customized prostheses**

### **Abstract**

Additive manufacturing is a key technology for the digital production of customized prostheses and orthoses. Considering that such assistive devices can be designed to meet specific biomechanical needs based on the actual contours of the patients' limbs, the ability of those having physical disabilities being able to produce their custom prostheses and orthoses at home would be groundbreaking, by current standards. To such an end, this research aims at selecting sustainable biopolymers that can be used as filaments to produce customized prosthetic sockets using low-cost additive manufacturing technology. Special focus was put into characterizing the use of recycled PLA reinforced with short carbon fibers as filaments for additive manufacturing. Numerical simulation results showed the potential of this sustainable material combination as an ecodesign solution for customized prostheses and orthoses. Such a solution should allow for patients being able to successfully produce and assemble their own customized assistive devices using fused deposition modelling.

Keywords: Additive Manufacturing, Customization, Biomechanics, Ecodesign, Sustainability.

## **5.1. Introduction**

Additive manufacturing (AM) has been referred as an effective alternative to traditional fabrication processes to manufacture customized prosthesis and orthosis, as it is not as material-wasting, time-consuming or as labor-intensive, when compared with conventional manufacturing [1]. These direct digital technologies are advanced manufacturing processes which allow for mass customization to develop and produce dedicated products [2] which may be adapted to their users' requirements.

Considering the advantages of designing prosthesis and orthosis to meet specific biomechanical needs based on the actual contours of the patients' limbs, current research focuses on the ability of those having physical disabilities being able to produce specific parts of their custom prostheses and orthoses at their homes using conventional low-cost AM devices. To improve the sustainability of such custom-made parts, the selection of dedicated eco-materials will be discussed to allow for their use in these AM processes.

### **5.1.1. Customization with Additive Manufacturing**

When compared with traditional manufacturing processes, AM presents several distinctive features [3], such as the ability of freeform manufacturing and the possibility to combine into a single component a whole assembly of parts. This latter feature is usually required by the need of breaking down a given product into separate parts to comply with the limits of conventional manufacturing. Both these AM characteristics allow for dedicated product customization with lower overall manufacturing costs [4] and with special focus on adapting the product performance to its user's specific needs.

AM customization does not rely solely on the final manufactured parts and/or product's features but is also referred to the ability to produced products and parts based on a wide range of material types and nature [5, 6]. These range from additive manufactured food products [7] to high performance aeronautic [8] and aerospace parts [9], with ever increasing new feedstock materials for AM [10].

When concerned to the AM of polymer-based products, the lower mechanical properties of this type of materials for structural applications usually require for alternative solutions to



comply with the strength requisites required for their end-use. Thus, the recent ability to produce polymer-based composites by AM [7, 11, 12] allow for an increased range of applications, thus broadening the structural use of polymer-based components and parts.

One particularly promising field of use for AM is the possibility to design and produce dedicated prosthesis and devices adapted to their users' needs [13, 14]. To such an end, AM has been reported as particularly beneficial in dental applications [15], in customized airway prosthesis [16], in bio-inspired heart valves [17], in craniofacial soft tissue prostheses [18], in customized tracheal stents [19], among many other successful applications, in which AM allows to design and manufacture custom prostheses and orthoses to their final users' requirements.

### **5.1.2. Additive Manufacturing Environmental Sustainability through Recycling**

The current effort to promote circular economy solutions amongst manufacturing processes allows highlighting the environmental benefits of AM [20, 21]. When compared to traditional manufacturing, AM is usually referred as being an environmentally sustainable way to produce tangible goods [22] as it allows for reduced material waste, lower energy use, and lesser emissions than those of conventional processes [23].

Considering the whole life cycle of AM products, the reuse of both waste materials and end-of-life AM parts through recycling is also an environmentally sustainable solution as it contributes to lower the environmental impacts of these manufacturing processes. Metal-based AM parts can be recycled for a wide range of engineering alloys [24], whereas the polymer-based AM parts can also be recycled, particularly if they are of a thermoplastic nature [25]. Cruz et al. [26] present an extensive literature review on the latter subject.

The use of natural fibers as reinforcement in AM engineering materials may also be perceived as an environmentally sustainable solution to incorporate biomaterials into AM composites to improve their mechanical, thermal, chemical, surface, and morphological properties [27]. However, as these AM composites are not mono-materials, increased challenges must be overcome to allow for their successful recyclability [28, 29].

## **5.2. Materials and Methods**

Current research focuses on the use of recycled PLA biopolymers with, and without carbon fiber reinforcement. To discuss the usability of these eco-materials in custom prosthesis design and manufacturing, a brief discussion will be carried-out about the materials and methods used in this study.

### **5.2.1. Recycled Reinforced PLA for Additive Manufacturing**

Due to its sustainable nature, minimal warping and ease of use, Polylactic Acid (PLA) is currently one of the highest biopolymers produced at a global scale [30]. The PLA filaments are also amongst the most popular materials used in open-source desktop 3D-printing [31] mainly due to its renewable resource nature. The increased adoption of virgin and recycled PLA in AM led to corresponding research efforts to characterize optimal process parameters, performance, and waste reuse [32–35].

The potential of PLA reinforced composite materials has been discussed and tested by different researchers to infer about its usability in many engineering fields, using mainly long natural and non-natural fibers [30, 36, 37]. In current research, PLA reinforced with carbon fibers was selected since these fibers are not significantly affected by the thermal cycles of the recycling process [38]. After shredding, the original end-of-life PLA parts and waste reinforced with long carbon fibers result in a homogeneous mix of short carbon reinforced particles with no preferential fiber alignment. The shredded particles will be used to create new filaments of rPLA with different percentages of carbon-fiber reinforcements. The mechanical properties of these rPLA-based eco-materials are based on the work carried-out by Farah et al. [39], Hu & Karki [40] and De Groot et al. [41].

### **5.2.2. Numerical Model**

With the numerical simulation, it is intended to characterize the magnitude of stresses that occur at the socket-type prosthesis level to aid inferring about the mechanical properties of different sustainable materials to be used in such type of assistive devices.

The numerical model presented in Fig. 1 was used to carry out different simulations based on the 2D axisymmetric approximation of the patient's residual limb contours and the prosthesis itself. This model, also used by the authors in previous research [42, 43], was adapted to support and discuss the results of current research. It consists of the patient's residual limb femur and the evolving soft tissues, as well as the dedicated prosthesis and liner used to better accommodate the socket-type device.

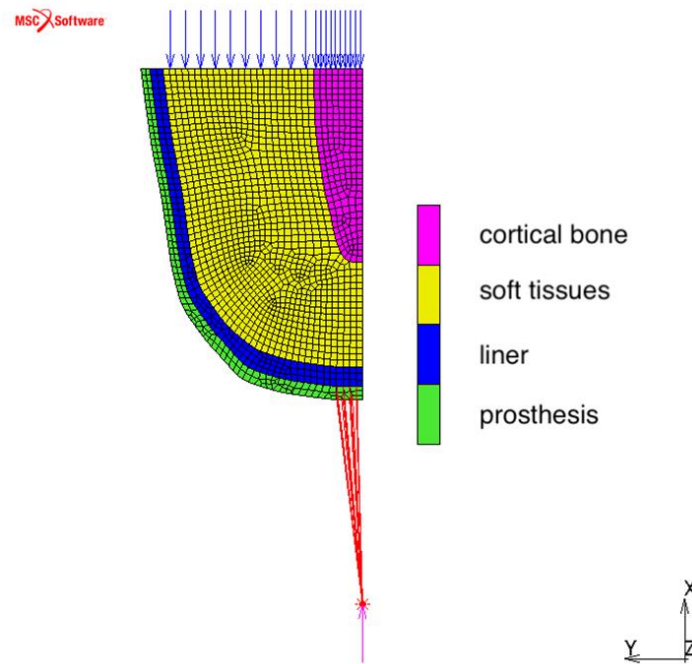


**Fig. 1.** Geometries, meshes and deformable bodies of the biomechanical model.

### Geometry and loading

The data that enabled creating the geometry of this model's anthropometry and customized prosthesis was acquired through the patient's medical digital imaging. Such data was interpolated using cubic splines. The prosthesis was considered to support a load of 70 kgf, which corresponds to the total weight of the user during the static stance. Loading is imposed in quasi-static conditions [44], as illustrated in Fig. 1.

## Materials

A conventional thermoplastic polymer (polypropylene) and five different eco-materials were considered for the composition of the socket-type prosthesis: an epoxy resin whose molecular structure is mostly of vegetable origin (SR GreenPoxy 56, produced by Sicomin [45]); a composite in which a SR GreenPoxy 56 resin matrix is reinforced with 40% natural jute fibers; a recycled PLA biopolymer, and two composites in which the recycled PLA biopolymer matrix is reinforced with 20% and 30% short carbon fibers.

## Finite Element Analysis (FEM)

Given the symmetry of the model (see Fig. 1), a 2D axisymmetric analysis was performed. The simulations with this model were made using the implicit module of MSC Marc Mentat 2018 [46].

A multifrontal direct sparse solver, the Paradiso solver, is used with a Newton-Raphson iterative procedure. For convergence testing, a relative force tolerance of 10% is used. An adaptative multicriteria stepping procedure is used for load increment was used for the initial time step (load increment) of  $1 \times 10^{-6}$ .

The numerical constrictions associated with the implicit method were overcome using a mesh adaptivity algorithm, the advancing front quadrilateral. An automatic algorithm was used for meshing, and linear quadrilateral axisymmetric solid elements with four nodes (Quad 10) were used.

The initial mesh dimensions of the elements were of 3 mm. This value was established in a previous iterative process and is considered an objective in the adaptive mesh algorithm. In this process, the mesh size may be reduced to a quarter of its initial value, depending on the strain change and the distortion that may take place in each element [42, 43]. In the structural analysis, large strain nonlinear procedures were used.

For the soft tissues' materials, the Neo-Hookean model presented in [47] was used, whereas, for the liner, Mooney-Rivlin behavior with three parameters [48] was considered.

On what concerns the hard materials – femur and socket – a linear elastic behavior was considered. The femur, the resin and thermoplastic materials were modeled as isotropic

linear elastic. The reinforce fibers – jute and carbon – were modeled as orthotropic linear elastic materials. The composite materials are modeled as anisotropic linear elastic materials.

### **Composite materials simulation**

For the composite materials numerical simulation, the Halpin-Tsai model for discontinuous fibers was used [49]. The composite material's elastic properties were computed in the MSC Patran 2019 software [50] considering the respective resin/fiber volume ratio. A 10 to 1 ratio was considered for the fibers' length vs diameter.

The fibers on the composite were later dispersed using a 2D short fiber model implemented in the MSC Patran 2019 software [50], with angles  $\alpha = 0^\circ$  and  $\phi = 45^\circ$ , a standard deviation of  $10^\circ$  through a random process, with zero correlation, using 1000 Monte Carlo iterations.

The composites were oriented so that axis 1 has, at each point, the direction of the tangent to the prosthesis profile shown in Fig. 1. Axis 2 has the direction of thickness and axis 3, the tangential direction [46].

## **5.3. Results and Discussion**

The results section of current research starts with both the biomechanical system and the custom socket-type prosthesis simulation to analyze the local stress fields resulting from the use of the prosthesis. In the end of this section, the results are discussed towards the usability of the rPLA biocomposite as a structural material in such custom assistive device.

### **5.3.1. Biomechanical system simulation**

In the contact between the system's various components, a Coulomb's bilinear friction model was used, with an average friction coefficient between the cortical bone and the soft tissues of  $\mu = 0.3$  [51].

A friction coefficient of  $\mu = 0.5$  was considered for the contact between the socket type prosthesis and the liner. For the liner and the soft tissues contacts, a friction coefficient of  $\mu = 0.65$  was used [43].

In the numerical model, the contact between deformable bodies is modelled by the finite sliding segment-to-segment contact algorithm. The separation criteria are based upon stresses (Lagrange multipliers): separation threshold is treated as residual stress of negligible magnitude ( $0.9 \times 10^{-6}$  MPa) [43].

### **Biological tissues**

The patient's soft tissues were modeled by a Neo-Hookean model for the muscle, with  $C_{10} = 4.25$  kPa and the volumetric behavior obtained only with the first term of the series,  $D_1 = 24.34$  MPa<sup>-1</sup>. The patient's femur was modelled as an isotropic, homogeneous, and linear elastic material. The cortical bone properties are considered along the longitudinal direction [52], with an elastic modulus,  $E = 11.5$  GPa, and Poisson's ratio,  $\nu = 0.31$  [43].

### **Non-biological materials**

When modelling the biomechanical model liner (see Fig. 1) the TEC Pro 18 polyurethane was considered. This material is produced by TEC Interface Systems, Waite Park, Minnesota, modeled by a the second-order Mooney-Rivlin model, with the following parameters:  $C_{10} = 1.5152 \times 10^{-6}$  kPa;  $C_{01} = 41.365$  kPa;  $C_{11} = 9.4846 \times 10^{-7}$  kPa; and the bulk modulus of 413.65 MPa. Considering that six different materials were considered for the prosthesis, a dedicated section for the details of their numerical simulation will be presented next [43].

## **5.3.2. Socket-type prostheses simulation**

To better visualize and quantify the stress field that occurs in the socket-type prosthesis, which is the main object of current research, the part of the model related to it was isolated from the rest of the numerical model components (see Fig. 1). As previously referred, a

conventional thermoplastic polymer (polypropylene) and five different eco-materials were considered for the composition of the socket-type prosthesis. The simulation for each of these material types will be presented and discussed in this section.

## Polypropylene

This thermoplastic material was modelled as homogeneous, isotropic, and linear elastic, with an elastic modulus ( $E$ ) of 1000 MPa and the Poisson's ratio  $\nu = 0.30$  [43]. Considering these parameters, a dedicated simulation for the polypropylene material for the prosthetic socket was carried out and the stress fields on the socket are shown in Fig. 2. The mean normal stress field is presented in Fig. 2a), whereas Fig. 2b) illustrates the von Mises stress field. It can be observed that the higher stress levels are located at the lower end of the patient's prosthesis, in the connection between the socket and the pylon. In the surrounding contact area with the pylon, compression stresses are observed. On the opposite side of the socket thickness, tensile stresses are generated. In this simulation, the mean normal stresses varied between -32 and 24 MPa and the equivalent von Mises stresses varied up to 64 MPa.

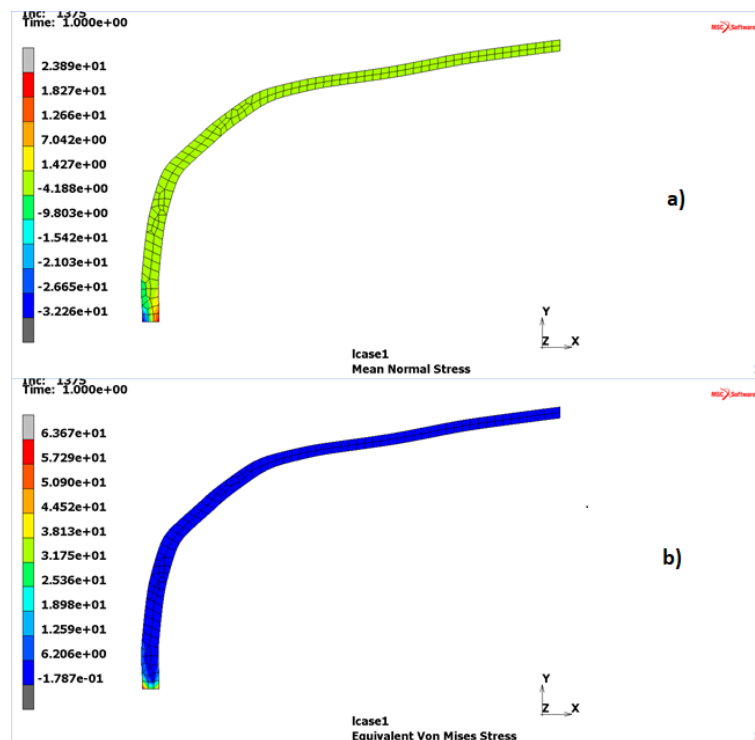


**Fig. 2.** Stress fields (in MPa) for the polypropylene socket-type prosthesis: a) Mean normal stress; b) Equivalent von Mises stress.

### SR GreenPoxy 56

This biopolymer was modelled as homogeneous, isotropic, and linear elastic, with an elastic modulus ( $E$ ) of 3000 MPa, a Poisson's ratio  $\nu = 0.39$  and the specific mass  $\rho = 1180 \text{ kg/m}^3$  [43]. The contact stresses on the socket-type prosthesis, namely the mean normal stresses and the equivalent von Mises stresses are shown in the numerical simulation presented in Fig. 3. Considering these parameters, a dedicated simulation for the SR GreenPoxy 56 resin was carried out and the stress fields on the socket are presented in Fig. 3. Thus, Fig. 3a) illustrates the mean normal stress field and Fig. 3b) shows the von Mises stress field.

As what occurred for the polypropylene, it can be observed that the higher stress levels are located at the lower end of the patient's prosthesis. However, the stress levels are lower for the SR GreenPoxy 56 resin than those for the thermoplastic polymer. In the surrounding area of the contact with the pylon compression stresses take place and, on the other side of the socket thickness, tensile stresses are observed. In this simulation, the mean normal stresses varied between -28 and 21 MPa and the equivalent von Mises stresses varied up to 55 MPa.

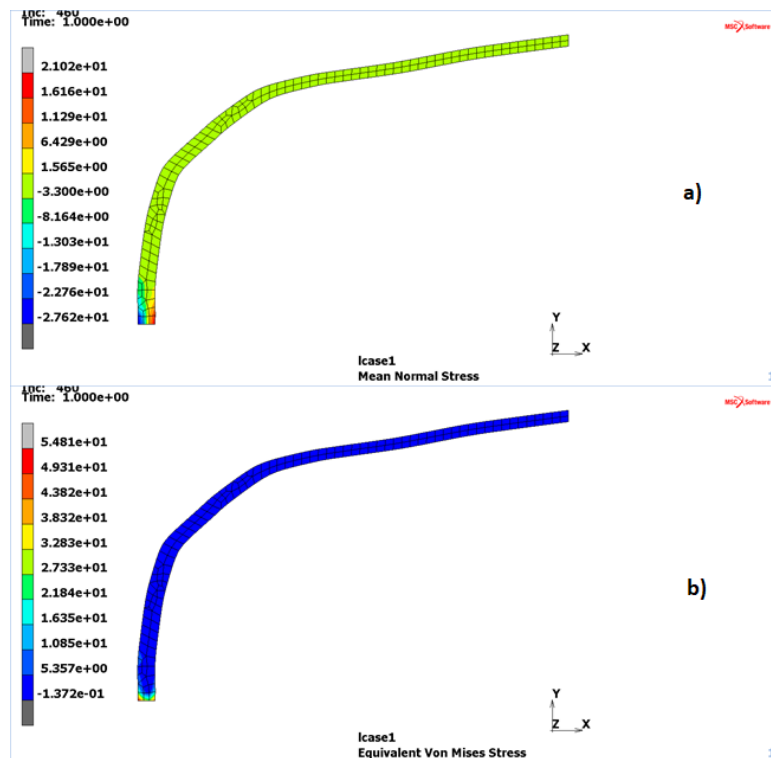


**Fig. 3.** Stress fields (in MPa) for the SR GreenPoxy 56 resin reinforced socket-type prosthesis: a) Mean normal stress; b) Equivalent von Mises stress.



### SR GreenPoxy 56 resin reinforced with 40% jute fibers

This biopolymer-based composite reinforced with 40% jute fibers was modelled as following: the jute fibers were considered as homogeneous whilst the resulting composite was modelled as 2D orthotropic and linear elastic, with an elastic modulus  $E_1 = 23949$  MPa and  $E_2 = 978$  MPa, the Poisson's ratio  $\nu_{12} = 0.374$  and  $\nu_{21} = 0.014$ , the shear modulus  $G_{12} = 411$  MPa and the specific mass  $\rho = 1440$  kg/m<sup>3</sup> [43]. For this biocomposite, a 60 to 40% resin-to-fiber volume ratio was considered. From the simulation in MSC Patran 2019, using the Halpin-Tsai model [49], the resulting elasticity matrix for this composite is presented in equation (1).

$$[C_{ij}] = \begin{bmatrix} 1.30 \times 10^5 & 1.39 \times 10^5 & 1.26 \times 10^5 & 3.07 \times 10^1 \\ 1.39 \times 10^5 & 1.59 \times 10^5 & 1.40 \times 10^5 & 5.04 \times 10^1 \\ 1.26 \times 10^5 & 1.40 \times 10^5 & 1.31 \times 10^5 & 5.32 \times 10^1 \\ 3.07 \times 10^1 & 5.04 \times 10^1 & 5.32 \times 10^1 & 2.10 \times 10^3 \end{bmatrix} (MPa) \quad (2)$$

The dedicated simulation with the SR GreenPoxy 56 composite reinforced with jute fibers was carried out and the stress field on the socket are available at Fig. 4. Again, as for previous simulations it can be observed that the higher stress levels are located at the lower end of the patient's prosthesis. The normal stress levels are lower for the SR GreenPoxy 56 resin than those for the GreenPoxy-Jute composite. However, the von Mises stresses have the opposite behavior. In the surrounding area of the contact with the pylon compression stresses take place, whereas on the other side of the socket thickness tensile stresses can be observed. In this simulation, the mean normal stresses varied between -57 and 59 MPa and the equivalent von Mises stresses varied up to 13 MPa.

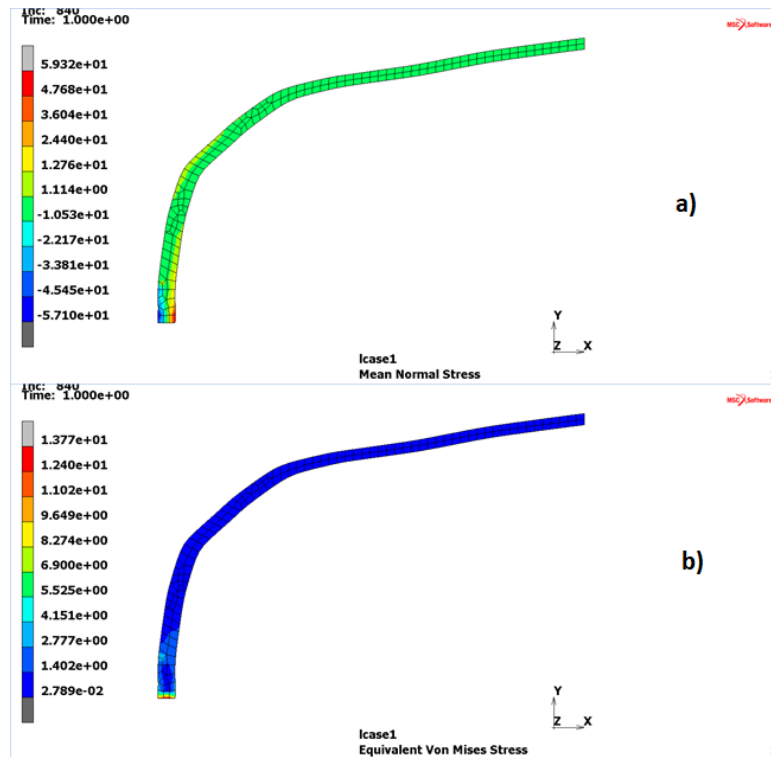


**Fig. 4.** Stress fields (in MPa) for the SR GreenPoxy 56 resin reinforced socket-type prosthesis with 40% jute fibers socket-type prosthesis: a) Mean normal stress; b) Equivalent von Mises stress.

### Recycled PLA biopolymer

The research conducted by Anderson [53] shows that for a short number of recycling cycles the mechanical properties of rPLA are similar to those of the virgin PLA. Consequently, both PLA and rPLA biopolymers can be modelled as homogeneous, isotropic, and linear elastic, with an elastic modulus ( $E$ ) of 3500 MPa, a Poisson's ratio  $\nu = 0.36$  and the specific mass  $\rho = 1252 \text{ kg/m}^3$  [39]. Considering these parameters, a dedicated simulation for the rPLA biopolymer used in the prosthetic socket was carried out and the stress fields on the socket are presented in Fig. 5. It can be observed that the PLA/rPLA biopolymer has similar stress fields as those observed for the GreenPoxy 56 resin. In this simulation, the mean normal stresses varied between -29 and 21 MPa and the equivalent von Mises stresses varied up to 57 MPa.

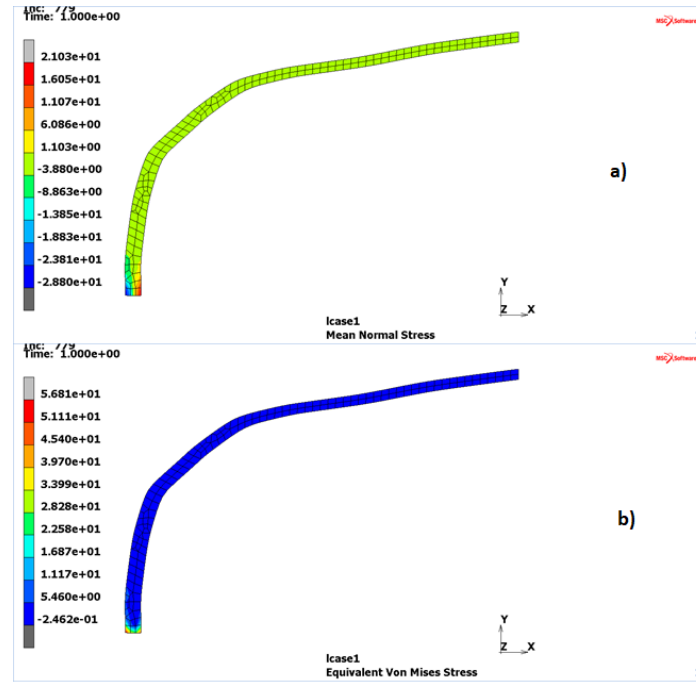


**Fig. 5.** Stress fields (in MPa) for the PLA/rPLA biopolymer socket-type prosthesis: a) Mean normal stress; b) Equivalent von Mises stress.

### Recycled PLA biopolymer composite (20% carbon fiber)

For the rPLA+20% carbon composite, the properties presented above for the PLA/rPLA biopolymer were considered for this composite's matrix. As for the carbon fibers, these were modeled as homogeneous, 2D orthotropic and linear elastic, with elastic modulus  $E_1 = 250$  GPa and  $E_2 = 22.4$  GPa, the Poisson's ratio  $\nu_{12} = 0.35$  and  $\nu_{21} = 0.0024$ , the shear modulus  $G_{12} = 22.1$  GPa and the specific mass  $\rho = 1760$  kg/m<sup>3</sup> [40, 41]. For the first PLA composite simulation, a rPLA\_0.2C with 80 to 20% resin-to-fiber volume ratio was considered. From the composite simulation in MSC Patran 2019 using the Halpin-Tsai model [49], the elasticity matrix was obtained for this composite as presented in equation (2).

$$[C_{ij}] = \begin{bmatrix} 1.86 \times 10^4 & 1.36 \times 10^4 & 1.42 \times 10^4 & 1.50 \times 10^1 \\ 1.36 \times 10^4 & 1.89 \times 10^4 & 1.36 \times 10^4 & 5.57 \times 10^0 \\ 1.42 \times 10^4 & 1.36 \times 10^4 & 1.86 \times 10^4 & 8.33 \times 10^0 \\ 1.50 \times 10^1 & 5.57 \times 10^0 & 8.33 \times 10^0 & 1.98 \times 10^3 \end{bmatrix} (MPa) \quad (2)$$

Considering these parameters, a dedicated simulation for the Recycled PLA biopolymer composite with 20% carbon fiber was carried out and the main results are shown in Fig. 6.

When compared with the rPLA biopolymer, a great increase in magnitude of the normal stress field can be observed, with a slight decrease of the von Mises stress field. In this simulation, the mean normal stresses varied between -48 and 44 MPa and the equivalent von Mises stresses varied up to 53 MPa.

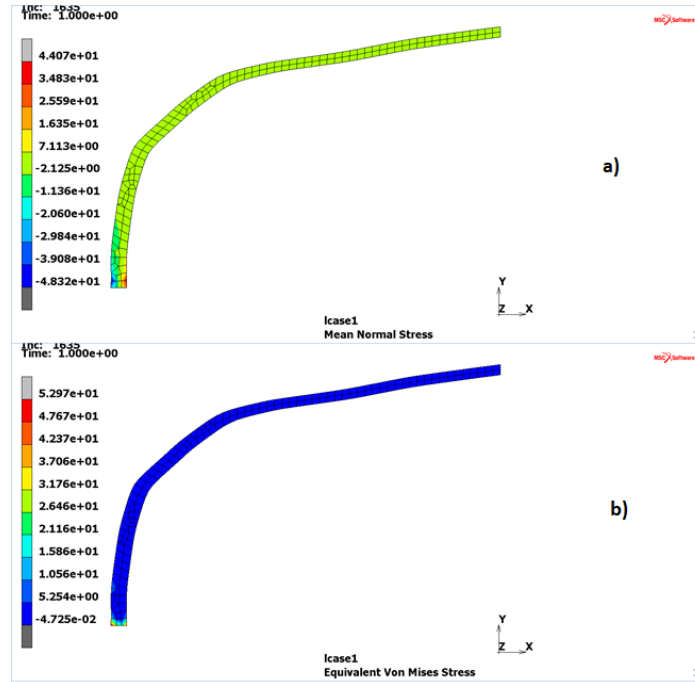


**Fig. 6.** Stress fields (in MPa) for the recycled PLA biopolymer reinforced with 20% short carbon fibers socket-type prosthesis: a) Mean normal stress; b) Equivalent von Mises stress.

### Recycled PLA biopolymer composite (30% carbon fiber)

For the second rPLA+30% carbon composite, the same properties for the recycled PLA matrix and carbon fiber were considered. However, a different PLA\_0.3C with 70 to 30% resin-to-fiber volume ratio was considered. From the composite simulation in MSC Patran 2019 using the Halpin-Tsai model [49], the elasticity matrix was obtained for this composite as presented in equation (3).

$$[C_{ij}] = \begin{bmatrix} 1.56 \times 10^5 & 1.76 \times 10^5 & 1.49 \times 10^5 & 3.68 \times 10^1 \\ 1.76 \times 10^5 & 2.16 \times 10^5 & 1.76 \times 10^5 & 1.15 \times 10^2 \\ 1.49 \times 10^5 & 1.76 \times 10^5 & 1.56 \times 10^5 & 1.25 \times 10^2 \\ 3.68 \times 10^1 & 1.15 \times 10^2 & 1.25 \times 10^2 & 2.83 \times 10^3 \end{bmatrix} (MPa) \quad (3)$$

Based on these parameters, a dedicated simulation for the rPLA biopolymer composite with 30% carbon fiber was carried out and the main results are illustrated in Fig. 7. When compared with the plain rPLA biopolymer results, a great increase in magnitude of the normal stress field has occurred and a great decrease of the von Mises stress field took place. In this simulation, the mean normal stresses varied between -49 and 51 MPa and the equivalent von Mises stresses varied up to 17 MPa.

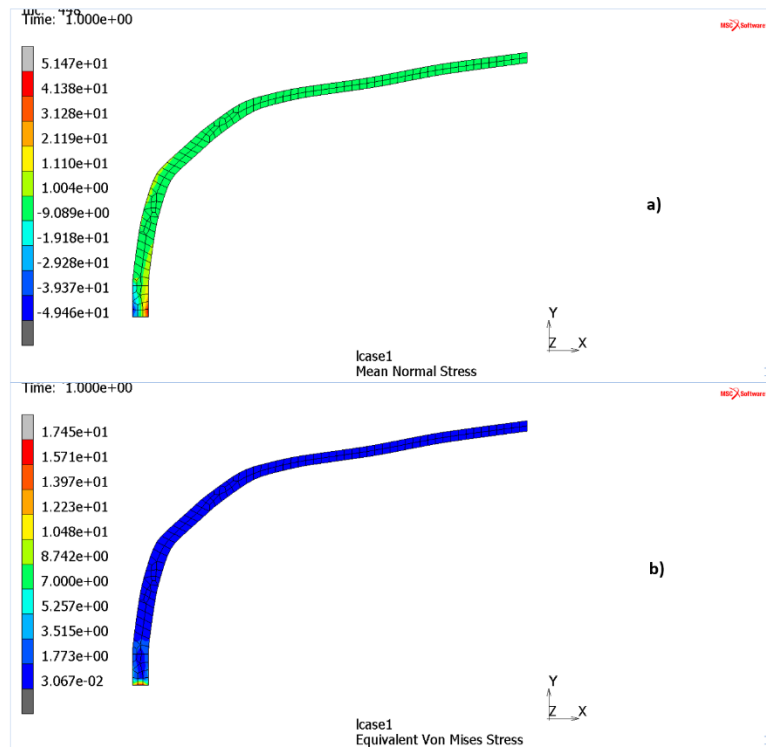


**Fig. 7.** Stress fields (in MPa) for the recycled PLA biopolymer reinforced with 30% short carbon fibers socket-type prosthesis: a) Mean normal stress; b) Equivalent von Mises stress.

### Contact stresses

To assess the effect of increased stiffness and anisotropy of the prosthesis material on the patient's comfort using it, as well as to analyze the transmission of forces at the interfaces of the different components of the prosthesis, Fig. 8 and Fig. 9, show, respectively, the field of contact stresses developed in the system for the rPLA biopolymer socket and the rPLA+30% carbon composite.

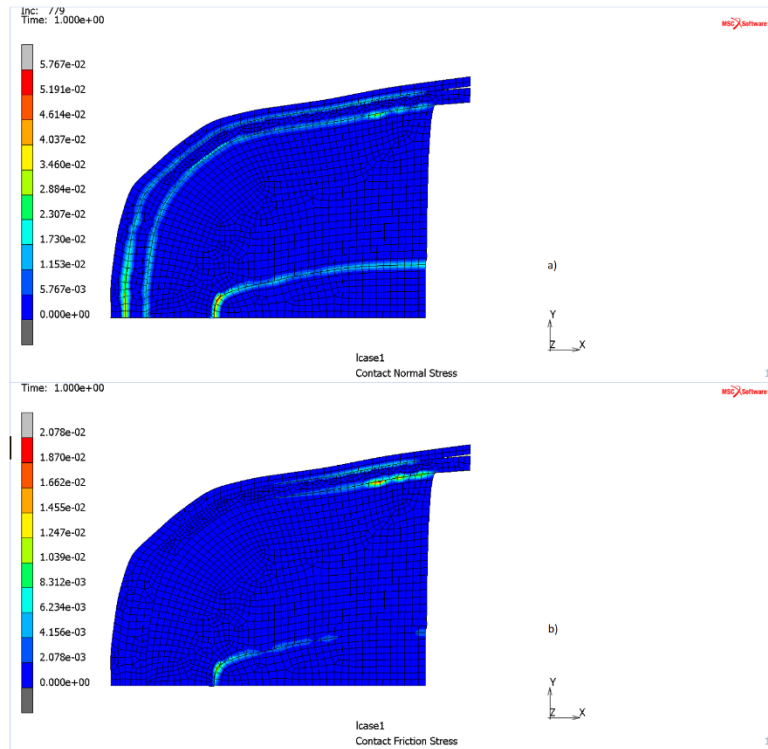


**Fig. 8.** Contact stress field (in MPa) developed in the system with rPLA biopolymer socket: a) Normal stress; b) Friction stress.

From the analysis of the results presented in both Fig. 8 and Fig. 9., it can be observed that the normal contact stresses in the polymer are significantly lower than for the composite, while the opposite occurs for the friction stresses.

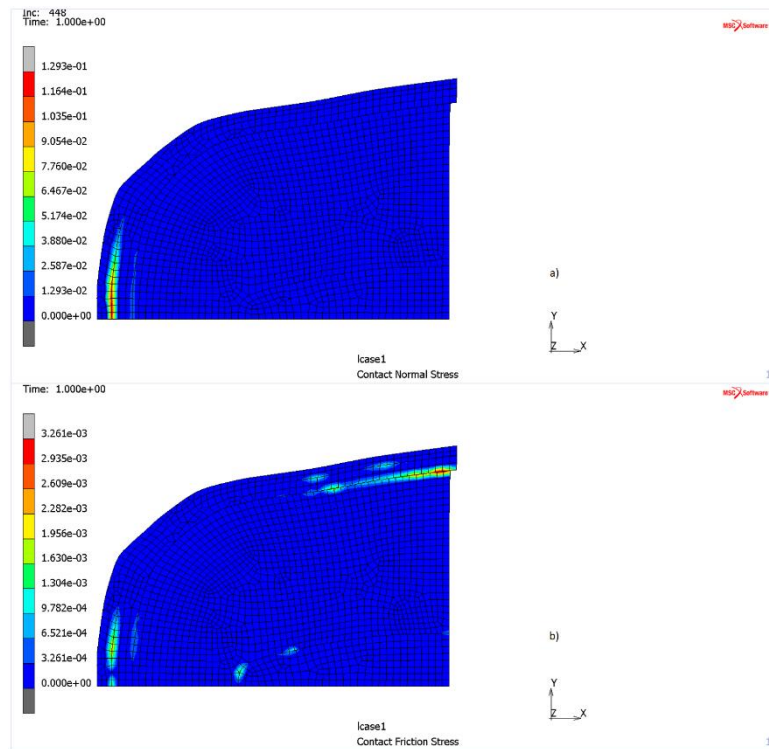


**Fig. 9.** Contact stress field (in MPa) developed in the system with the socket of rPLA biopolymer reinforced with 30% short carbon fibers: a) Normal stress; b) Friction stress.

### Components of stresses

To assess the influence of the components of stresses in the mean normal stress and in the von Mises stress fields, Fig. 10 and Fig. 11 show, respectively, the field of components of stresses developed in the socket of rPLA biopolymer and the rPLA+30% carbon composite.

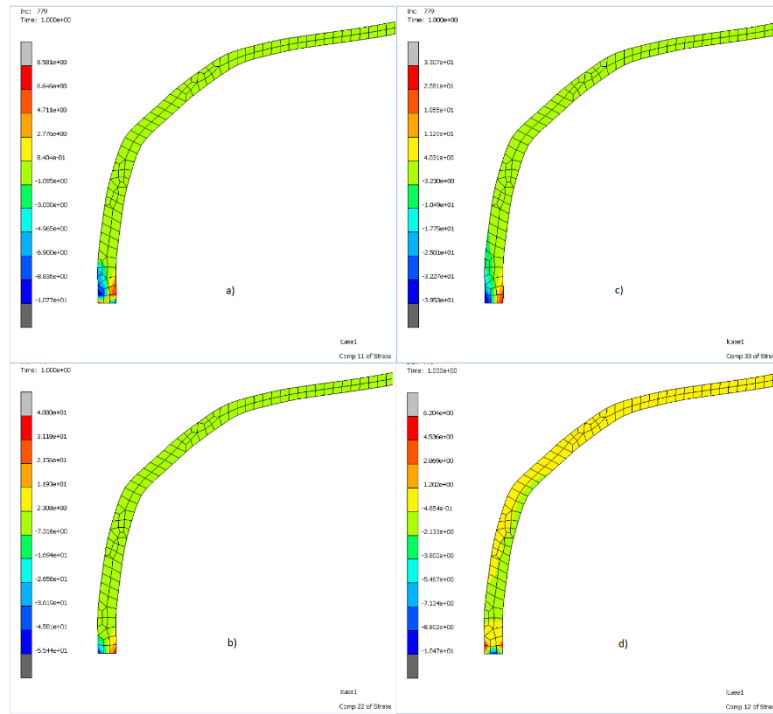


**Fig. 10.** Components stress fields (in MPa) developed in PLA biopolymer socket: a) Axial stress; b) Radial stress; c) Normal stress in tangential direction; d) Shear stress.

From the analysis of the results presented in both Fig. 10 and Fig. 11, it can be observed that all the components of normal stresses in the composite have similar magnitudes, which result in lower von Mises stresses and increased mean normal stresses.



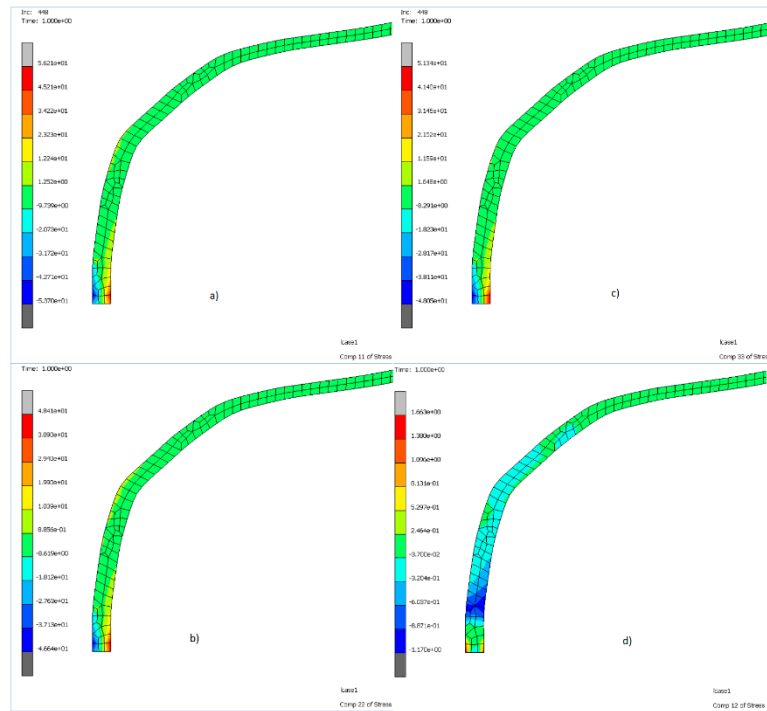


**Fig. 11.** Components stress fields (in MPa) developed in socket of recycled PLA reinforced with 30% short carbon fibers:  
 a) Axial stress; b) Radial stress; c) Normal stress in tangential direction; d) Shear stress.

**Discussion**

The recycled PLA biopolymer composite reinforced with short carbon fibers has special relevance for the current customized prosthesis development scenario. Particularly, the 70 to 30% resin-to-fiber volume ratio presents the most promising results. Thus, although the GreenPoxy composite may include more environmentally friendly materials, this latter biocomposite cannot be transformed into an extrudable filament and, therefore, cannot be used in low-cost fused deposit modelling additive processes.

To compare the proposed rPLA biocomposite with other alternative materials for the customized socket-type prosthesis, various numerical simulations were carried-out towards inferring about the suitability of use to satisfy the requirements for the application under research. The results of these simulations were shown in Fig. 2 to Fig. 7, in which it was observed that the highest stress levels were located at the lower end of the prosthesis geometry. Fig. 12 shows the nodes of the numerical model located on such critical area.

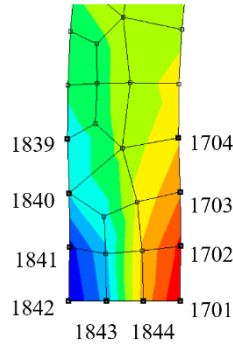


**Fig. 12.** Identification of nodes located at the critical zone of all the numerical model simulations.

### **Raghava-Caddell-Atkins equivalent stresses**

Considering that solely the von Mises plasticity criterion would not present satisfactory results when applied to polymeric materials, as it did not include the dependence of the hydrostatic pressure and assumed equal values of yield stress to compression and tension Raghava et al. [54], proposed a new plasticity criterion adapting the von Mises model to include the effect of the hydrostatic pressure.

Later, Caddell et. al. [55] confirmed the validity of the modified criterion to be used as the yield criteria for polymeric materials. The elasticity limit function  $F(\sigma_{ij})$  according to the Raghava-Caddell-Atkins criterion can be expressed as follows:

$$F(\sigma_{ij}) = (\sigma_1 - \sigma_2)^2 + (\sigma_1 - \sigma_3)^2 + (\sigma_2 - \sigma_3)^2 + 2(\sigma_1 + \sigma_2 + \sigma_3)(C - T) = 2CT \quad (4)$$

in which C and T refer to the absolute values of the yield stress, respectively in compression and traction.

Groot et. al. [41], mentioned the modified von Mises criteria to be efficient when considering the effect of hydrostatic pressure to assess the yield of reinforced resins. Conversely, in current research, the Raghava-Caddell-Atkins criterion was used to assess the yield stresses on the socket-type prosthesis when applied to different materials. When analyzing the mechanical behavior of the polymer-based composites, it was considered that the yield occurs in the matrix.

## Summary of the results

For the polymers and resins considered, the respective yield strengths to compression and tension were obtained according to the Table 1.

**Table 1.** Yield strengths to compression and tension for the considered polymers and resins.

	Polypropylene	GreenPoxy	PLA/rPLA
<b>Compressive strength</b>	40 MPa	79 MPa	13600 psi = 93,79 MPa 68 MPa
<b>Tensile strength</b>	20 MPa	50 MPa	9531 psi = 65,73 MPa 40 MPa
<b>C-T</b>	20 MPa	29 MPa	28,06 MPa
<b>References</b>	(matweb.com, 2021; polymerdatabase.com, 2021)	(Perrier, n.d.)	(Anderson, 2017; makerbot.com, 2021)

Table 2 and Table 3 present the results for the von Mises equivalent stresses ( $\sigma_{\text{Von Mises}}$ ), the hydrostatic stresses ( $\sigma_{\text{kk}}$ ) and the Raghava-Caddell-Atkins equivalent stresses ( $\sigma_{\text{RCA}}$ ) at the nodes on the critical zone (see Fig. 8), for the various materials. For the various polymers and resins, these values are compared with the respective yield strength and the reference stress for the Raghava-Caddell-Atkins criterion.

**Table 2.** Summary of all the simulation results for the Polypropylene, GreenPoxy and Composite GreenPoxy +40% jute materials.

NODE	Polipropylene			GreenPoxy			GreenPoxy+40% jute composite		
	$\sigma_{\text{vonMises}}$	$\sigma_{\text{kk}}$	$\sigma_{\text{RCA}}$	$\sigma_{\text{vonMises}}$	$\sigma_{\text{kk}}$	$\sigma_{\text{RCA}}$	$\sigma_{\text{vonMises}}$	$\sigma_{\text{kk}}$	$\sigma_{\text{RCA}}$
<b>1839</b>	10,48	-7,67	16,22	6,60	-9,37	17,76	2,40	-25,90	27,51
<b>1840</b>	14,01	-10,13	19,97	8,88	-12,58	21,06	3,23	-34,83	31,94
<b>1841</b>	34,75	-25,28	41,39	24,16	-24,65	36,03	3,62	-57,10	40,85
<b>1842</b>	63,67	-32,26	<b>68,55</b>	54,81	-27,62	<b>61,68</b>	11,09	-41,04	36,24
<b>1843</b>	35,98	-17,84	40,63	33,04	-15,89	39,40	13,25	-22,48	28,77
<b>1844</b>	30,69	10,28	33,87	27,09	8,47	31,30	13,77	14,34	24,61
<b>1701</b>	53,86	23,89	58,13	46,91	21,02	53,01	9,32	56,08	41,39
<b>1702</b>	25,28	17,25	31,37	18,02	17,60	28,90	3,10	59,32	<b>41,59</b>
<b>1703</b>	12,13	8,42	17,77	8,01	10,72	19,36	3,26	35,06	32,05
<b>1704</b>	7,71	4,39	12,13	5,13	5,73	13,88	2,10	22,59	25,68
Strength [MPa]			<b>28,28</b>			<b>62,80</b>			<b>62,80</b>

**Table 3.** Summary of all the simulation results for the Recycled PLA, rPLA+20% carbon composite and rPLA+30% carbon composite materials.

NODE	Recycled PLA			rPLA +20% carbon composite			rPLA +30% carbon composite		
	$\sigma_{\text{vonMises}}$	$\sigma_{\text{kk}}$	$\sigma_{\text{RCA}}$	$\sigma_{\text{vonMises}}$	$\sigma_{\text{kk}}$	$\sigma_{\text{RCA}}$	$\sigma_{\text{vonMises}}$	$\sigma_{\text{kk}}$	$\sigma_{\text{RCA}}$
1839	7,58	-8,31	17,05	4,41	-14,41	20,59	3,27	-21,60	24,83
1840	10,20	-11,18	20,44	5,93	-19,40	24,08	4,39	-29,04	28,88
1841	26,68	-24,00	37,21	15,32	-48,32	39,88	4,07	-49,46	<b>37,48</b>
1842	56,81	-28,80	<b>63,53</b>	52,97	-21,08	<b>58,28</b>	11,32	-32,23	32,13
1843	34,28	-16,74	40,56	29,71	-13,12	35,37	16,58	-17,36	27,60
1844	27,08	8,21	31,04	19,87	7,21	24,44	17,45	10,74	24,62
1701	47,40	21,03	53,26	46,12	28,16	54,01	9,25	44,87	36,67
1702	19,66	16,60	29,20	12,04	44,07	37,17	3,81	51,47	38,19
1703	9,01	9,18	18,40	5,52	18,04	23,17	4,47	29,55	29,14
1704	5,77	4,89	13,06	3,54	11,58	18,37	2,88	19,04	23,30
Strength [MPa]			52			52			52

On what concerns to the normal stresses, it can be observed that, in general, the highest stresses take place on the most distal part of the socket-type prosthesis, at the interface between the socket and the liner. Conversely, considering the equivalent von Mises stresses, it can also be observed that the higher stresses occur on the most distal part of the socket-type prosthesis.

By observing the summarized results presented in Table 2 and Table 3 it is possible to verify that only the composites of SR GreenPoxy 56 resin reinforced with 40% jute fibers and of recycled PLA biopolymer reinforced with 30% short carbon fibers meet, with a safety margin, the requirements to support the loads necessary to this application. These are very positive results in that it opens the possibility to build a socket-type prosthesis through additive manufacturing, such as with the Fused Deposition Modelling (FDM) technology. Nonetheless, the resulting mechanical properties shall also be assessed and validated using an experimental setup.

Analyzing the results presented in Fig. 4 and Fig. 7, it can be observed that both the GreenPoxy+40% jute and the rPLA+30% carbon composites have similar behaviors. When compared, the GreenPoxy-jute composite has slightly lower normal stresses than the rPLA-carbon composite, whereas when considering the von Mises stresses, these are slightly higher for the GreenPoxy-jute composite than for the rPLA-carbon composite. As previous mentioned, for current case-study, the rPLA biopolymer composite is preferred towards the GreenPoxy due to its applicability in additive manufacturing. Thus, further analysis will be restricted to the recycled PLA biopolymer reinforced with 30% carbon fibers.

Considering the stress fields presented in both Fig. 10 and Fig. 11, it can be observed that the increased mechanical behavior of the rPLA composite, when compared to the rPLA biopolymer, is due to the higher stiffness of the composite in the axial direction (Fig. 10a and Fig. 11a)), which is the thickness direction of the critical zone. The stiffness increase derives from the dispersion of short carbon fibers in the direction of the socket thickness. Thus, a particular attention must be paid to this fact during the manufacturing of the prosthesis, as such increase in stiffness leads to the transmission of efforts to the soft tissues in a more uniform way, resulting in better comfort for the patient, as can be observed from the results presented in Fig. 9 and Fig. 10. In fact, as the shear stresses are amongst the main causes for diseases produced by prosthesis in lower limb amputations [42], these are significantly lower for the rPLA+30% carbon composite, which further supports the preferred selection of this material for the current case-study's socket-type prosthesis.

## **5.4. Summary and Conclusions**

This study analyzed the use of recycled reinforced PLA as feedstock material for additive manufacturing to produce customized socket-type prostheses.

Based on the actual anatomical contour of the patients' residual limb, numerical simulations were carried out both at the biomechanical system and the custom socket-type prosthesis to analyze the local stress fields resulting from the use of the prosthesis.

These numerical analyses were carried out considering a conventional thermo-plastic polymer (polypropylene) and five different eco-materials, namely a bioepoxy resin SR GreenPoxy 56 with and without natural jute fibers reinforcement, and recycled PLA biopolymer with and without short carbon fibers as reinforcement.

Analyzing the results, for the given custom geometry of the prosthesis, only the GreenPoxy-jute composite with 40% reinforcement fibers and the rPLA biopolymer reinforced with 30% carbon fibers met the design criteria to be used on such assistive device. However, for the current case-study, the rPLA biopolymer composite is preferred towards the GreenPoxy composite due to its applicability as filaments for additive manufacturing.

In conclusion, the numerical simulation results showed the potential of the rPLA biopolymer reinforced with 30% carbon fibers as an ecodesign solution for customized prostheses and orthoses. This recycled feedstock material should allow for patients being able to successfully produce and assemble their own customized assistive devices using fused deposition modelling.

## **References**

- [1] Wang Y, Tan Q, Pu F, et al (2020) A Review of the Application of Additive Manufacturing in Prosthetic and Orthotic Clinics from a Biomechanical Perspective. *Engineering* 6:1258–1266
- [2] Mahamood RM, Akinlabi ET (2016) Achieving Mass Customization Through Additive Manufacturing. In: Schlick C, Trzecieliński S (eds) *Advances in Ergonomics of Manufacturing: Managing the Enterprise of the Future*. Springer International Publishing, Cham, pp 385–390
- [3] Thompson MK, Moroni G, Vaneker T, et al (2016) Design for Additive Manufacturing: Trends, opportunities, considerations, and constraints. *CIRP Annals* 65:737–760. <https://doi.org/10.1016/j.cirp.2016.05.004>
- [4] Ko H, Moon SK, Hwang J (2015) Design for additive manufacturing in customized products. *International Journal of Precision Engineering and Manufacturing* 16:2369–2375. <https://doi.org/10.1007/s12541-015-0305-9>
- [5] Bhatia A, Sehgal AK (2021) Additive manufacturing materials, methods and applications: A review. *Materials Today: Proceedings*. <https://doi.org/10.1016/j.matpr.2021.04.379>
- [6] Pajonk A, Prieto A, Blum U, Knaack U (2022) Multi-material additive manufacturing in architecture and construction: A review. *Journal of Building Engineering* 45:103603. <https://doi.org/10.1016/j.jobbe.2021.103603>
- [7] Siacor FDC, Chen Q, Zhao JY, et al (2021) On the additive manufacturing (3D printing) of viscoelastic materials and flow behavior: From composites to food manufacturing. *Additive Manufacturing* 45:102043. <https://doi.org/10.1016/j.addma.2021.102043>

- [8] Blanco D, Rubio EM, Marín MM, Davim JP (2021) Advanced materials and multi-materials applied in aeronautical and automotive fields: a systematic review approach. *Procedia CIRP* 99:196–201. <https://doi.org/10.1016/j.procir.2021.03.027>
- [9] Blakey-Milner B, Gradl P, Snedden G, et al (2021) Metal additive manufacturing in aerospace: A review. *Materials & Design* 209:110008. <https://doi.org/10.1016/j.matdes.2021.110008>
- [10] Praveena BA, Lokesh N, Abdulrajak B, et al (2021) A comprehensive review of emerging additive manufacturing (3D printing technology): Methods, materials, applications, challenges, trends and future potential. *Materials Today: Proceedings*. <https://doi.org/10.1016/j.matpr.2021.11.059>
- [11] Liu G, Xiong Y, Zhou L (2021) Additive manufacturing of continuous fiber reinforced polymer composites: Design opportunities and novel applications. *Composites Communications* 27:100907. <https://doi.org/10.1016/j.coco.2021.100907>
- [12] Yuan S, Li S, Zhu J, Tang Y (2021) Additive manufacturing of polymeric composites from material processing to structural design. *Composites Part B: Engineering* 219:108903. <https://doi.org/10.1016/j.compositesb.2021.108903>
- [13] Chen RK, Jin Yan, Wensman J, Shih A (2016) Additive manufacturing of custom orthoses and prostheses-A review. *Additive Manufacturing* 12:77–89
- [14] Wang Y, Tan Q, Pu F, et al (2020) A Review of the Application of Additive Manufacturing in Prosthetic and Orthotic Clinics from a Biomechanical Perspective. *Engineering* 6:1258–1266. <https://doi.org/10.1016/j.eng.2020.07.019>
- [15] Revilla-León M, Fountain J, Piedra-Cascón W, et al (2021) Workflow of a fiber-reinforced composite fixed dental prosthesis by using a 4-piece additive manufactured silicone index: A dental technique. *The Journal of Prosthetic Dentistry* 125:569–575. <https://doi.org/10.1016/j.prosdent.2020.02.030>
- [16] Schweiger T, Moscato F, Hoetzenecker K (2021) Commentary: Three-dimensional-printed, customized airway prosthesis—is it justified to walk the extra mile? *JTCVS Techniques*. <https://doi.org/10.1016/j.xjtc.2021.09.025>

- [17] Coulter FB, Schaffner M, Faber JA, et al (2019) Bioinspired Heart Valve Prosthesis Made by Silicone Additive Manufacturing. *Matter* 1:266–279.  
<https://doi.org/10.1016/j.matt.2019.05.013>
- [18] Miechowicz S, Wojnarowska W, Majkut S, et al (2021) Method of designing and manufacturing craniofacial soft tissue prostheses using Additive Manufacturing: A case study. *Biocybernetics and Biomedical Engineering* 41:854–865.  
<https://doi.org/10.1016/j.bbe.2021.05.008>
- [19] Colpani A, Fiorentino A, Ceretti E (2020) Design and Fabrication of Customized Tracheal Stents by Additive Manufacturing. *Procedia Manufacturing* 47:1029–1035.  
<https://doi.org/10.1016/j.promfg.2020.04.318>
- [20] Diegel O, Singamneni S, Reay S, Withell A (2010) Tools for Sustainable Product Design: Additive Manufacturing. *Journal of Sustainable Development* 3:
- [21] Javaid M, Haleem A, Singh RP, et al (2021) Role of additive manufacturing applications towards environmental sustainability. *Advanced Industrial and Engineering Polymer Re-search* 4:312–322. <https://doi.org/10.1016/j.aiepr.2021.07.005>
- [22] Siva Rama Krishna L, Srikanth PJ (2021) Evaluation of environmental impact of additive and subtractive manufacturing processes for sustainable manufacturing. *Materials Today: Proceedings* 45:3054–3060. <https://doi.org/10.1016/j.matpr.2020.12.060>
- [23] Javaid M, Haleem A, Singh RP, et al (2021) Role of additive manufacturing applications towards environmental sustainability. *Advanced Industrial and Engineering Polymer Re-search* 4:312–322. <https://doi.org/10.1016/j.aiepr.2021.07.005>
- [24] Moghimian P, Poirié T, Habibnejad-Korayem M, et al (2021) Metal powders in additive manufacturing: A review on reus-ability and recyclability of common titanium, nickel and aluminum alloys. *Additive Manufacturing* 43:102017.  
<https://doi.org/10.1016/j.addma.2021.102017>
- [25] Zander NE (2019) Recycled Polymer Feedstocks for Material Extrusion Additive Manufacturing. pp 37–51
- [26] Cruz Sanchez FA, Boudaoud H, Camargo M, Pearce JM (2020) Plastic recycling in additive manufacturing: A systematic literature review and opportunities for the circular



economy. *Journal of Cleaner Production* 264:121602.

<https://doi.org/10.1016/j.jclepro.2020.121602>

[27] Tonk R (2021) Natural fibers for sustainable additive manufacturing: A state of the art review. *Materials Today: Proceedings* 37:3087–3090.

<https://doi.org/10.1016/j.matpr.2020.09.017>

[28] Sauerwein M, Doubrovski E, Balkenende R, Bakker C (2019) Exploring the potential of additive manufacturing for product design in a circular economy. *Journal of Cleaner Production* 226:1138–1149. <https://doi.org/10.1016/j.jclepro.2019.04.108>

[29] Bernatas R, Dageou S, Despax-Ferreres A, Barasinski A (2021) Recycling of fiber reinforced composites with a focus on thermoplastic composites. *Cleaner Engineering and Technology* 5:100272. <https://doi.org/10.1016/j.clet.2021.100272>

[30] Ilyas RA, Sapuan SM, Harussani MM, et al (2021) Polylactic Acid (PLA) Biocomposite: Processing, Additive Manufacturing and Advanced Applications. *Polymers* 13:1326. <https://doi.org/10.3390/polym13081326>

[31] Kuznetsov V, Solonin A, Urzhumtsev O, et al (2018) Strength of PLA Components Fabricated with Fused Deposition Technology Using a Desktop 3D Printer as a Function of Geometrical Parameters of the Process. *Polymers* 10:313.

<https://doi.org/10.3390/polym10030313>

[32] Beltrán FR, Arrieta MP, Moreno E, et al (2021) Evaluation of the Technical Viability of Distributed Mechanical Recycling of PLA 3D Printing Wastes. *Polymers* 13:1247. <https://doi.org/10.3390/polym13081247>

[33] Chacón JM, Caminero MA, García-Plaza E, Núñez PJ (2017) Additive manufacturing of PLA structures using fused deposition modelling: Effect of process parameters on mechanical properties and their optimal selection. *Materials & Design* 124:143–157. <https://doi.org/10.1016/j.matdes.2017.03.065>

[34] Anderson I (2017) Mechanical Properties of Specimens 3D Printed with Virgin and Recycled Polylactic Acid. *3D Printing and Additive Manufacturing* 4:110–115.

<https://doi.org/10.1089/3dp.2016.0054>

[35] Cicala G, Giordano D, Tosto C, et al (2018) Polylactide (PLA) Filaments a Biobased Solution for Additive Manufacturing: Correlating Rheology and

Thermomechanical Properties with Printing Quality. *Materials* 11:1191.

<https://doi.org/10.3390/ma11071191>

[36] Lee CH, Padzil FNBM, Lee SH, et al (2021) Potential for Natural Fiber Reinforcement in PLA Polymer Filaments for Fused Deposition Modeling (FDM) Additive Manufacturing: A Review. *Polymers* 13:1407. <https://doi.org/10.3390/polym13091407>

[37] Maqsood N, Rimašauskas M (2021) Delamination observation occurred during the flexural bending in additively manufactured PLA-short carbon fiber filament reinforced with continuous carbon fiber composite. *Results in Engineering* 11:100246.

<https://doi.org/10.1016/j.rineng.2021.100246>

[38] Liu W, Huang H, Zhu L, Liu Z (2021) Integrating carbon fiber reclamation and additive manufacturing for recycling CFRP waste. *Composites Part B: Engineering* 215:.

<https://doi.org/10.1016/j.compositesb.2021.108808>

[39] Farah S, Anderson DG, Langer R (2016) Physical and mechanical properties of PLA, and their functions in widespread applications — A comprehensive review.

*Advanced Drug Delivery Reviews* 107:367–392

[40] Hu Z, Karki R (2015) Prediction of mechanical properties of three-dimensional fabric composites reinforced by transversely isotropic carbon fibers. *Journal of Composite Materials* 49:1513–1524. <https://doi.org/10.1177/0021998314535960>

[41] de Groot R, Peters MCRB, de Haan' YM, et al (1987) Failure Stress Criteria for Composite Resin

[42] Ramalho A, Ferraz M, Gaspar M, Capela C (2020) Development of a preliminary finite element model to assess the effects of friction on the residual limb of a transfemoral amputee. *Materials Today: Proceedings* 33:1859–1863.

<https://doi.org/https://doi.org/10.1016/j.matpr.2020.05.199>

[43] Ramalho A, Ferraz M, Gaspar M, Capela C (2022) Influence of Materials and their Constitutive Laws on the Stress Fields produced in the Residual Limb of a Transfemoral Amputation. *Lecture Notes in Mechanical Engineering* - In Press

[44] Lin C-C, Chang C-H, Wu C-L, et al (2004) Effects of liner stiffness for trans-tibial prosthesis: a finite element contact model. *Medical Engineering & Physics* 26:1–9.

[https://doi.org/10.1016/S1350-4533\(03\)00127-9](https://doi.org/10.1016/S1350-4533(03)00127-9)

- [45] Sicomin (2015) SR GreenPoxy 56 Technical Datasheet
- [46] MSC Software Corporation (2018) Marc 2018.0 Theory and User Information. Newport Beach, CA 92660 USA:
- [47] Portnoy S, Siev-Ner I, Shabshin N, Gefen A (2011) Effects of sitting postures on risks for deep tissue injury in the residuum of a transtibial prosthetic-user: a biomechanical case study. *Computer Methods in Biomechanics and Biomedical Engineering* 14:1009–1019. <https://doi.org/10.1080/10255842.2010.504719>
- [48] Łagan S, Liber-Kneć A (2018) The determination of mechanical properties of prosthetic liners through experimental and constitutive modelling approaches. *Czasopismo Techniczne* 3:197–209. <https://doi.org/10.4467/2353737XCT.18.048.8343>
- [49] Shokrieh MM, Moshrefzadeh-Sani H (2016) On the constant parameters of Halpin-Tsai equation. *Polymer* 106:14–20. <https://doi.org/10.1016/j.polymer.2016.10.049>
- [50] MSC Patran (2008) Materials Application - Theory - Composite Materials. In: Patran 2008 r1, Reference Manual Part 4: Functional Assignments. Santa Ana, CA 92707 USA, pp 88–160
- [51] Shacham S, Castel D, Gefen A (2010) Measurements of the Static Friction Coefficient Between Bone and Muscle Tissues. *Journal of Biomechanical Engineering* 132:1–4. <https://doi.org/10.1115/1.4001893>
- [52] Ivarsson B, Crandall J, Hall G (2004) Biomechanics. In: F. Kreith (ed) *Handbook of Mechanical Engineering*, 2nd ed. CRC Press, Boca Raton
- [53] Anderson I (2017) Mechanical Properties of Specimens 3D Printed with Virgin and Recycled Polylactic Acid. *3D Printing and Additive Manufacturing* 4:110–115. <https://doi.org/10.1089/3dp.2016.0054>
- [54] Raghava S, Caddell RM, Yeh G S Y (1973) The macroscopic yield behaviour of polymers. *Journal of Materials Science* 8:225–232. <https://doi.org/https://doi.org/10.1007/BF00550671>
- [55] Caddell RM, Raghava RS, Atkins AG (1974) Pressure dependent yield criteria for polymers. *Materials Science and Engineering* 13:113–120. [https://doi.org/https://doi.org/10.1016/0025-5416\(74\)90179-7](https://doi.org/https://doi.org/10.1016/0025-5416(74)90179-7)

[56] matweb.com (2021) <http://www.matweb.com/reference/compressivestrength.aspx>

[57] polymerdatabase.com (2021)

<http://polymerdatabase.com/Commercial%20Polymers/PP.html>

[58] Perrier A (2016) Influence du vieillissement hydrique sur le comportement mécanique de l'interface fil/matrice dans les composites chanvre/époxy. Chanvre/Époxy. L'École Nationale Supérieure de Mécanique et D'Aérotechnique

[59] makerbot.com (2021)

[https://downloads.makerbot.com/legal/MakerBot\\_R\\_\\_PLA\\_and\\_ABS\\_Strength\\_Data.pdf](https://downloads.makerbot.com/legal/MakerBot_R__PLA_and_ABS_Strength_Data.pdf)

## 6. Summary, Discussion and Conclusions

Some partial goals were defined to try to answer the question that was raised by the defined research gap. Through the development of specific exploratory research-studies, which resulted in four publications, an attempt was made to answer each envisaged goal.

### Summary and Discussion

The preliminary model of the biomechanical system carried out in the **first paper** allowed for the development of three numerical models that demonstrated that, in general, the greatest stresses in the biological parts were located in the proximal part of the soft tissues, near the liner, due to friction. The third developed model revealed that the normal stresses were more evenly distributed across these surfaces when compared to what was observed in the first and second models. In addition, the shear stresses for the same model were significantly lower than for the other ones. These disparities can be justified by the preload that was considered only in the third model, which affected the stress distributions within the soft tissues. As shear stresses are one of the main causes of injuries in this type of prosthetic devices, the obtained results positively affect the patient's comfort and health.

The development of an improved model of the biomechanical system, as well as the definition of more realistic mechanical and tribological properties of the materials made in the **second and third papers**, resulted in simulations that made it possible to compare the effect of the constitutive laws on the stress field produced across the entire system.

The improved model was obtained by the segmentation of a patient's medical image of the stump. However, this could also be achieved using low-cost home-available devices, such as using a flatbed scanner. Casting a patient's stump could be performed to obtain a true geometry of the stump. Then, by removing the plaster and sawing it in half, it could be possible to get the needed profile to be scanned along with a ruler next to it, as to help obtain a real scale. Using the image obtained by the scanner, it would be possible to segment the points to obtain a real 2D profile, similar to that developed by segmenting a medical image of a patient's stump. In addition, although it is outside the scope of this exploratory study,

one could saw the plaster into four or even eight equal parts to obtain several sections that would provide more information for the creation of a more accurate geometry/model.

Simulations performed with the hyperelastic models have shown that, at the biological tissue level, the highest normal stresses occurred at the interface between the femur and the soft tissues (at the distal part of the femur) for the Neo-Hookean model, and between the liner and the soft tissues (at the distal part of the stump) for the Ogden model. Regarding shear stresses, the highest occurred at the interface between the liner and the soft tissues (at the proximal part of the liner) both for the Neo-Hookean and Ogden models. It could also be observed that for the Ogden model, in the area where the normal stresses were the highest, the shear stresses were negligible since there was no slip.

Simulations carried out with each of the considered materials – polypropylene thermoplastic and SR GreenPoxy 56 – have shown that the stresses occurring at the level of the prosthesis exceeded their strength. Thus, a composite material consisting of the more sustainable SR GreenPoxy 56 material reinforced with natural jute fibers had to be considered for further simulations to be performed. These simulations have shown that the overall reduction of friction between the liner and the soft tissues has somewhat consistently reduced the shear stresses at that same interface.

At last, the comparison between the performed simulations for the hyperelastic numerical models with their equivalent elastic models have shown that, at the biological tissues level, a significant decrease in the normal contact stresses and a slight increase in the shear contact stresses were observed. These results have shown that the constitutive laws used to characterize the involved materials significantly influence the developed contact stress fields in the biomechanical system, results that can be justified by the fact that biological tissues represent most of the volume of the present numerical model.

The attempt to select sustainable biopolymers to produce customized prosthetic sockets led to the development of the **fourth and final paper**.

To evaluate the suitability of different materials to this type of medical application, an adaptation of the previously developed model was made, and some more numerical simulations were performed. Six different materials were considered: one conventional thermoplastic polymer (polypropylene) and five different eco-materials, namely a bioepoxy

resin SR GreenPoxy 56 without reinforcement and with a 40% natural jute fibers reinforcement, and a recycled PLA biopolymer without reinforcement and with a 20% and 30% carbon fibers reinforcement.

The carried-out simulations have shown that the highest stress levels were consistently located at the lower end of the socket-type prosthesis. As such, the critical nodes of the numerical model for that area were analyzed. This analysis revealed that only the composites SR GreenPoxy 56 reinforced with 40% natural jute fibers and recycled PLA biopolymer reinforced with 30% carbon fibers safely met the requirements to support the loads involved in this application. However, the shear stresses observed for the former composite proved to be significantly higher than for the latter. Given this fact, and since the SR GreenPoxy 56 composite cannot be made into an extrudable filament for application in additive manufacturing processes, the recycled PLA biopolymer reinforced with 30% carbon fibers exhibited the most promising results.

## **Conclusions**

Since this was an exploratory study, the methodology of this work was not fully defined, so there could be different or improved methods for carrying it out. Nevertheless, the objectives set for this preliminary study were generally well accomplished.

This research allowed for the development of both a preliminary finite element model, and a subsequently improved model, that have proven to be effective when assessing the effects of friction on the residual limb of a transfemoral amputee. The results obtained made it possible to evaluate the influence that the coefficient of friction between the components that make up the whole biomechanical system - prosthesis, liner, soft tissue, and femur - has on the distribution of the developed contact stress field, thus affecting the patient's comfort and health.

The carried out numerical simulations result has proven that materials and their constitutive laws do indeed have a great influence on the developed contact stress field. It also contributed to correctly define the properties of all the materials that constitute the biomechanical model, and to assess the suitability of the considered materials.

Lastly, some of the considered materials have shown great potential to be used for the manufacture of socket-type prostheses, namely the composites of SR GreenPoxy 56 reinforced with 40% natural jute fibers and recycled PLA biopolymer reinforced with 30% carbon fibers. However, the latter has proved to be the most appropriate for the present case study since it can be transformed in filament form. This opens the possibility of producing customized parts of a prosthetic device using low-cost home-available additive manufacturing processes.

### **Future Work**

We realize that the accomplished study may be only the beginning of a broader study. As a next step, it would be relevant to make the transition from the theory to the reality through experimental preparations, to compare and evaluate in practical terms the results obtained.



The previously presented flowchart can be improved to incorporate some steps to be carried out in a future work (Figure 16).

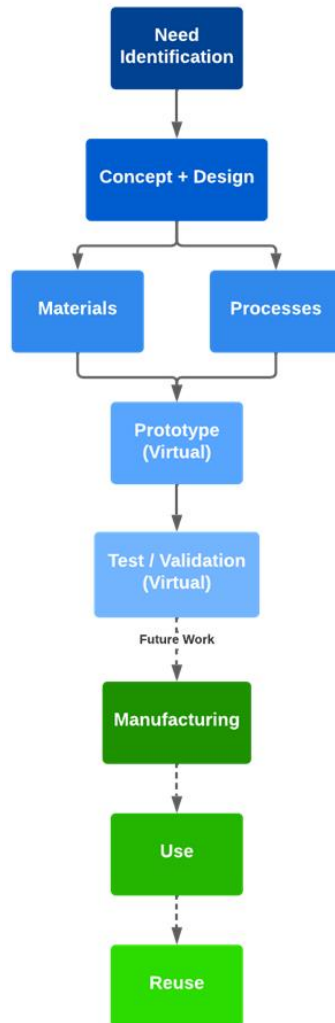


**Figure 16** - Improved flowchart that encompasses possible steps for the development of future work.

Firstly, it would be relevant to try to manufacture the sustainable material that exhibited promising results for the biomedical application at stake, as is the case of the composite of recycled bio-polymer PLA reinforced with 30% short carbon fibers, and to transform it in filament form so that it could be used with additive manufacturing technologies, such as Fused Deposition Modelling (FDM). Furthermore, despite being outside the scope of this study, it could also be interesting to produce the composite of SR GreenPoxy 56 reinforced with 40% jute fibers, as it has also shown very positive results and consists in a more environmentally friendly material.

With the manufacture of the most promising composite for this study, a real prototype could be built to assess the results obtained through the various carried out simulations. Should the experimental procedures show positive results, one could move on to a patient's use of a customized socket-type prosthesis made with home-available low-cost additive manufacturing technologies.

Finally, being a sustainable material in which its properties are not significantly affected by the thermal cycles of the recycling process, it could be milled for new filament production, contributing to a circular economy.

## References

- Adams, R. C., Advani, S., Alman, D. E., Andressen, F. R., Armstrong, K. B., Astrom, B. T., & Bandyopadhyay, A. (2001). ASM Handbook Composites (Volume 21). In *Fiber Technology for Fiber-Reinforced Composites*. <https://doi.org/10.1016/B978-0-08-101871-2.00006-0>
- Adepu, S., Ramakrishna, S., Costa-Pinto, R., & Oliveira, A. L. (2021). *molecules* *Controlled Drug Delivery Systems: Current Status and Future Directions*. <https://doi.org/10.3390/molecules26195905>
- Akbari Aghdam, H., Sheikhabaei, E., Hajihashemi, H., Kazemi, D., & Andalib, A. (2019). The impacts of internal versus external fixation for tibial fractures with simultaneous acute compartment syndrome. *European Journal of Orthopaedic Surgery and Traumatology*, 29(1), 183–187. <https://doi.org/10.1007/s00590-018-2275-y>
- Ambrosio, L. (2017). *Biomedical composites* (Second). Woodhead Publishing, Elsevier. <https://doi.org/https://doi.org/10.1016/C2015-0-02024-X>
- Anderson, I. (2017). Mechanical Properties of Specimens 3D Printed with Virgin and Recycled Polylactic Acid. *3D Printing and Additive Manufacturing*, 4(2), 110–115. <https://doi.org/10.1089/3dp.2016.0054>
- Bahl, S. (2020). Fiber reinforced metal matrix composites - A review. *Materials Today: Proceedings*, 39, 317–323. <https://doi.org/10.1016/j.matpr.2020.07.423>
- Bansal, N. P., & Lamon, J. (2014). *Ceramic Matrix Composites: Materials, Modeling and Technology*. Wiley. <https://doi.org/10.1002/9781118832998>
- Barbero, E. J. (2017). *Introduction to Composite Materials Design* (Third). CRC Press. <https://doi.org/https://doi.org/10.1201/9781315296494>
- Berthelot, J.-M., & Cole, M. (199 C.E.). *Composite Materials: Mechanical Behavior and Structural Analysis*. Springer. <https://doi.org/https://doi.org/10.1007/978-1-4612-0527-2>
- Chawla, K. K. (2012). *Composite Materials: Science and Engineering* (Third). Springer. <https://doi.org/https://doi.org/10.1007/978-0-387-74365-3>
- Day, M. C., Wadey, R., & Strike, S. (2019). Living with limb loss: everyday experiences of “good” and “bad” days in people with lower limb amputation. *Disability and Rehabilitation*, 41(20), 2433–2442. <https://doi.org/10.1080/09638288.2018.1467502>

- Francis, L. F., Stadler, B. J. H., & Roberts, C. C. (2016). *Materials Processing*. Academic Press.
- Freiman, S. W., & Mecholsky, J. J. (2019). *The Fracture of Brittle Materials: Testing and Analysis* (2nd Edition). Wiley.
- Fujihara, K., Teo, K., Gopal, R., Loh, P. L., Ganesh, V. K., Ramakrishna, S., Foong, K. W. C., & Chew, C. L. (2004). Fibrous composite materials in dentistry and orthopaedics: Review and applications. In *Composites Science and Technology* (Vol. 64, Issue 6, pp. 775–788). Elsevier BV. <https://doi.org/10.1016/j.compscitech.2003.09.012>
- Gay, D. (2014). *Composite Materials: Design and Applications* (third). CRC Press. <https://doi.org/10.1177/0892705714554493>
- Gebreslassie, B., Gebreselassie, K., & Esayas, R. (2018). Patterns and Causes of Amputation in Ayder Referral Hospital, Mekelle, Ethiopia: A Three-Year Experience. *Ethiopian Journal of Health Sciences*, 28(1), 31–36. <https://doi.org/10.4314/ejhs.v28i1.5>
- Gholampour, A., & Ozbakkaloglu, T. (2020). A review of natural fiber composites: properties, modification and processing techniques, characterization, applications. In *Journal of Materials Science* (Vol. 55, Issue 3, pp. 829–892). Springer New York LLC. <https://doi.org/10.1007/s10853-019-03990-y>
- Gibson, R. F. (2016). *Principles of Composite Material Mechanics, Fourth Edition* (Fourth). CRC Press.
- Guo, Z., Poot, A. A., & Grijpma, D. W. (2021). Advanced polymer-based composites and structures for biomedical applications. In *European Polymer Journal* (Vol. 149). Elsevier Ltd. <https://doi.org/10.1016/j.eurpolymj.2021.110388>
- Hsissou, R., Seghiri, R., Benzekri, Z., Hilali, M., Rafik, M., & Elharfi, A. (2021). Polymer composite materials: A comprehensive review. *Composite Structures*, 262, 113640. <https://doi.org/10.1016/J.COMPSTRUCT.2021.113640>
- Huang, H. M. (2020). Medical application of polymer-based composites. In *Polymers* (Vol. 12, Issue 11, pp. 1–5). MDPI AG. <https://doi.org/10.3390/polym12112560>
- Jayamani, E., Jie, T. J., & bin Bakri, M. K. (2021). Life cycle assessment of sustainable composites. In *Advances in Sustainable Polymer Composites* (pp. 245–265). Elsevier. <https://doi.org/10.1016/b978-0-12-820338-5.00011-4>
- Junqueira, D. M., Gomes, G. F., Silveira, M. E., & Ancelotti, A. C. (2019). Design Optimization and Development of Tubular Isogrid Composites Tubes for Lower Limb Prosthesis. *Applied Composite Materials*, 26(1), 273–297. <https://doi.org/10.1007/s10443-018-9692-2>

- Karuppiah, A. (2016). *Predicting The Influence of Weave Architecture on the Stress Relaxation Behavior of Woven Composite Using Finite Element Based Micromechanics*. <https://doi.org/10.13140/RG.2.2.17881.16482>
- Krauklis, A. E., Karl, C. W., Gagani, A. I., & Jørgensen, J. K. (2021). Composite material recycling technology—state-of-the-art and sustainable development for the 2020s. In *Journal of Composites Science* (Vol. 5, Issue 1). MDPI AG. <https://doi.org/10.3390/jcs5010028>
- Krishnakumar, S., & Senthilvelan, T. (2021). Polymer composites in dentistry and orthopedic applications-a review. *Materials Today: Proceedings*, 46, 9707–9713. <https://doi.org/10.1016/j.matpr.2020.08.463>
- Kumar, D. (2019). Manufacturing Processes and Applications of Composites Materials. *International Research Journal of Engineering and Technology*. <https://doi.org/10.15660/AUOFMTE.2010-2.1896>
- Lee, D. E., Koo, H., Sun, I. C., Ryu, J. H., Kim, K., & Kwon, I. C. (2012). Multifunctional nanoparticles for multimodal imaging and theragnosis. *Chemical Society Reviews*, 41(7), 2656–2672. <https://doi.org/10.1039/c2cs15261d>
- Lim Goh, K., Thilan De Silva, R., & Thomas, S. (2020). *Interfaces in Particle and Fibre Reinforced Composites: Current Perspectives on Polymer, Ceramic, Metal and Extracellular Matrices*. Woodhead Publishing. <https://doi.org/https://doi.org/10.1016/C2017-0-03930-7>
- Liu, S., Qin, S., He, M., Zhou, D., Qin, Q., & Wang, H. (2020). Current applications of poly(lactic acid) composites in tissue engineering and drug delivery. In *Composites Part B: Engineering* (Vol. 199). Elsevier Ltd. <https://doi.org/10.1016/j.compositesb.2020.108238>
- Maghsoudi-Ganjeh, M., Lin, L., Wang, X., & Zeng, X. (2019). Bioinspired design of hybrid composite materials. *International Journal of Smart and Nano Materials*, 10(1), 90–105. <https://doi.org/10.1080/19475411.2018.1541145>
- Maji, P. K., Banerjee, A. J., Banerjee, P. S., & Karmakar, S. (2014). Additive manufacturing in prosthesis development - A case study. *Rapid Prototyping Journal*, 20(6), 480–489. <https://doi.org/10.1108/RPJ-07-2012-0066>
- makerbot.com. (2021, October 18). [https://downloads.makerbot.com/legal/MakerBot\\_R\\_\\_PLA\\_and\\_ABS\\_Strength\\_Data.pdf](https://downloads.makerbot.com/legal/MakerBot_R__PLA_and_ABS_Strength_Data.pdf).
- matweb.com. (2021, October 18). <http://www.matweb.com/reference/compressivestrength.aspx>.

- Mazumder, S., Nayak, A. K., Ara, T. J., & Hasnain, M. S. (2019). Hydroxyapatite composites for dentistry. In *Applications of Nanocomposite Materials in Dentistry* (pp. 123–143). Elsevier. <https://doi.org/10.1016/B978-0-12-813742-0.00007-9>
- McKeen, L. W. (2019). *The Effect of UV Light and Weather on Plastics and Elastomers (Fourth Edition): Introduction to Plastics and Polymers* (Fourth Edition, pp. 1–20). William Andrew. <https://doi.org/10.1016/B978-0-12-816457-0.00001-0>
- Pasăre, M. M., Luca, L., & Dimitrov, R. (2019). Aspects of Composite Materials Evolution. *Fiability & Durability / Fiabilitate Si Durabilitate*, 55–59. [https://web.archive.org/web/20201124111609id\\_/https://www.utgjiu.ro/rev\\_mec/mecanica/pdf/2019-02/07\\_DIMITROV.pdf](https://web.archive.org/web/20201124111609id_/https://www.utgjiu.ro/rev_mec/mecanica/pdf/2019-02/07_DIMITROV.pdf)
- Moura, M. F. S. F. de, Morais, A. B. de, & Magalhães, A. G. de. (2009). *Materiais Compósitos: Materiais, Fabrico e Comportamento Mecânico* (2<sup>a</sup>). Publindústria.
- Nasar, A. (2019). Hydroxyapatite and its coatings in dental implants. In *Applications of Nanocomposite Materials in Dentistry* (Issue ii). Elsevier Inc. <https://doi.org/10.1016/B978-0-12-813742-0.00008-0>
- Niendorf, K., & Raeymaekers, B. (2021). Additive Manufacturing of Polymer Matrix Composite Materials with Aligned or Organized Filler Material: A Review. In *Advanced Engineering Materials* (Vol. 23, Issue 4). John Wiley and Sons Inc. <https://doi.org/10.1002/adem.202001002>
- Nurhanisah, M. H., Hashemi, F., Paridah, M. T., Jawaid, M., & Naveen, J. (2018). Mechanical properties of laminated kenaf woven fabric composites for below-knee prosthesis socket application. *IOP Conference Series: Materials Science and Engineering*, 368(1). <https://doi.org/10.1088/1757-899X/368/1/012050>
- Nurhanisah, M. H., Saba, N., Jawaid, M., & Paridah, M. T. (2017). Design of prosthetic leg socket from kenaf fibre based composites. *Green Energy and Technology*, 0(9783319493817), 127–141. [https://doi.org/10.1007/978-3-319-49382-4\\_6](https://doi.org/10.1007/978-3-319-49382-4_6)
- Pellico, J., Gawne, P. J., & T. M. De Rosales, R. (2021). Radiolabelling of nanomaterials for medical imaging and therapy. In *Chemical Society Reviews* (Vol. 50, Issue 5, pp. 3355–3423). Royal Society of Chemistry. <https://doi.org/10.1039/d0cs00384k>
- Perrier, A. (n.d.). *Influence du vieillissement hydrique sur le comportement mécanique de l'interface fil/matrice dans les composites chanvre/époxy*. <https://tel.archives-ouvertes.fr/tel-01447566>
- polymerdatabase.com. (2021, October 18). <http://polymerdatabase.com/Commercial%20Polymers/PP.html>.

- Rakshit, R., & Das, A. K. (2019). A review on cutting of industrial ceramic materials. In *Precision Engineering* (Vol. 59, pp. 90–109). Elsevier Inc. <https://doi.org/10.1016/j.precisioneng.2019.05.009>
- Rathbone, M. J., Siegel, R. A., & Juergen, S. (2012). *Fundamentals and Applications of Controlled Release Drug Delivery*. Springer. <https://doi.org/10.1007/978-1-4614-0881-9>
- Reddy Nagavally, R. (2016). Composite Materials - History, Types, Fabrication Techniques, Advantages, And Applications. In *Proceedings of 29th IRF International Conference, Materials Science*.
- Saeedifar, M., & Zarouchas, D. (2020). Damage characterization of laminated composites using acoustic emission: A review. In *Composites Part B: Engineering* (Vol. 195). Elsevier Ltd. <https://doi.org/10.1016/j.compositesb.2020.108039>
- Sastri, V. R. (2013). *Plastics in Medical Devices: Properties, Requirements, and Applications* (Second). William Andrew, Elsevier. <https://doi.org/https://doi.org/10.1016/C2012-0-05946-7>
- Scholz, M. S., Blanchfield, J. P., Bloom, L. D., Coburn, B. H., Elkington, M., Fuller, J. D., Gilbert, M. E., Muflahi, S. A., Pernice, M. F., Rae, S. I., Trevarthen, J. A., White, S. C., Weaver, P. M., & Bond, I. P. (2011). The use of composite materials in modern orthopaedic medicine and prosthetic devices: A review. In *Composites Science and Technology* (Vol. 71, Issue 16, pp. 1791–1803). <https://doi.org/10.1016/j.compscitech.2011.08.017>
- Silva, M., Mateus, A., Oliveira, D., & Malça, C. (2017). An alternative method to produce metal/plastic hybrid components for orthopedics applications. *Proceedings of the Institution of Mechanical Engineers, Part L: Journal of Materials: Design and Applications*, 231(1–2), 179–186. <https://doi.org/10.1177/1464420716664545>
- Soemardi, T. P., Irawan, A. P., Soemardi, T. P., Widjajalaksmi, K., & Reksoprodjo, A. H. S. (2011). Tensile and Flexural Strength of Ramie Fiber Reinforced Epoxy Composites for Socket Prosthesis Application. *International Journal of Mechanical and Materials Engineering (IJMME)*, 6(1), 46–50.
- Stenvall, E., Flodberg, G., Pettersson, H., Hellberg, K., Hermansson, L., Wallin, M., & Yang, L. (2020). Additive manufacturing of prostheses using forest-based composites. *Bioengineering*, 7(3), 1–18. <https://doi.org/10.3390/bioengineering7030103>
- T. Hanawa, Yoshimitsu Okazaki, Sachiko Hiromoto, Mitsuo Niinomi, & Y. Yan. (2019). Metals for Biomedical Devices. In *Mitsuo Niinomi*. Woodhead Publishing, Elsevier. <https://doi.org/https://doi.org/10.1016/C2017-0-03429-8>

- Vitali, A., Regazzoni, D., Rizzi, C., & Colombo, G. (2017). Design and Additive Manufacturing of Lower Limb Prosthetic Socket. In *ASME 2017 International Mechanical Engineering Congress and Exposition*.  
<https://doi.org/10.1115/IMECE2017-71494>
- Wang, M., Nong, Q., Liu, Y., & Yu, H. (2021). Design of lower limb prosthetic sockets: a review. *Expert Review of Medical Devices*, 1–11.  
<https://doi.org/10.1080/17434440.2022.2020094>
- Wang, M., & Zhao, Q. (2018). Biomedical composites. In *Biomedical Composites* (p. 19). Elsevier Inc. <https://doi.org/10.1533/9781845697372>
- Yi, X., Du, S., & Zhang, L. (2018). *Composite Materials Engineering, Volume 1. Different Types of Composite Materials* (Vol. 1). <https://doi.org/10.1007/978-981-10-5696-3>



# Attachments

## Attachment 1



Available online at [www.sciencedirect.com](http://www.sciencedirect.com)

ScienceDirect

materialstoday:  
PROCEEDINGS

2020 The 10th International Conference on Key Engineering Materials

### Development of a preliminary finite element model to assess the effects of friction on the residual limb of a transfemoral amputee

Armando Ramalho<sup>a,b,1</sup>, Miguel Ferraz<sup>c</sup>, Marcelo Gaspar<sup>c</sup>,

Carlos Capela<sup>b,c</sup>

<sup>a</sup>*Polytechnic Institute of Castelo Branco, Castelo Branco, Portugal*

<sup>b</sup>*Centre for Mechanical Engineering, Materials and Processes (CEMMPRE), Coimbra, Portugal*

<sup>c</sup>*Polytechnic Institute of Leiria, Leiria, Portugal*

---

#### Abstract

The use of numerical modelling tools allows optimizing the development of complex anatomical artefacts, such as customized prostheses for lower limb amputees. These numerical tools make it possible to characterize the interfacial interactions taking place between different parts of the prosthesis and the residual limb. This allows for understanding which rectifications and fittings having to be made on the custom design of the artificial body part without the need for manufacturing and donning prostheses. To such end, current research focused on the development of a preliminary Finite Element Model to assess the effects of friction on the residual limb of a transfemoral amputee, as the friction on the contact between the soft tissues, the liner and the prosthesis of the amputee is of major importance for his/her health and comfort.

[copyright information to be updated in production process]

*Keywords: Finite Element Analysis; Prosthetic liner; Interfacial stresses; Amputee; Patient comfort and health; Customized medical devices.*

#### 1. Introduction

In the current paper, a preliminary study was carried out as part of a broader project that intends to use numerical modelling tools in order to optimize the development of customized prostheses for lower limbs of transfemoral amputees. The main goals of using the Finite Element Method (FEA) as a numerical modelling tool in the development of this prosthesis are the following: 1. Facilitate the understanding of the interfacial interaction between the different parts of the prosthesis and the residual limb; further, the field of stresses in the soft tissues is assessed to enable the evaluation of the stresses in areas not available in vivo studies. 2. Facilitate the prosthesis rectifications and fitting that enable the custom design without the need to build and donning prostheses; this process allows reducing the physical and psychological impact on the life of the patient. To help in the distribution and cushioning of the loads transferred between the socket and the soft tissues in the residual limb, soft prosthetic liners are usually interposed between both parts [1].

The aim of the FEA in this project is to assess the effect of the prosthetic liner material properties in the interfacial stresses between the parts of the prosthesis and the residual limb. The load distribution effect on the stresses generated inside the residual soft tissues will be also assessed.

---

<sup>1</sup> Corresponding author. Tel.: +351 272 339 300 fax: +351 272 339 301.  
E-mail address: [aramalho@ipcb.pt](mailto:aramalho@ipcb.pt)

The finite element model will be validated in specific geometries and through the clinical study of amputated patients. At this stage of the project, a patient with a transfemoral amputation was selected, and the necessary approvals are still being analyzed by the local ethics committees.

To generate the Finite Element Model (FEM) the following tasks will be carried-out:

1. Geometric modelling of the stump and the socket. The patient morphology acquired by medical images will be segmented using the software Matlab and Rhinoceros 3D, in order to obtain the stump and bones surfaces. The inner socket surface will be furnished by the cad manufacture software. The geometry of the liner will be inputted and parametrized.

2. Meshes. The surfaces will be imported to software MSC Patran were the solid model will be prepared, meshed and parameterized.

3. Material properties. The material properties obtained in the literature [2-4] will be adapted to the model taking into account the experimental results.

4. Boundary conditions – slip model. The contact-slip models in the literature [5] will be adapted to the model taking into account the experimental results.

5. Boundary conditions – loading. The loading will be done in two steps. In a first step will be simulated the donning and fitting of prosthesis [6]. In a second step were superimposed a loading taking into account the experimentally measured three-dimensional ground reaction forces and moments using a force platform while the patient walked – the forces and moments were transferred to the top surface of the bones [7, 8].

6. Procedures. The FEM will be run in the MSC Marc software.

7. Validation of the FEM. The model will be validated with the experimental results published in the literature [5, 7-10] and with the obtained experimental results.

In the current stage of this project, the anatomical characteristics of the patient cannot be used. Therefore, a preliminary study related to the above-mentioned task 4 was carried out. In this study, a preliminary FEA was developed to assess the effects of the friction coefficient on the contacts of the parts of the biomechanical model – socket, liner, stump and residual femoral bone – in the stress field at the stump. In fact, the friction coefficient on the contact between the soft tissues, the liner and the prosthesis of the amputee is of major importance for patient health and comfort. The effect of the friction coefficient on the positioning of the prosthesis was studied by W.C.C. Lee and M. Zhang [11]. The effect of the friction coefficient between the femur and soft tissues was studied by J.F. Ramirez and J.A. Vélez [10]. The importance of the liner in the patient's health and comfort drove many investigations [6, 12, 13]. Accurate assessment of stress distribution between the skin and prosthetic devices is also very important in robotics [14, 15]. In the current preliminary study, the effect of friction on the contact of all of these parts of the biomechanical model will be assessed.

## 2. Finite element model

The Finite Element Model used in this research was based on the one by M.B. Silver-Thorn and D.S. Childress [8], with a simplified and adapted geometry to the anatomical shapes of the patient, as well as to the scope of this preliminary study.

*Geometry.* In this exploratory research, the simplified geometry of the model (Fig.1.a) is an approximation to the patient's residual limb anthropometry, being the femur approximated to a spherical-end cylinder. Considering muscle atrophy, the simplified shape of the stump was considered as a conical trunk with its base on the distal end, a diameter of 160 mm and a 10-degree slope. The liner was modelled as a 6 mm thick conical surface fitted to the stump. Finally, the socket type prosthesis was also modelled as a conical surface fitted to the liner, with an overall thickness of 3 mm.

*Mechanical Properties of Materials.* The materials of current research - soft tissues, liner (pelite [3]), cortical bone [4] and prosthesis (propylene) - are all defined as an isotropic, homogeneous, and linear elastic material, that have an elastic modulus (E) and Poisson's ratio ( $\nu$ ) as follows: Soft tissues - E=0.06 MPa,  $\nu=0.45$  (approximately incompressible); Liner - E=0.38 MPa,  $\nu=0.49$  (approximately incompressible); Cortical bone - E=11.5 GPa,  $\nu=0.31$ ; Prosthesis - E=1 GPa,  $\nu=0.30$ .

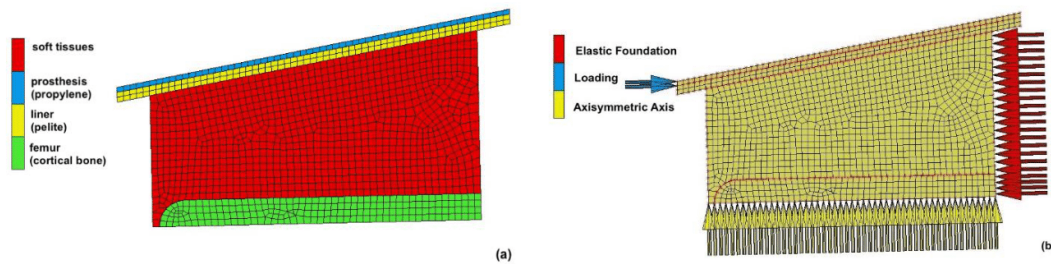


Fig. 1. (a) Numerical model geometry and materials; (b) Boundary conditions of the model.

**Boundary conditions.** An elastic foundation, with a stiffness value of  $E=0.06$  MPa, was considered for the proximal part of the model. This condition was intended to approximate the interaction of the stump with the rest of the body. To make contact modelling less dependent on the finite element mesh, the interaction between bodies was modelled using the segment-to-segment algorithm [16], which uses the Augmented Lagrangian constraint method that allows the contact between organic surfaces to be more efficiently approximated. Three numerical models were developed in order to assess the effect of the friction coefficients on the stresses developed at the biomechanical model's soft tissues:

- *Model 1* was based on a Coulomb's bilinear friction model, with an average friction coefficient between the cortical bone and the soft tissues of  $\mu=0.415$  [4]. A friction coefficient of  $\mu=0.6$  was also considered on the contact between the prosthesis and the liner [11], whilst for the contact between the liner and the soft tissues, the friction coefficient was of  $\mu=0.8$  [12].
- *Model 2* is similar to Model 1 and was created to validate the numerical model, allowing comparing the results with those of different authors [8, 10]. In this model, the contact between soft tissues and femur was modelled as glued.
- *Model 3* was based on Model 1 with a prestress in the liner, with both horizontal and vertical ring loads of 40 N. Distributing compressive stresses over the residual limb, particularly in sensitive regions with bony prominences, is desirable [6]. Some manufacturers customize their liner to impose these compressions in the donning process. The preload imposed in model 3 generates an initial pressure similar to that considered by that author.

**Loading.** The prosthesis is considered to support the patient's total weight (70 kgf), during the static stance. Loading is imposed quasi-static conditions [17], as illustrated in Fig.1.b.

**Finite element analysis.** Given the symmetry of the model, a 2D axisymmetric analysis was performed. This simplification allowed for a more efficient analysis with reduced computational cost. The simulations with this model were made using the implicit module of MSC Marc Mentat 2018. This method, when applied to models that suffer large deformations, can cause several convergence problems related to kinematic nonlinearities, mesh distortion, shear locking, etc. However, the implicit method allows for efficient use of contact models for materials with nonlinear constitutive relationships.

Current exploratory research is the preliminary foundation of a broader project that aims at developing dedicated FEA models of customized anatomic geometries and characterize the mechanical behaviour of constitutive materials. The numerical constrictions associated with the implicit method were overcome using mesh adaptivity algorithms. Due to the geometric complexity of the models at which this work aims being applied to, an automatic algorithm was used for meshing, and linear quadrilateral axisymmetric solid elements with four nodes (Quad 10) were used. The initial mesh dimensions of the elements were of 4 mm. This value was established in a previous iterative process and is considered as an objective in the adaptive mesh algorithm. In this process, the mesh size may be reduced to a quarter of its initial value, depending on the strain change and the distortion that may occur in each element.

### 3. Results and discussion

The von Mises stress distribution (in MPa), for Models 1, 2 and 3 are shown on Fig.2. It can be observed that for Model 1 (Fig.2.a) and Model 2 (Fig.2.b), in the biological parts, the highest stresses occur in the proximal part, for

the soft tissues near the liner. When compared with the results by other authors [8, 10] the numerical model can be validated. Whereas the geometry and loading are different, von Mises stresses have the same orders of magnitude and similar distributions, although in the present study the effect of friction between the prosthesis, liner and soft tissues is visible. The obtained results allow assessing the influence of the friction coefficient between the prosthesis, the liner and the soft tissues on the stress distribution of the whole biomechanical system.

In Model 3 (Fig.2.c), at the soft tissues, the highest stresses occur in the proximal part, near the liner. When compared with previous Model 1 and 2, in Model 3 one can observe that the von Mises stress is higher. From the analysis of the von Mises stress distribution, we cannot conclude about the influence of friction between the bodies in the biomechanical model.

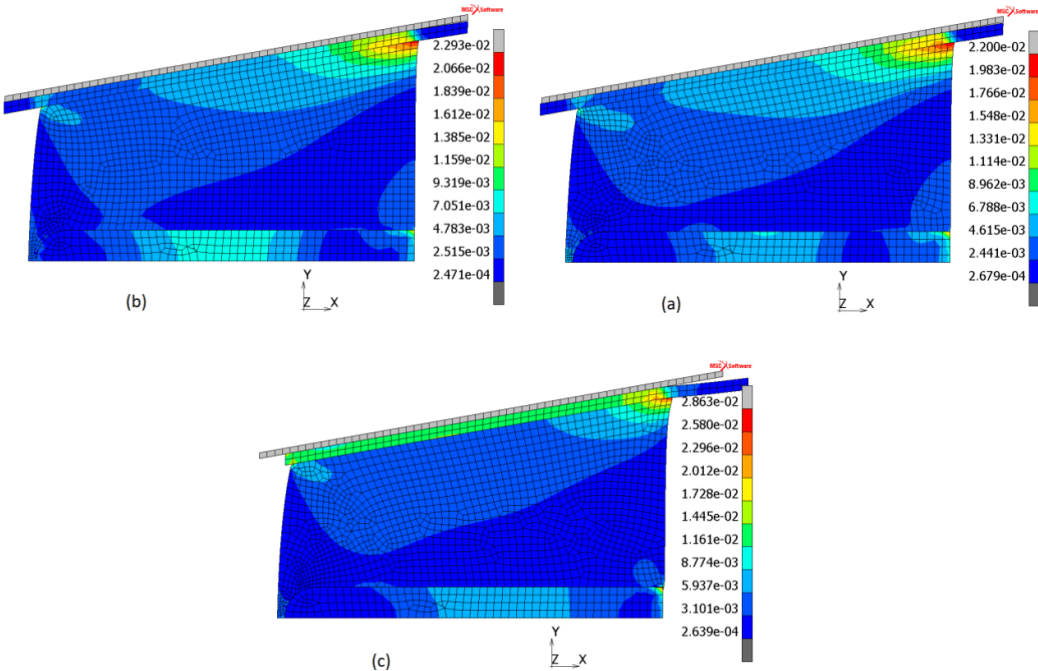


Fig. 2. (a) Von Mises stress distribution (MPa) for Model 1; (b) for Model 2; (c) and for Model 3.

Fig.3 shows the normal and shear contact stresses, between all the solids, for Model 1. Both images plot the contact stresses between the prosthesis and the liner, between the soft tissues and the liner, as well as between the soft tissues and the patients' femur. Fig.3.a presents the normal stresses for Model 1, whereas Fig.3.b show the tangential stresses for the same Model.

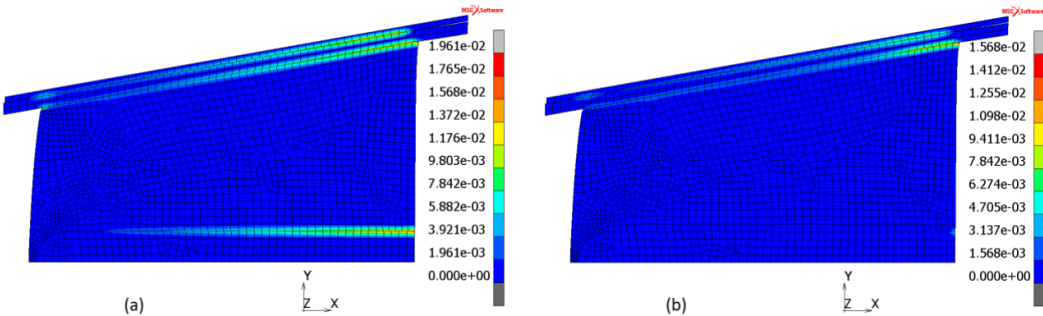


Fig. 3. (a) Normal contact stresses for Model 1; (b) Shear contact stresses of Model 1.



Fig.4 presents the normal and shear contact stresses, between all the solids, for Model 2. In Fig.4.a, normal stresses between the prosthesis and the liner, between the soft tissues and the liner, as well as between the soft tissues and the patients' femur can be observed. Fig.4.b shows the shear stresses that occur between the same biological solids of the patient.

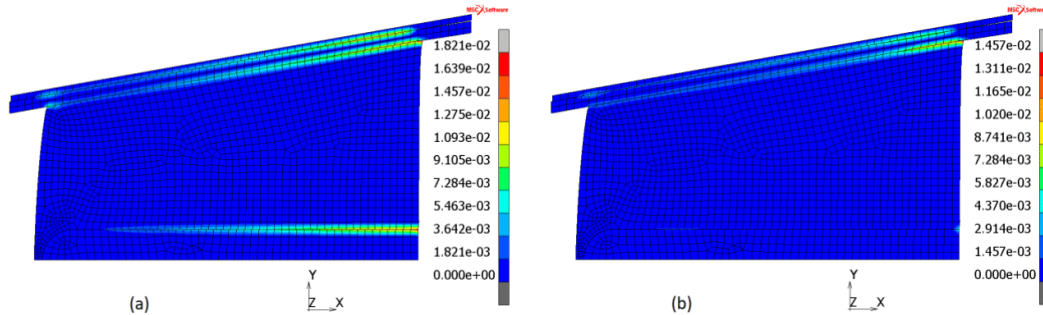


Fig. 4. (a) Normal contact stresses for Model 2; (b) Shear contact stresses of Model 2.

When compared, at the biological solids' interfaces, the normal and shear contact stress distribution for both Model 1 (Fig.3) and Model 2 (Fig.4) show to be similar. However, for Model 2 (Fig.4), the stress distribution in the soft tissues near the femur and the liner is more homogeneous than for Model 1 (Fig.3), and the influence of stress has a less superficial effect, extending to deeper layers.

For Model 3, the normal and shear contact stresses, between all the solids, are presented in Fig.5. As for previous Model 1 (Fig.3) and Model 2 (Fig.4), both images plot the contact stresses between the prosthesis and the liner, between the soft tissues and the liner, as well as between the soft tissues and the patients' femur. Fig.5.a presents the normal stresses for Model 3, whereas Fig.5.b show the shear stresses for the same Model.

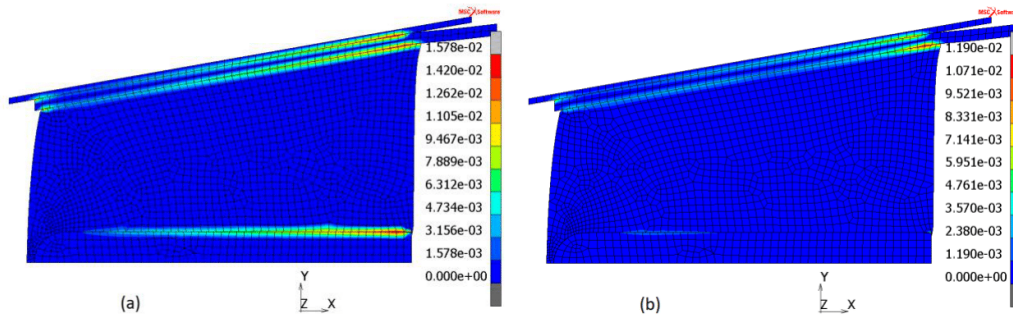


Fig. 5. (a) Normal contact stresses for Model 3; (b) Shear contact stresses of Model 3.

When observing Fig.5.a, on Model 3, the normal stresses are evenly distributed over the entire surface of the liner and much of the surface of the femur, than those of Model 1 (Fig.3.a) and Model 2 (Fig.4.a). When analyzing the shear stresses that take place between contacting bodies on Model 3 (Fig.5.b), these show to be significantly lower than those of Model 1 (Fig.3.b) and Model 2 (Fig.5.b). This 24% shear contact stress reduction is due to the effect of the prestress on the liner that affects the stress distribution inside the soft tissues. This positively affects the patient's comfort and health, as shear stresses are one of the main cause of injuries on this type of prosthetic devices [18].

#### 4. Conclusions

The developed Finite Element Model reveals to be effective when assessing the effects of friction on the residual limb of a transfemoral amputee.

The results obtained allow evaluating the influence of the friction coefficient between the prosthesis, the liner and the soft tissues on the stress distribution of the whole biomechanical system.

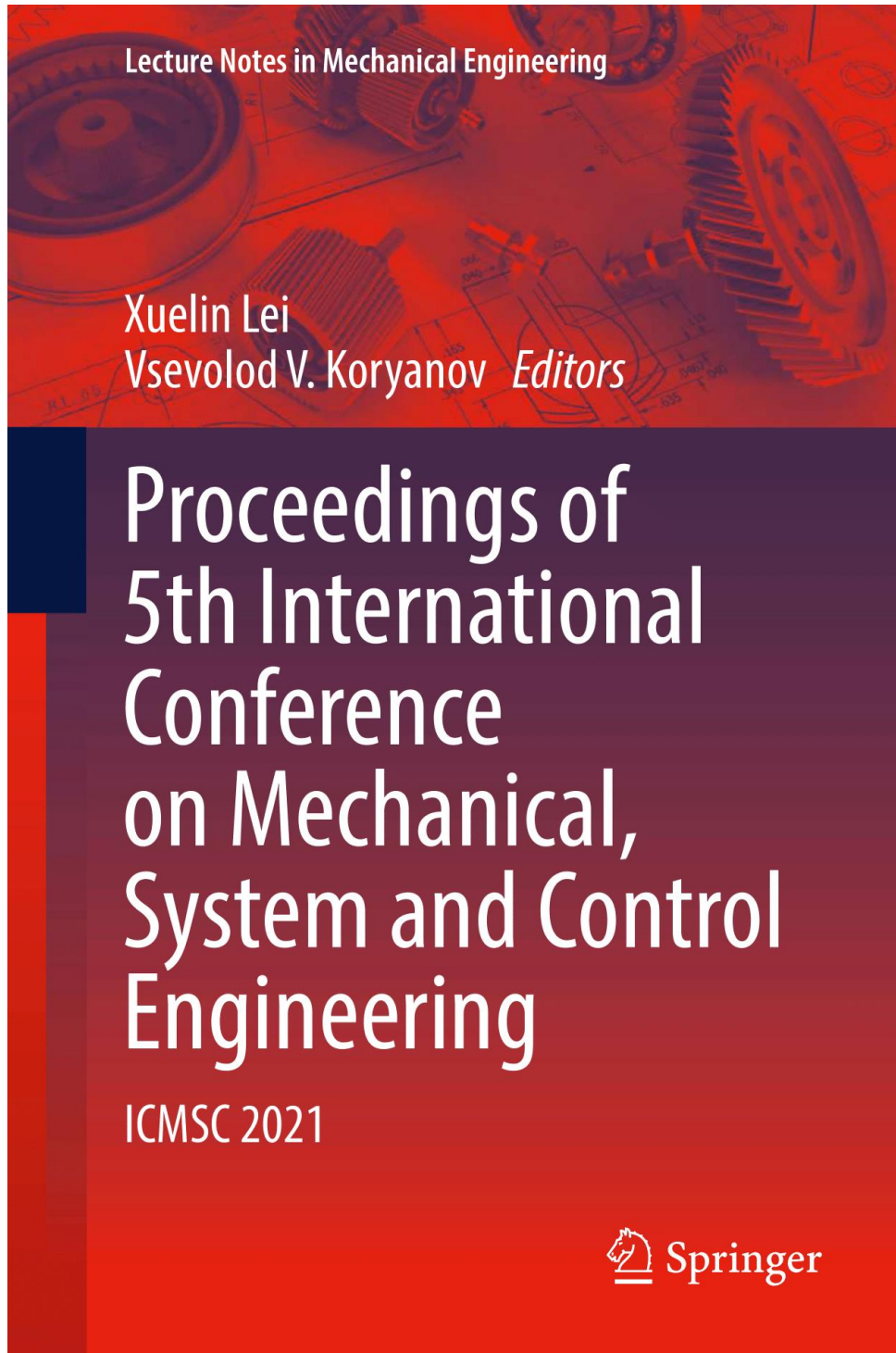
The friction between the bodies of the biomechanical model has a great influence on the stress distribution that takes place in the soft tissues, thus enhancing or compromising the patient's comfort and health.

The FEA Model 3, with a prestress on the liner, improves the effect of friction on the biomechanical model. The uniform pressure in the contact between the liner and the soft tissues due to the prestress lowers the contact shear stresses, which is one of the main causes of injuries on patients using this type of prosthetic devices.

#### References


- [1] Klute, Glenn K., Brian C. Glaister and Jocelyn S. Berge. "Prosthetic liners for lower limb amputees: A review of the literature." *Prosthetics and Orthotics International* 34(2) (2010) 146-153.
- [2] Sanders, Joan E., Brian S. Nicholson, Santosh G. Zachariah, Damon V. Cassisi, Ari Karchin and John R. Fergason. "Testing of elastomeric liners used in limb prosthetics: Classification of 15 products by mechanical performance." *Journal of Rehabilitation Research & Development* 41(2) (2004) 175-186.
- [3] Steege, J. W. and D.S. Schnur. "Prediction of pressure in the below knee socket interface by finite element analysis." *ASME Symposium on Biomechanics of Normal and Pathological Gait* 1987.
- [4] Ivarsson, B. J., J. R. Crandall, G. W. Hall and W. D. Pilkey. "Biomechanics", in: F. Kreith (Ed.) *Handbook of Mechanical Engineering* (2004) CRC Press, Boca Raton.
- [5] Lee, Winson C. C., Ming Zhang, David A. Boone and Bill Contoyannis. "Finite element analysis to determine the effect of monolimb flexibility on structural strength and interaction between residual limb and prosthetic socket." *Journal of Rehabilitation Research & Development* 41(6A) (2004) 775-786.
- [6] Boutwell, Erin, Rebecca Stine, Andrew Hansen, Kerice Tucker and Steven Gard. "Effect of prosthetic gel liner thickness on gait biomechanics and pressure distribution within the transtibial socket." *Journal of Rehabilitation Research & Development* 49(2) (2012) 227-240.
- [7] Jiaa, Xiaohong, Ming Zhanga and Winson C. C. Lee. "Load transfer mechanics between trans-tibial prosthetic socket and residual limb – dynamic effects." *Journal of Biomechanics* 37 (2004) 1371-1377.
- [8] Silver-Thorn, M. Barbara and Dudley S. Childress. "Parametric Analysis Using the Finite Element Method to Investigate Prosthetic Interface Stresses for Persons with Trans-tibial Amputation." *Journal of Rehabilitation Research and Development* 33(3) (1996) 227-238.
- [9] Sanders, Joan E. and Colin H. Daly. "Normal and shear stresses on a residual limb in a prosthetic socket during ambulation: Comparison of finite element results with experimental measurements." *Journal of Rehabilitation Research & Development* 30(2) (1993) 191-204.
- [10] Ramirez, Juan Fernando and Jaime Andrés Vélez. "Incidence of the boundary condition between bone and soft tissue in a finite element model of a transfemoral amputee." *Prosthetics and Orthotics International* 36(4) (2012) 405-414.
- [11] Lee, Winson C. C. and Ming Zhang. "Using computational simulation to aid in the prediction of socket fit: a preliminary study." *Med Eng Phys* 29(8) (2007) 923-929.
- [12] Cavaco, A., A. Ramalho, S. Pais and L. Durães. "Mechanical and structural characterization of tibial prosthetic interfaces before and after aging under simulated service conditions." *Journal of the Mechanical Behavior of Biomedical Materials* 43C (2014) 78-90.
- [13] Derler, S., G. U. Schrade and L.-C. Gerhardt. "Tribology of human skin and mechanical skin equivalents in contact with textiles." *Wear* 263(7-12) (2007) 1112-1116.
- [14] Misra, S., K. B. Reed, B. W. Schafer, K. T. Ramesh and A. M. Okamura. "Mechanics of Flexible Needles Robotically Steered through Soft Tissue." *Int J Rob Res.* 29(13) (2010) 1640-1660.
- [15] Pacchierotti, C., L. Meli, F. Chinello, M. Malvezzi and D. Prattichizzo. "Cutaneous haptic feedback to ensure the stability of robotic teleoperation systems." *Int J Rob Res.* 34(14) (2015) 1773-1787.
- [16] Laursen, T. A. and J. C. Simo. "Algorithmic symmetrization of Coulomb frictional problems using augmented Lagrangians." *Computer Methods in Applied Mechanics and Engineering*, 108 (1993) 133-146.
- [17] Lin, Chih-Chieh, Chih-Han Chang, Chu-Lung Wu, Kao-Chi Chung and I-Chen Liao. "Effects of liner stiffness for trans-tibial prosthesis: a finite element contact model." *Med Eng Phys* 26(1) (2004) 1-9.
- [18] Sanders, Joan E., Colin H. Daly and Ernest M. Burgess. "Interface shear stresses during ambulation with a below-knee prosthetic limb." *Journal of Rehabilitation Research & Development* 29(4) (1992) 1-8.

## Attachment 2




## Lecture Notes in Mechanical Engineering

### Series Editors

Francisco Cavas-Martínez , Departamento de Estructuras, Construcción y Expresión Gráfica Universidad Politécnica de Cartagena, Cartagena, Murcia, Spain

Fakher Chaari, National School of Engineers, University of Sfax, Sfax, Tunisia

Francesca di Mare, Institute of Energy Technology, Ruhr-Universität Bochum, Bochum, Nordrhein-Westfalen, Germany

Francesco Gherardini , Dipartimento di Ingegneria “Enzo Ferrari”, Università di Modena e Reggio Emilia, Modena, Italy

Mohamed Haddar, National School of Engineers of Sfax (ENIS), Sfax, Tunisia

Vitalii Ivanov, Department of Manufacturing Engineering, Machines and Tools, Sumy State University, Sumy, Ukraine

Young W. Kwon, Department of Manufacturing Engineering and Aerospace Engineering, Graduate School of Engineering and Applied Science, Monterey, CA, USA

Justyna Trojanowska, Poznan University of Technology, Poznan, Poland



**Lecture Notes in Mechanical Engineering (LNME)** publishes the latest developments in Mechanical Engineering—quickly, informally and with high quality. Original research reported in proceedings and post-proceedings represents the core of LNME. Volumes published in LNME embrace all aspects, subfields and new challenges of mechanical engineering. Topics in the series include:

- Engineering Design
- Machinery and Machine Elements
- Mechanical Structures and Stress Analysis
- Automotive Engineering
- Engine Technology
- Aerospace Technology and Astronautics
- Nanotechnology and Microengineering
- Control, Robotics, Mechatronics
- MEMS
- Theoretical and Applied Mechanics
- Dynamical Systems, Control
- Fluid Mechanics
- Engineering Thermodynamics, Heat and Mass Transfer
- Manufacturing
- Precision Engineering, Instrumentation, Measurement
- Materials Engineering
- Tribology and Surface Technology

To submit a proposal or request further information, please contact the Springer Editor of your location:

**China:** Ms. Ella Zhang at [ella.zhang@springer.com](mailto:ella.zhang@springer.com)

**India:** Priya Vyas at [priya.vyas@springer.com](mailto:priya.vyas@springer.com)

**Rest of Asia, Australia, New Zealand:** Swati Meherishi at [swati.meherishi@springer.com](mailto:swati.meherishi@springer.com)

**All other countries:** Dr. Leontina Di Cecco at [Leontina.dicecco@springer.com](mailto:Leontina.dicecco@springer.com)

To submit a proposal for a monograph, please check our Springer Tracts in Mechanical Engineering at <https://link.springer.com/bookseries/11693> or contact [Leontina.dicecco@springer.com](mailto:Leontina.dicecco@springer.com)

**Indexed by SCOPUS. All books published in the series are submitted for consideration in Web of Science.**

More information about this series at <https://link.springer.com/bookseries/11236>

Xuelin Lei · Vsevolod V. Koryanov  
Editors

Proceedings of 5th  
International Conference  
on Mechanical, System  
and Control Engineering

ICMSC 2021

 Springer

*Editors*

Xuelin Lei  
East China University of Science  
and Technology  
Shanghai, China

Vsevolod V. Koryanov  
Bauman Moscow State Technical  
University  
Moscow, Russia

ISSN 2195-4356                      ISSN 2195-4364 (electronic)  
Lecture Notes in Mechanical Engineering  
ISBN 978-981-16-9631-2              ISBN 978-981-16-9632-9 (eBook)  
<https://doi.org/10.1007/978-981-16-9632-9>

© The Editor(s) (if applicable) and The Author(s), under exclusive license to Springer Nature Singapore Pte Ltd. 2022

This work is subject to copyright. All rights are solely and exclusively licensed by the Publisher, whether the whole or part of the material is concerned, specifically the rights of translation, reprinting, reuse of illustrations, recitation, broadcasting, reproduction on microfilms or in any other physical way, and transmission or information storage and retrieval, electronic adaptation, computer software, or by similar or dissimilar methodology now known or hereafter developed.

The use of general descriptive names, registered names, trademarks, service marks, etc. in this publication does not imply, even in the absence of a specific statement, that such names are exempt from the relevant protective laws and regulations and therefore free for general use.

The publisher, the authors and the editors are safe to assume that the advice and information in this book are believed to be true and accurate at the date of publication. Neither the publisher nor the authors or the editors give a warranty, expressed or implied, with respect to the material contained herein or for any errors or omissions that may have been made. The publisher remains neutral with regard to jurisdictional claims in published maps and institutional affiliations.

This Springer imprint is published by the registered company Springer Nature Singapore Pte Ltd.  
The registered company address is: 152 Beach Road, #21-01/04 Gateway East, Singapore 189721, Singapore

## Contents

### Materials Science and Engineering

<b>Effect of Fibre Treatment on Tensile Properties in Bamboo Fibre Extraction: A Review Paper</b> .....	3
Moviyndiran Muniandy, Sukri Mustapa, Nurdin Ali, Waluyo Adi Siswanto, Azrin Hani Abdul Rashid, and Mohd Idrus Mohd Masirin	
<b>Spray Solution Combustion Synthesis of NiCu Hollow Spheres</b> .....	11
Zhanna Yermekova, German Trusov, and Sergey I. Roslyakov	
<b>Approach to the Selection of Classification Features for Integrated and Combined Technological Processes of Metal Ware Manufacturing</b> .....	19
Marina Polyakova, Ekaterina Lopatina, and Aleksandr Gulin	
<b>Synthesis and Characterization of PSf-CQD Nanocomposite Membrane via Non-solvent Induced Phase Separation Technique</b> .....	25
Persia Ada N. de Yro, Dianne Y. Amor, Sweetheart Meryl G. Navarro, Gerald Mari O. Quiachon, and Sharyjel R. Cayabyab	
<b>Study of the Movement of the Descent Vehicle with an Inflatable Device Made of a Special Material Taking into Account the Arising Asymmetry</b> .....	35
Vsevolod V. Koryanov, Andrey S. Kukharenko, Lang Shuobin, and Danhe Chen	
<b>Electrode Shape Design and Current Density Distribution for Stable Plasma Beam Incinerator</b> .....	45
Grich Kongphet, Tanakorn Wongwuttanasatian, and Amnart Suksri	

<b>Influence of Materials and Their Constitutive Laws on the Stress Fields Produced in the Residual Limb of a Transfemoral Amputation</b> .....	53
Armando Ramalho, Miguel Ferraz, Marcelo Gaspar, and Carlos Capela	
<b>Study of the Elastic Field of a Plane Strain Orthotropic Composite Plate Subjected to Uniform Tension</b> .....	67
S K Deb Nath	
<b>Comparison of Papaya Cushioning Materials by Ellipsoid Evaluation Method</b> .....	77
Mayuree Inwan, Ratiya Thuwapanichayanan, and Supakit Sayasoonthorn	
<b>Development of Polyamide–Polysulfone Thin Film Composites with Copper–treated Zeolites as Additives for Enhanced Hydrophilicity</b> .....	87
Sharyjel R. Cayabyab, Justine de Guzman, and Persia Ada de Yro	
<b>Dynamics and Mechanical Engineering</b>	
<b>Numerical RANS Researches of Aerodynamics a Propeller Ring and Fuselage Interference for Thrust Increases</b> .....	101
Vitaliy V. Gubskiy, Olga V. Pavlenko, and Albert V. Petrov	
<b>The Numerical Simulation of the Flow Feature and Fluid Force Around an In-Line Oscillating Circular Cylinder by the Vortex Method</b> .....	109
Yoshifumi Yokoi	
<b>Dynamic Modeling and Dynamic Response Analysis of Annular Composite Beam Structure</b> .....	117
Bingheng Zhu, Dengqing Cao, Youxia Li, and Tianxi Liu	
<b>Experimental Flow Visualization of Novel Aircraft Architectures</b> .....	127
V. I. Chernousov, A. A. Krutov, and E. A. Pigusov	
<b>Investigation of the Movement of the Descent Vehicle in the Atmosphere of the Planet with Inflatable Braking Mechanical Devices, Taking into Account Various Perturbations at an Average Altitude of Movement</b> .....	133
Vsevolod Koryanov, Lang Shuobin, Leo Richier, and Danhe Chen	
<b>The Use of Numerical Modeling for the Formation of Recommendations for Conducting Experiments on Ballistic Tracks</b> .....	141
S. N. Iljukhin, V. V. Koryanov, V. O. Moskalenko, and A. G. Toporkov	
<b>Cost Benefit of a Small-Scale Vertical Axis Wind Turbine for Residential use in Honduras</b> .....	149
Sophia Eloise Ayestas and Alicia María Reyes Duke	

Contents	vii
<b>Nonlinear Dynamical Modeling and Vibration Responses of A T-Shaped Beam Structure</b> .....	161
Shuai Chen, Dengqing Cao, Youxia Li, and Zhigang Chen	
<b>Machinery and Control Technology</b>	
<b>Topological Optimization of the Milling Head</b> .....	171
Karel Raz, Zdenek Chval, and Martin Stepanek	
<b>Comparison Study of Single Valve and Sequential Valve Mode on the Effect of Steam Turbine Heat Rate</b> .....	179
Atang Salam, Fajar Purnomo, and Wahyu Caesarendra	
<b>Experimental Study of Wing-Tip Vortex Core Circulation in Near-Field</b> .....	191
Robert Stepanov and Alexander Kusyumov	
<b>Thermal Contact Conductance Relation on Asperities Location</b> .....	199
Ekaterina S. Golubtsova and Mikhail V. Murashov	
<b>A Modeling and Modal Analysis Method for Folded Plate</b> .....	209
Kaiyuan Tian, Dengqing Cao, and Kaiping Yu	
<b>Effect of Current Carrying Length in Electric Pulse Aided Deformation</b> .....	217
A. Subrahmanyam, M. Dakaiah, Rahul Kumar Verma, and N. Venkata Reddy	
<b>A Preliminary Study of Shock Calibration Machine for Accelerometer Calibration</b> .....	225
Supavee Prangphanta, Kunaphot Sukchoksirichaiporn, Patchayaporn Doungkum, Thira Jearsiripongkul, Somthana Panyadilok, Adisorn Tongkum, and Krit Jiamjiroch	
<b>Failure Probability Estimation of Thermally Stable Diamond Composite Rock Cutting Tips in Underground Roadway Development</b> .....	233
Yong Sun, Xingsheng Li, and Hua Guo	
<b>Transtibial Prosthetic Socket Produced Using Additive Manufacturing</b> .....	243
Karel Raz, Zdenek Chval, and Martin Stepanek	

## About the Editors

**Dr. Xuelin Lei** holds a Ph.D. in Mechanical Engineering from Shanghai Jiaotong University in 2015. He has worked in the School of Mechanical and Power Engineering of East China University of Science and Technology. Dr. Lei also presided over a series of research projects such as Youth Program of National Natural Science Foundation of China, sub-project of National Science and Technology Major Project, Chinese Postdoctoral Science Foundation and Open Fund of State Key Laboratory of Tribology at Tsinghua University.

**Dr. Vsevolod V. Koryanov** is the first deputy head of the Department of Dynamics and Flight Control of Rockets and Spacecraft's at Bauman Moscow State Technical University, Russia. He has authored over 160 published scientific papers and 3 textbooks. He has published papers in journals of national and international repute. He has mentored several scholars for their master's and Ph.D. theses. He teaches courses such as theory of space flight, ballistics of rockets and space vehicles, and theory of space vehicles flight. In 2013, he was awarded Yu. A. Gagarin medal of the Russian Federation of Cosmonautics.

# Influence of Materials and Their Constitutive Laws on the Stress Fields Produced in the Residual Limb of a Transfemoral Amputation



Armando Ramalho, Miguel Ferraz, Marcelo Gaspar, and Carlos Capela

## 1 Introduction

The friction coefficient between the various components of a prosthesis and the contacting biological tissues has a significant influence on the intensity of the shear stresses generated at the interfaces of the biological materials of lower limb osteotomized patients [1, 2]. Furthermore, the distribution of shear stresses at the interface between the liner and the soft tissues is referred to as one of the leading causes of pressure ulcers in patients with transfemoral amputation [3].

Even though it is widely recognized that the materials' constitutive laws have a significant influence on the stress fields generated at the residual limb (when interacting with the combined socket prosthesis), most simulations of these biomechanical systems using the finite element method (FEM) still use linear elastic models [4–7]. Thus, such linear elastic models are mostly suitable for simulating most rigid materials, *e.g.*, cortical bone and the vast majority of hard sockets prosthesis.

---

A. Ramalho (✉)  
Polytechnic Institute of Castelo Branco, Castelo Branco, Portugal  
e-mail: [aramalho@ipcb.pt](mailto:aramalho@ipcb.pt)

M. Ferraz · M. Gaspar · C. Capela  
Polytechnic Institute of Leiria, Leiria, Portugal  
e-mail: [marcelo.gaspar@ipleiria.pt](mailto:marcelo.gaspar@ipleiria.pt)

C. Capela  
e-mail: [carlos.capela@ipleiria.pt](mailto:carlos.capela@ipleiria.pt)

A. Ramalho · C. Capela  
Centre for Mechanical Engineering, Materials and Processes (CEMMPRE), Univ Coimbra,  
Coimbra, Portugal

M. Gaspar  
Centre for Rapid and Sustainable Product Development (CDRSP), Leiria, Portugal

© The Author(s), under exclusive license to Springer Nature Singapore Pte Ltd. 2022  
X. Lei and V. V. Koryanov (eds.), *Proceedings of 5th International Conference  
on Mechanical, System and Control Engineering*, Lecture Notes  
in Mechanical Engineering, [https://doi.org/10.1007/978-981-16-9632-9\\_7](https://doi.org/10.1007/978-981-16-9632-9_7)

53



However, this model is not suitable for more flexible materials when subjected to large deformations, namely the liners and the soft tissues [8–10].

In most simulations using FEM, the soft tissues are generally approached as homogeneous and isotropic materials. Nonetheless, the use of software that allows generating geometries with various components collected from medical images (*e.g.*, Materialize) provide for the simulation of these materials in a more realistic way, thus separating the soft tissues into their main components—skin, fat, muscle, blood vessels, fascia—and allowing for considering the anisotropy of their properties [9].

The mechanical characterization of biomaterials that allows the definition of its constitutive law is widely available in the current literature [8, 10]. However, this characterization is limited when considering biological materials. This is mainly due to the fact that these materials' characterization is strongly endogenous. In most simulations using the FEM of biomechanical systems, soft tissues are characterized by a linear elastic model. Nonetheless, this approach does not seem adequate when these biological materials are subject to large deformations. Thus, according to the literature, hyperelastic models are the most used for nonlinear soft tissue mechanical characterization [9, 11, 12]. The main hyperelastic models used in the simulation of soft tissues' constitutive law are the Mooney-Rivlin model (in their Mooney second and third-order variants) and the Neo-Hookean model, the Yeoh model and the Ogden model.

In this study, the stress field at the prosthesis interfaces (of a patient with trans-femoral amputation) is assessed using FEM numerical simulation. The influence of the constitutive law applied in modelling the mechanical behaviour of the liner material, and the soft tissues, are analyzed and discussed. Additionally, the friction coefficient between the prosthesis and the liner, the liner and the skin and between the soft tissues and the femur are also analyzed and discussed. The model previously presented by the authors in Ramalho et al. [1] is improved in terms of the geometry and the materials characterization. For the manufacturing of the prosthesis, propylene thermoplastic is compared with the use of an epoxy resin in which the majority of the molecular structure is of vegetable origin (SR GreenPoxi 56) produced by Sicomin. In most of the simulations presented, a composite material is used for prosthesis manufacturing in which the GreenPoxi resin is reinforced with natural jute fibres. This composite is modelled as a linear elastic material with anisotropic behaviour.

## 2 Finite Element Model

### 2.1 Geometry

The two-dimensional finite element model previously presented by the authors in Ramalho et al. [1] has been improved in terms of geometry definition. Several points were collected from the femur and limb profiles presented in Hoellwarth et al. [13]. These points allowed for modelling the profiles of these organic components using

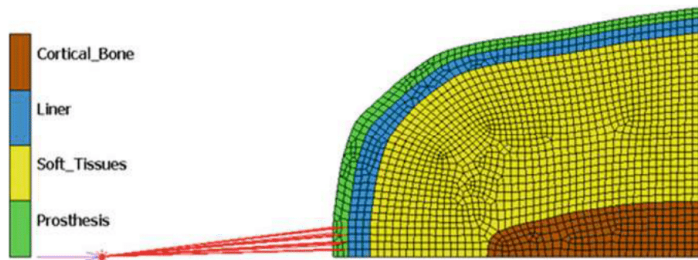


**Fig. 1** Geometry, mesh and deformable bodies of the numerical model

cubic spline interpolation. The previous 2D axisymmetric formulation was maintained. An elastic foundation is used to support the patient's limb. To increase the damping effect, the liner's thickness was reinforced in the distal part of the stem [4, 7]. The connection between the socket and the pylon, taking into account its rigidity, is modelled through a REB2 type connection [14].

Three materials were considered to build the socket type prosthesis model: the thermoplastic previously used in Ramalho et al. [1], propylene, the SR GreenPoxi 56 resin produced by Sicomin and a composite in which the SR GreenPoxi 56 is reinforced with natural jute fibres. Considering the mechanical properties of these materials, the prosthesis's thickness was increased in the distal part of the stump, where the stresses in the prosthesis are higher.

The geometry, finite element mesh, and the model's various components are presented in Fig. 1.

## 2.2 Mechanical Properties of the Materials—Constitutive Laws

**Biologic Materials.** The femur is modelled as an isotropic, homogeneous and linear elastic material. The cortical bone properties are considered along the longitudinal direction [15], with an elastic modulus,  $E = 11.5$  GPa, and Poisson's ratio,  $\nu = 0.31$ .

For the soft tissues, two different models were used: the Neo-Hookean model (presented in Portnoy et al. [12]) for the muscle, with  $C_{10} = 4.25$  kPa and the volumetric behaviour obtained only with the first term of the series,  $D1 = 24.34$  MPa<sup>-1</sup>; the first order Ogden model (presented in Kallin et al. [9]) for the muscle, with the ground state shear modulus  $\mu = 1907$  kPa, strain hardening  $\alpha = 4.6$  and volumetric behaviour obtained only with the first term of the series,  $D1 = 10.5$  MPa<sup>-1</sup>.

To compare the results using the hyperelastic model with those of the linear elastic model (after acquiring the stress field in the soft tissues), the properties of an equivalent elastic material were computed. The volume deformation energy was equivalent

to that absorbed in both simulated hyperelastic models for the equivalent elastic material. In this process, the Poisson's ratio was fixed at  $\nu = 0.45$ , corresponding to an approximately incompressible situation. The equivalent elasticity coefficients' values were  $E_{\text{equNH}} = 0.0534$  MPa (Neo-Hookean model) and  $E_{\text{equO}} = 0.0196$  MPa (Ogden model).

**Liner.** When modelling the liner, the experimental results presented in Sanders et al. [10] were used. Four different liners were chosen from each presented stiffness classes, ordered from  $C_1$  to  $C_4$  by increasing stiffness value. For the more rigid class,  $C_1$ , an elastomer was selected, the Fillauer Silicone liner, produced by Fillauer, Inc., Chattanooga, Tennessee; for the next class,  $C_2$  a polyurethane, TEC Pro 18, produced by TEC Interface Systems, Waite Park, Minnesota; for class  $C_3$  an elastomer, Iceross Comfort, produced by Ossur USA, Inc., Columbia, Maryland was chosen; for the most flexible class, a gel was selected, the Super Stretch, made by ALPS, St. Petersburg, Florida. The selection of these materials was based not only on their stiffness value but also considering the corresponding friction coefficient between that material and human skin. These friction coefficient values were also ordered in different classes ( $F_1$  to  $F_4$ ), from the highest to the lowest.

The experimental results were approximated fitting time-independent data by differential evolution, using the finite element software MSC Marc 2018 [14]. In the approximation, the results available in Sanders et al. [10], corresponding to the tensile, compression and pure shear tests, were taken into account. Among the hyperelastic models (H M) available, the best approximations for the selected liners corresponded to the second-order Mooney-Rivlin (M-R) and Yeoh models, shown in Table 1. The friction coefficient (FC) shown in the table refers to the friction between the liner and the skin. Also is defined a stiffness class (S C) and a friction class (Fr C) for the liners.

On an initial exploratory study, the constitutive equations presented in Łagan and Liber-Kneć [16] were used on the liner, for a Neo-Hookean model, with  $C_{10} = 23$  kPa and the bulk modulus of 230 MPa.

**Prosthesis.** For the socket type prosthesis composition, three different materials were analyzed: propylene thermoplastic; an epoxy resin in which most of the molecular structure is of vegetable origin (SR GreenPoxi 56 produced by Sicomin) and a composite material in which an SR GreenPoxi 56 resin matrix is reinforced with jute fibres.

The propylene thermoplastic is modelled as homogeneous, isotropic and linear elastic, based on the mechanical properties presented in Silver-Thorn and Childress [17], with an elastic modulus ( $E$ ) of 1000 MPa and the Poisson's ratio  $\nu = 0.30$ .

SR GreenPoxi 56 resin is also modelled as homogeneous, isotropic and linear elastic, based on the properties presented in Perrier [18] with an elastic modulus ( $E$ ) of 3000 MPa, a Poisson's ratio  $\nu = 0.39$  and the specific mass  $\rho = 1180$  kg/m<sup>3</sup>.

The jute fibre is modelled as homogeneous, 2D orthotropic and linear elastic, based on the properties presented in Suthenthiraveerappa and Gopalan [19], with elastic modulus  $E_1 = 23,949$  MPa and  $E_2 = 978$  MPa, the Poisson's ratio  $\nu_{12} =$

0.374 and  $\nu_{21} = 0.014$ , the shear modulus  $G_{12} = 411$  MPa and the specific mass  $\rho = 1440$  kg/m<sup>3</sup>.

Based on the Halpin–Tsai model for discontinuous fibres, the composite material's elastic properties (SR GreenPoxi 56 resin matrix reinforced with jute fibres) were computed in the MSC Patran 2019 software [20] considering a 60/40% for the resin/fibre volume ratio. A 10 to 1 ratio was considered for the fibres' length vs diameter.

The fibre of this composite was later dispersed using a 2D short fibre model implemented in the MSC Patran 2019 software [20], with angles  $\alpha = 0^\circ$  and  $\phi = 45^\circ$ , a standard deviation of  $10^\circ$  through a random process, with zero correlation, using 1000 Monte Carlo iterations. The elasticity matrix of this composite is represented in Eq. (1). The composite was oriented so that axis 1 has, at each point, the direction of the tangent to the prosthesis profile shown in Fig. 1. Axis 2 has the direction of thickness and axis 3, the radial direction [14].

$$[C_{ij}] = \begin{bmatrix} 1.30 \times 10^5 & 1.39 \times 10^5 & 1.26 \times 10^5 & 3.07 \times 10^1 \\ 1.39 \times 10^5 & 1.59 \times 10^5 & 1.40 \times 10^5 & 5.04 \times 10^1 \\ 1.26 \times 10^5 & 1.40 \times 10^5 & 1.31 \times 10^5 & 5.32 \times 10^1 \\ 3.07 \times 10^1 & 5.04 \times 10^1 & 5.32 \times 10^1 & 2.10 \times 10^3 \end{bmatrix} \text{ (MPa)}. \quad (1)$$

**Table 1** Hyperelastic models used for various liners

Liner	S C	FC/Fr C	H M	Parameters and coefficients
Fillauer silicone	C <sub>1</sub>	$\mu_f = 0.6$	Yeoh	$C_{10} = 0.923252$ kPa
		F3		$C_{20} = 2.18386e-05$ kPa
				$C_{30} = 44.9592$ kPa
TEC Pro 18	C2	$\mu_f = 1$	M-R	$C_{10} = 1.5152e-06$ kPa
		F1		$C_{01} = 41.365$ kPa
TEC Pro 18 L	C2	$\mu_f = 0.65$		$C_{11} = 9.4846e-7$ kPa
		F1		Bulk Modulus = 413,650 kPa
Iceross comfort	C3	$\mu_f = 0.4$	M-R	$C_{10} = 2.19397e-05$ kPa
		F4		$C_{01} = 20.775$ kPa
				$C_{11} = 1.28457e-05$ kPa
				Bulk Modulus = 207,750 kPa
Super stretch gel	C4	$\mu_f = 0.65$	M-R	$C_{10} = 1.23146e-04$ kPa
		F2		$C_{01} = 10.5949$ kPa
				$C_{11} = 2.89243e-9$ kPa
				Bulk Modulus = 105,905 kPa

### 2.3 Friction Model

In the contact between the system's various components, a Coulomb's bilinear friction model was used, with an average friction coefficient between the cortical bone and the soft tissues of  $\mu = 0.3$  [21]. A friction coefficient of  $\mu = 0.5$  was considered for the contact between the socket type prosthesis made of SR GreenPoxi 56 and the liner [22]. When the prosthesis is made of propylene, a friction coefficient of  $\mu = 0.6$  between the prosthesis and the liner was kept [1]. On the contact between the liner and the soft tissues, the friction coefficient varies, considering each of the liners, the values shown in Table 1. In the numerical model, the contact between deformable bodies is modelled by the finite sliding segment-to-segment contact algorithm. The separation criteria are based upon stresses (Lagrange multipliers): separation threshold is treated as residual stress of negligible magnitude ( $0.9e-06$  MPa).

### 2.4 Finite Element Analysis

Given the symmetry of the model, a 2D axisymmetric analysis was performed. The simulations with this model were made using the implicit module of MSC Marc Mentat 2018 [14]. A multifrontal direct sparse solver, the Paradiso solver, is used with a Newton–Raphson iterative procedure. For convergence testing, a relative force tolerance of 10% is used. An adaptative multicriteria stepping procedure is used for load increment—was used the initial time step (load increment) of  $1e-06$ . The numerical constrictions associated with the implicit method were overcome using a mesh adaptivity algorithm, the advancing front quadrilateral. An automatic algorithm was used for meshing, and linear quadrilateral axisymmetric solid elements with four nodes (Quad 10) were used. The initial mesh dimensions of the elements were 3 mm. This value was established in a previous iterative process and is considered an objective in the adaptive mesh algorithm. In this process, the mesh size may be reduced to a quarter of its initial value, depending on the strain change and the distortion that may take place in each element [1]. In the structural analysis, large strain nonlinear procedures were used. Based on an automatic algorithm depending on the constitutive law, the Multiplicative Updated Lagrange procedure is preferential for hyperelastic materials.

### 2.5 Loading

The prosthesis is considered to support the patient's total weight (70 kgf) during the static stance. Loading is imposed in quasi-static conditions [1], as illustrated in Fig. 1.

### 3 Numerical Simulations Planning

A preliminary simulation was carried out to compare the effect of the constitutive law on the stress field produced at the prosthesis's different components. Model 3, presented in Ramalho et al. [1], was simulated varying only the liner and soft tissues' constitutive law. The geometry and all of the remaining parameters were maintained. For the soft tissues, the Neo-Hookean model presented in Portnoy et al. [12] was used, whereas, for the liner, a Neo-Hookean behaviour with the parameters of in Łagan and Liber-Kneć [16] was considered. The constitutive law used for soft tissues has a much less rigid behaviour than that of the previously used linear elastic model. In addition, the volumetric compressibility is also much lower in the constitutive law. Thus, much higher deformation and normal (80%) and shear stresses (40%) were observed for the same loading. However, it appears that this variation is much smaller in terms of biological tissues. The resulting normal and shear stress fields (MPa) are shown in Fig. 2.

This pilot simulation allowed outlining a set of simulations to be carried out with the geometry presented in Fig. 1. In addition to the influence of the constitutive law, the simulations focused on the effect of friction. When comparing models, it was essential to take into account the stiffness and the volumetric compressiveness. Considering that the study presented in Sanders et al. [10] provides the required data for the range of liners available in the market, it was decided to use that data for the parameters of current work, according to Table 1.

The first simulations led to the rupture of the propylene-based prosthesis. Thus, considering the more sustainable nature of the bio epoxy and the improved mechanical properties, the GreenPoxi 56 resin was selected for current research with and without the reinforcement of natural jute fibres. Thus, to study the influence of friction and the constitutive law of materials in the stress fields produced in the biological tissues of a patient with a transfemoral amputation, the simulations presented in Table 2 were carried out.

### 4 Results and Discussion

The biological tissues use most of the volume of the numerical model. This verifies that the constitutive law used in its modelling has a significant effect on the results.

Figure 3 shows the stress distribution (MPa) in the biological tissues of the A5 model, which is considered representative of the generic distribution that occurred in the various simulations in which the soft tissues were characterized with the Neo-Hookean model.

On what concerns the normal stresses, it can be observed that at the biological tissues level, the highest stresses take place at the interface between the femur and the soft tissues (on the distal part of the femur at the osteotomized section).



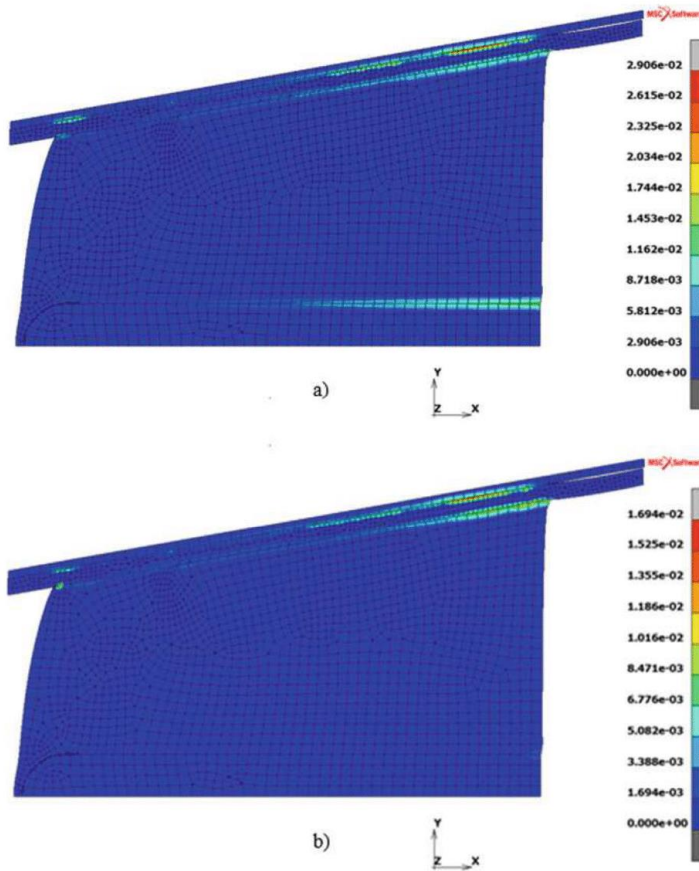


**Fig. 2** Preliminary study. **a** Normal contact stresses. **b** Shear contact stresses

On what refers to the shear stresses, it can also be observed that the higher stresses occur either at the interface between the liner and the soft tissues (in the proximal part of the liner), or close to the femur (in the region adjacent to that in which the maximum normal tensions take place). This distribution varies significantly in intensity for the various simulations.

Figure 4 shows the stress distribution (MPa) in the biological tissues of the A8 simulation, which is considered representative of the generic distribution that

**Table 2** Characterization of the performed simulations

Simulation	Soft tissues constitutive law	Prosthesis material	Liner
A1	Neo-Hookean	Propylene	TEC Pro 18
A2	Neo-Hookean	GreenPoxi 56	TEC Pro 18
A3	Neo-Hookean	GreenPoxi 56	TEC Pro 18L
A4	Neo-Hookean	Composite	Fillauer Silicone
A5	Neo-Hookean	Composite	TEC Pro 18
A6	Neo-Hookean	Composite	Iceross Comfort
A7	Neo-Hookean	Composite	Super Stretch Gel
A8	Ogden	Composite	TEC Pro 18
A9	Elastic equivalent Neo-Hookean	Composite	ElasEqTEC Pro 18
A10	Elastic equivalent Ogden	Composite	ElasEqTEC Pro 18
A11	Neo-Hookean	Composite	TEC Pro 18L
A12	Elastic equivalent Neo-Hookean	Composite	TEC Pro 18L

occurred in the various models in which the soft tissues were characterized with the Ogden model.

This figure shows that at the biological tissues' level, the maximum normal stress occurs at the interface between the liner and the soft tissues (on the distal part of the stump).

On what concerns the shear stresses, the highest stresses occur at the interface between the liner and the soft tissues (in the proximal part of the liner). This distribution varies significantly in intensity for the various simulations.

Finally, it can be observed that in the area where the normal contact stresses are highest, the shear stresses are neglectable, as there is no slip.

The highest values of normal and shear contact stresses that take place at the interfaces of the various components of the prosthesis ( $\sigma$  and  $\tau$ ) and the biological tissues ( $\sigma_B$  and  $\tau_B$ ) are shown in Table 3, as well as the equivalent Von Mises ( $\sigma_{VM}$ ) stress that occurs in the prosthesis (hard socket).

In the initial simulations (A1-A3), it can be observed that the stiffness increase of the prosthesis material leads to a slight decrease in contact stresses, as well as in the equivalent Von Mises stress that occurs in the prosthesis. The significant material stiffness increase does not lead to a very substantial change in the maximum stresses



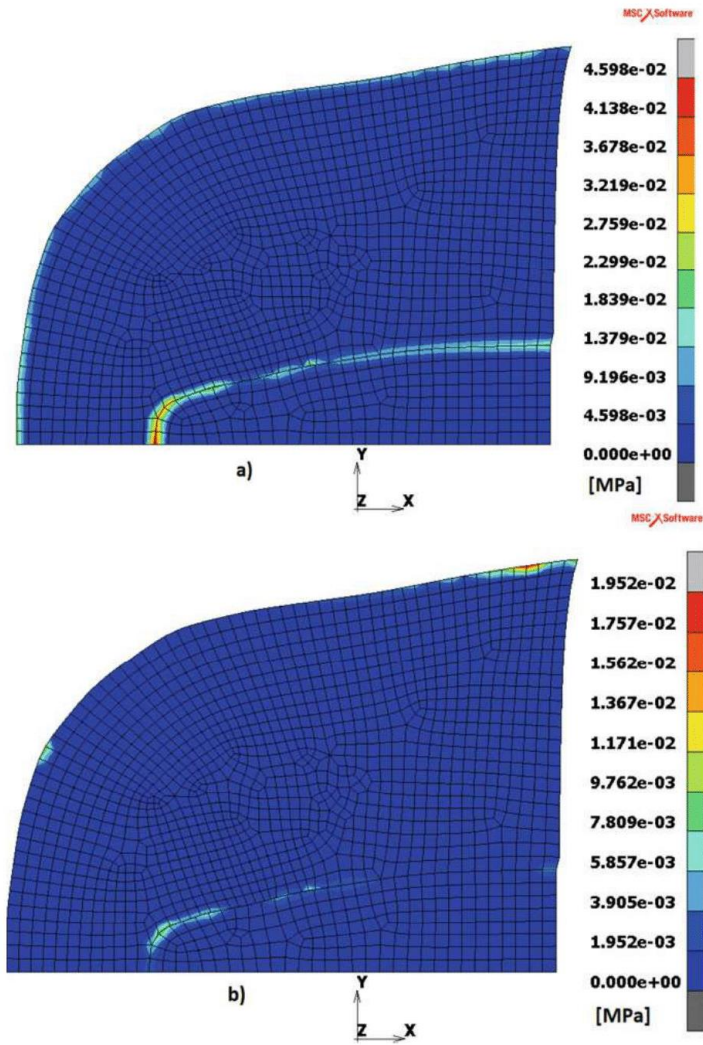


**Fig. 3** Contact stresses at biological tissues, A5 model. **a** Normal stresses. **b** Shear stresses

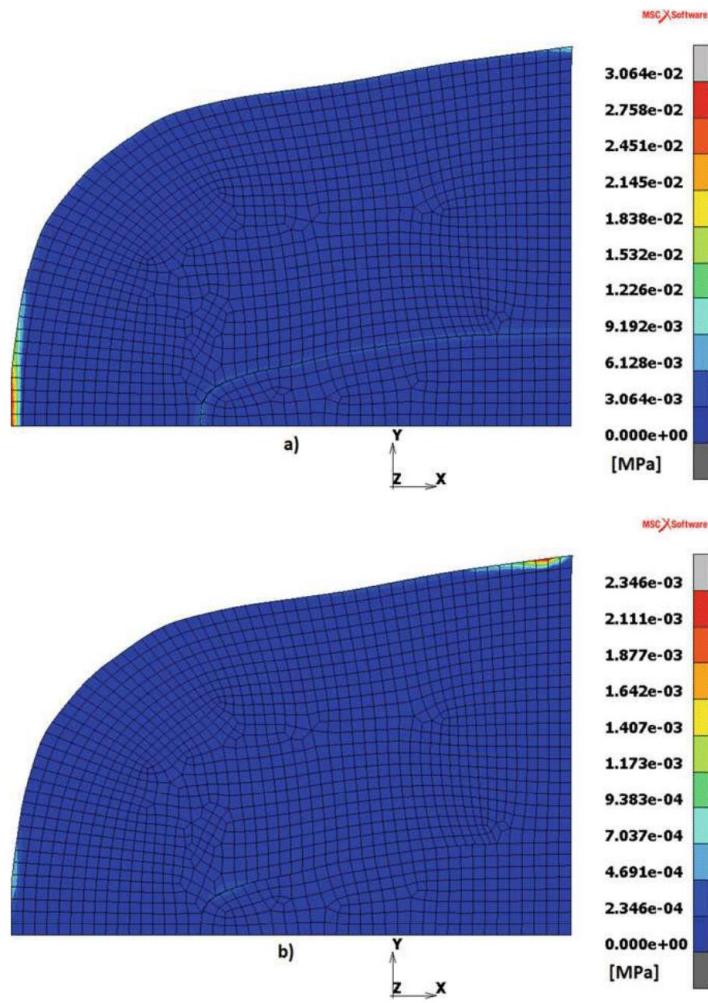


Fig. 4 Contact stresses at biological tissues, A8 model. a Normal stresses. b Shear stresses

**Table 3** Summary of the simulation results

Simulation	$\sigma$ (kPa)	$\tau$ (kPa)	$\sigma_B$ (kPa)	$\tau_B$ (kPa)	$\sigma_{VM}$ (MPa)
A1	68.24	17.94	68.24	17.94	63.84
A2	56.27	14.43	56.27	14.43	55.45
A3	44.86	3.09	14.53	3.09	54.81
A4	46.45	13.67	46.45	13.37	14.78
A5	67.84	19.52	45.98	19.52	13.77
A6	51.57	9.40	51.57	7.38	14.87
A7	68.57	19.50	36.29	10.37	13.59
A8	21.86	4.04	30.64	2.35	10.16
A9	60.47	18.88	60.47	17.93	14.99
A10	33.17	5.58	11.35	5.58	13.10
A11	50.06	14.52	50.06	14.52	14.34
A12	45.12	18.11	45.12	16.52	14.98

due to the influence of the prosthesis's small thickness on the overall stiffness of the structure. In the case of A3 simulation, reducing the friction coefficient between the liner and the soft tissues leads to a significant decrease in the normal and shear stresses at the interfaces. It is observed that the stresses that take place in the prosthesis exceed the resistance stresses of the materials [16, 20]. The use of a short fibre composite has the particularity of increasing the stiffness of the material and also of the whole prosthesis. According to Eq. (1), this occurs by decreasing the membrane effect with the significant increase in stiffness in the direction of thickness, resulting from the short fibres' orientation. The substantial increase in normal stresses observed along direction 2 (alongside the thickness) leads to a significant decrease in the equivalent Von Mises stress that occurs in the prosthesis, also leading to some changes in the distribution in the contact stress field (A2 and A5).

The decrease in friction between the liner and the soft tissues seems to lower, with some consistency, the shear stresses. When comparing the evolution of these shear stresses in simulations A5, A7, A4 and A6, the inconsistency between the results of A7 and A4 can be explained due to the Yoeh model used in A4. This effect is more evident when comparing the results of simulations A5 and A11, in which the only change observed is for the friction coefficient between the liner and the soft tissues, which changes from 1 to 0.65. The friction decrease leads to an increase in the normal contact stress and a reduction in the shear contact stress. These results, focusing on the friction coefficient variation, are consistent with those presented in Zhang et al. [23].

The effect of the constitutive law used in the characterization of soft tissues, and the liner, can be observed when comparing the use of hyperelastic models in simulations A11, A5 and A8 with the equivalent linear elastic simulations A12, A9 and A10. Thus, at the biological tissues level, one can observe a significant decrease in the normal contact stresses and a slight increase in the shear contact stresses.

## 5 Conclusions

The developed Finite Element Model reveals to be effective when assessing the effects of friction on the residual limb of a transfemoral amputee.

The results obtained allow evaluating the influence of the friction coefficient between the prosthesis, the liner and the soft tissues on the whole biomechanical system's stress distribution.

The stiffness and the anisotropy of the prosthesis material effectively influence the contact stresses field developed in the residual limb of a transfemoral amputation.

The friction between the liner and the soft tissues has an effective influence on the field of contact stresses developed in the residual limb of a transfemoral amputation.

The constitutive laws used to characterize liner and soft-tissue materials effectively influences the fields of contact stresses developed in the residual limb of a transfemoral amputation.

**Acknowledgements** This research is sponsored by national funds through FCT—Fundação para a Ciência e a Tecnologia, under the project UIDB/00285/2020.

## References

1. Ramalho A, Ferraz M, Gaspar M, Capela C (2020) Development of a preliminary finite element model to assess the effects of friction on the residual limb of a transfemoral amputee. *Mater Today Proc* 33:1859–1863
2. Ramírez JF, Vélez JA (2012) Incidence of the boundary condition between bone and soft tissue in a finite element model of a transfemoral amputee. *Prosthet Orthot Int* 36(4):405–414
3. Sanders JE, Daly CH, Burgess EM (1992) Interface shear stresses during ambulation with a below-knee prosthetic limb. *J Rehabil Res Dev* 29(4):1–8
4. Zhang M, Mak AFT, Roberts VC (1998) Finite element modelling of a residual lower-limb in a prosthetic socket: a survey of the development in the first decade. *Med Eng Phys* 20(5):360–373
5. Misra S, Ramesh KT, Okamura AM (2008) Modeling of tool-tissue interactions for computer-based surgical simulation: a literature review. *Presence (Camb)* 17(5):463
6. Mackerle J (2006) Finite element modeling and simulations in orthopedics: a bibliography 1998–2005. *Comput Methods Biomech Biomed Engin* 9(3):149–199
7. Gholizadeh H, Abu Osman NA, Eshraghi A, Ali S, Razak NA (2014) Transtibial prosthesis suspension systems: systematic review of literature. *Clin Biomech* 29(1):87–97
8. Cagle JC, Hafner BJ, Taffin N, Sanders JE (2018) Characterization of prosthetic liner products for people with transtibial amputation. *J Prosthetics Orthot* 30(4):187–199
9. Kallin S, Rashid A, Salomonsson K, Hansbo P (2019) Comparison of mechanical conditions in a lower leg model with 5 or 6 tissue types while exposed to prosthetic sockets applying finite element analysis. *ArXiv*, 1–27
10. Sanders JE, Nicholson BS, Zachariah SG, Cassisi DV, Karchin A, Ferguson JR (2004) Testing of elastomeric liners used in limb prosthetics: classification of 15 products by mechanical performance. *J Rehabil Res Dev* 41(2):175–185
11. Misra S, Reed KB, Schafer BW, Ramesh KT, Okamura AM (2010) Mechanics of flexible needles robotically steered through soft tissue. *Int J Rob Res* 29(13):1640–1660
12. Portnoy S, Siev-Ner I, Shabshin N, Gefen A (2011) Effects of sitting postures on risks for deep tissue injury in the residuum of a transtibial prosthetic-user: a biomechanical case study. *Comput Meth Biomech Biomed Engin* 14(11):1009–1019

13. Hoellwarth JS, Al Muderis M, Rozbruch SR (2020) Cementing Osseointegration implants results in loosening: case report and review of literature. *Cureus* 12(2)
14. MSC Software Corporation (2018) *Marc 2018.0 Theory and User Information*. Newport Beach, CA 92660 USA
15. Ivarsson BJ, Crandall JR, Hall GW, Pilkey WD (2004) Biomechanics. In: Kreith F (ed) *Handbook of mechanical engineering*, 2nd edn. CRC Press, Boca Raton
16. Łagan S, Liber-Kneć A (2018) The determination of mechanical properties of prosthetic liners through experimental and constitutive modelling approaches. *Czas Tech* 3:197–209
17. Silver-Thorn DS, Childress MB (1996) Parametric analysis using the finite element method to investigate prosthetic interface stresses for persons with trans-tibial amputation. *J Rehabil Res Dev* 33(3):227–238
18. Perrier A (2016) Influence du Vieillissement Hydrique Sur le Comportement Mécanique de l'Interface Fil/Matrice Dans des Composites Chanvre/Époxy. L'École Nationale Supérieure de Mécanique et D'Aérotechnique
19. Suthenthiraveerappa V, Gopalan V (2017) Elastic constants of tapered laminated woven jute/epoxy and woven aloe/epoxy composites under the influence of porosity. *J Reinf Plast Compos* 36(19):1453–1469
20. MSC Software Corporation (2008) *Materials application—theory—composite materials*, in *Patran 2008 r1, Reference Manual Part 4: Functional Assignments*, 88–160, Santa Ana, CA 92707 USA
21. Shacham S, Castel D, Gefen A (2010) Measurements of the static friction coefficient between bone and muscle tissues. *J Biomech Eng* 132(8):1–4
22. Persson BNJ (2016) Silicone rubber adhesion and sliding friction. *Tribol Lett* 62(2):1–5
23. Zhang M, Lord M, Turner-Smith AR, Roberts VC (1995) Development of a non-linear finite element modelling of the below-knee prosthetic socket interface. *Med Eng Phys* 17(8):559–566

## Attachment 3

12<sup>o</sup> Congresso Nacional de Mecânica Experimental – CNME2020  
Monte Real, Leiria, Portugal  
3-5 de março de 2021  
Carlos Capela, Rui B. Ruben, Mário S. Correia, *et al.* (editores)

### EFEITO DO ATRITO NO MEMBRO RESIDUAL NUMA AMPUTAÇÃO TRANSFEMORAL – INFLUÊNCIA DO MODELO CONSTITUTIVO DOS MATERIAIS

Armando Ramalho <sup>1,2</sup>, Miguel Ferraz <sup>3</sup>, Marcelo Gaspar <sup>4</sup>, Carlos Capela <sup>2,5</sup>

<sup>1</sup> Instituto Politécnico de Castelo Branco, Portugal, aramalho@ipcb.pt

<sup>2</sup> CEMMPRE, Universidade de Coimbra, Portugal

<sup>3</sup> Instituto Politécnico de Leiria, Portugal, 2170169@my.ipleiria.pt

<sup>4</sup> CPRSP, Instituto Politécnico de Leiria, Portugal, marcelo.gaspar@ipleiria.pt

<sup>5</sup> Instituto Politécnico de Leiria, Portugal, carlos.capela@ipleiria.pt

#### RESUMO

Neste artigo é avaliado o efeito das propriedades mecânicas e tribológicas dos materiais na interação entre os diversos componentes da prótese numa amputação transfemoral, através de uma análise por elementos finitos. O modelo numérico é desenvolvido sobre o software MSC.marc. O atrito vai influenciar a distribuição de tensões entre as diversas interfaces – prótese/liner, liner/tecidos moles e tecidos moles/osso cortical. A distribuição das tensões de corte junto às interfaces, influencia o conforto do paciente, sendo uma das principais causas da geração de úlceras de pressão nos pacientes amputados que usam este tipo de próteses.

É analisada a influência dos modelos constitutivos utilizados na modelação dos tecidos moles e do liner, na distribuição de tensão. Em concreto são comparados os resultados obtidos com a utilização de um modelo linear elástico com os obtidos com modelos hiperelásticos.

Palavras-chave: Método dos elementos finitos / Tensões de contacto / Amputação transfemoral / Modelos constitutivos / Atrito

#### 1. INTRODUÇÃO

A distribuição das tensões de corte na interface entre o liner e os tecidos moles é uma das principais causas do desenvolvimento de úlceras de pressão nos pacientes com amputação transfemoral, Sanders *et al.* (1992).

O coeficiente de atrito tem grande influência na intensidade das tensões de corte que se desenvolvem ao nível das interfaces das próteses nos pacientes amputados nos membros inferiores, Ramalho *et al.* (2020).

No presente artigo é avaliado o campo de tensões nas interfaces de uma prótese de um paciente com amputação transfemoral, através de simulação numérica por elementos finitos sendo analisada a influência dos modelos reológicos utilizados na modelação do comportamento mecânico do material do liner e dos tecidos moles. O modelo anteriormente apresentado pelos autores em Ramalho *et al.* (2020), é melhorado ao nível da geometria e da caracterização dos materiais. Na definição dos modelos hiperelásticos, são utilizados os parâmetros e caracterização mecânica apresentados em Kallin *et al.* (2019) e Sanders *et al.* (2004).

12<sup>o</sup> Congresso Nacional de Mecânica Experimental – CNME2020  
 Monte Real, Leiria, Portugal  
 3-5 de março de 2021  
 Carlos Capela, Rui B. Ruben, Mário S. Correia, *et al.* (editores)

## 2. DESCRIÇÃO

O modelo bidimensional de elementos finitos anteriormente apresentado pelos autores em Ramalho *et al.* (2020), foi melhorado ao nível da definição da geometria. Foram obtidos diversos pontos nos perfis do fémur e do coto apresentados em Hoellwarth (2020). Estes pontos permitiram a obtenção dos perfis através de interpolação por splines cúbicas. Manteve-se a formulação 2D axi-simétrica anteriormente utilizada. No suporte do coto é utilizado uma fundação elástica.

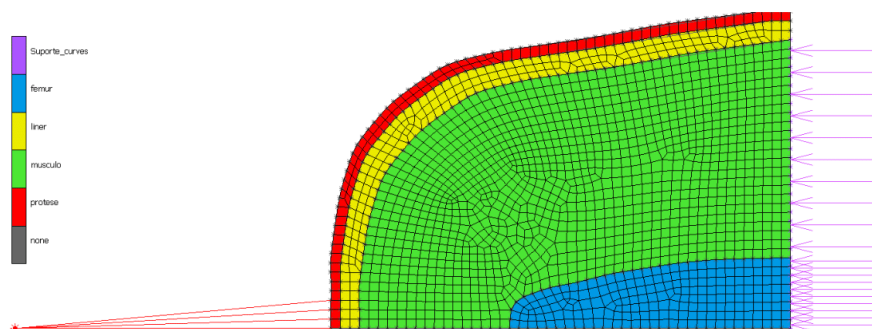


Fig. 1 – Modelo numérico

O modelo de escorregamento foi adaptado para permitir a caracterização hiperelástica do liner e dos tecidos moles. Para suportar as grandes deformações, manteve-se o algoritmo de refinamento automático da malha, baseado na deformação ao nível dos elementos.

## 3. CONCLUSÕES

O modelo numérico desenvolvido produz resultados coerentes com os apresentados por outros autores. A rigidez e a anisotropia do material da prótese influenciam o campo de tensões de contato desenvolvido no membro residual de uma amputação transfemoral. Os modelos constitutivos usados para caracterizar os materiais do liner e dos tecidos moles influenciam os campos de tensões de contato desenvolvidos no membro residual.

## REFERÊNCIAS

- Hoellwarth, J.S., Al Muderis, M., Rozbruch, R.S. (2020). Cementing Osseointegration Implants Results in Loosening: Case Report and Review of Literature. *Cureus* 12(2): e7066. DOI10.7759/cureus.7066.
- Kallin, S., Rashid, A., Salomonsson, K. and Hansbo, P. Comparison of mechanical conditions in a lower leg model with 5 or 6 tissue types while exposed to prosthetic sockets applying finite element analysis. *ArXiv*, pp. 1–27, 2019.
- Ramalho, A., Ferraz, M., Gaspar, M., Capela, C. (2020). Development of a preliminary finite element model to assess the effects of friction on the residual limb of a transfemoral amputee. *Mater. Today Proc.*, vol. 33, pp. 1859–1863, doi: 10.1016/j.matpr.2020.05.199.
- Sanders, J.E., Daly, C.H., Burgess, E.M. (1992). Interface shear stresses during ambulation with a below-knee prosthetic limb, *Journal of Rehabilitation Research & Development*, 29(4): 1-8.
- Sanders, J.E., Nicholson, B.S., Zachariah, S.G., Cassisi, D.V., Karchin, A., Ferguson, J.R. (2004). Testing of elastomeric liners used in limb prosthetics: Classification of 15 products by mechanical performance, *Journal of Rehabilitation Research & Development*, Vol. 41, No. 2, 175-186.



## Attachment 4

### Publishing Agreement

**SPRINGER NATURE**

for Contributions in Collected Works

---

This Publishing Agreement (this “**Agreement**”) has been approved by and entered into between:

**Marcelo Gaspar [0000-0003-3153-6468], School of Technology and Management, Polytechnic of Leiria, Leiria, Portugal**

**Miguel Ferraz [0000-0003-3748-3133], School of Technology and Management, Polytechnic of Leiria, Leiria, Portugal**

**Armando Ramalho [0000-0003-0500-0459], Polytechnic Institute of Castelo Branco, Castelo Branco, Portugal**

**Joel Vasco [0000-0001-8185-8145], School of Technology and Management, Polytechnic of Leiria, Leiria, Portugal**

**Carlos Capela [0000-0003-3334-4945], School of Technology and Management, Polytechnic of Leiria, Leiria, Portugal**

**Marcelo Rudolfo Calvete Gaspar** serves as corresponding author (the “**Corresponding Author**”)

on the one part and

Springer Nature Switzerland AG  
Gewerbstrasse 11, 6330 Cham, Switzerland

(the “**Publisher**”)

on the other part;  
together hereinafter referred to as the “**Parties**”.

The Publisher intends to publish the Author’s contribution in a collected work provisionally entitled:

**Progress in Digital and Physical Manufacturing - Proceedings of ProDPM’21**

(the “**Work**”)

edited by: **Dr. Henrique de Amorim Almeida, Joel Oliveira Correia Vasco, Anabela Gonçalves Rodrigues Marto, Carlos Alexandre Bento Capela, Flávio Gabriel da Silva Craveiro, Helena Maria Coelho da Rocha Terreiro Galha Bártole, Luis Manuel de Jesus Coelho, Mário António Simões Correia, Milena Maria Nogueira Vieira, Rui Miguel Barreiros Ruben**

(the “**Editor**”)

The Publisher intends to publish the Work under the imprint Springer.

The Work may be published in the book series **Springer Tracts in Additive Manufacturing**.

#### 1. Contracting Authors

When the Author is more than one person then, unless otherwise indicated in this Agreement or agreed in writing by the Publisher:

(a) the expression “**Author**” as used in this Agreement will apply collectively for all such persons (each a “**co-author**”);

(b) the Corresponding Author hereby warrants and represents that all co-authors of the contribution have expressly agreed that the Corresponding Author has full right, power and authority to sign this



Agreement on their behalf, that the Corresponding Author is entitled to act on their behalf, and that they shall be bound by the Corresponding Author, with respect to all matters, responsibilities, notices and communications related to this Agreement; the Corresponding Author shall obtain authorisations and make them available to the Publisher on request; and  
(c) each co-author is jointly and severally responsible for the Author's obligations under this Agreement which apply to each co-author individually and to the co-authors collectively and the Publisher shall not be bound by any separate agreement or legal relationship as between the co-authors.

## 2. Subject of the Agreement

2.1 The Author will prepare a contribution provisionally entitled:

### **Recycled Reinforced PLA as Ecodesign Solution for Customized Prostheses**

The expression "**Contribution**" as used in this Agreement means the contribution as identified above, and includes without limitation all related material delivered to the Publisher by or on behalf of the Author whatever its media and form (including text, graphical elements, tables, videos and/or links) in all versions and editions in whole or in part.

2.2 The Contribution may contain links (e.g. frames or in-line links) to media enhancements (e.g. additional documents, tables, diagrams, charts, graphics, illustrations, animations, pictures, videos and/or software) or to social or functional enhancements, complementing the Contribution, which are provided on the Author's own website or on a third party website or repository (e.g. maintained by an institution) subject always to the Author providing to the Editor, at the latest at the delivery date of the manuscript for the Contribution, an accurate description of each media enhancement and its respective website or repository, including its/their owner, nature and the URL. The Publisher is entitled to reject the inclusion of, or suspend, or delete links to all or any individual media enhancements.

2.3 In the event that an index is deemed necessary, the Author shall assist the Editor in its preparation (e.g. by suggesting index terms), if requested by the Editor.

## 3. Rights Granted

3.1 The Author hereby grants to the Publisher the perpetual, sole and exclusive, worldwide, transferable, sub-licensable and unlimited right to publish, produce, copy, distribute, communicate, display publicly, sell, rent and/or otherwise make available the Contribution in any language, in any versions or editions in any and all forms and/or media of expression (including without limitation in connection with any and all end-user devices), whether now known or developed in the future, in each case with the right to grant further time-limited or permanent rights. The above rights are granted in relation to the Contribution as a whole or any part and with or in relation to any other works.

Without limitation, the above grant includes: (a) the right to edit, alter, adapt, adjust and prepare derivative works; (b) all advertising and marketing rights including without limitation in relation to social media; (c) rights for any training, educational and/or instructional purposes; and (d) the right to add and/or remove links or combinations with other media/works.

The Author hereby grants to the Publisher the right to create, use and/or license and/or sub-license content data or metadata of any kind in relation to the Contribution or parts thereof (including abstracts and summaries) without restriction.

The Publisher also has the right to commission completion of the Contribution in accordance with the Clause "**Author's Responsibilities – Delivery and Acceptance of the Manuscript**" and of an updated version of the Contribution for new editions of the Work in accordance with the Clause "**New Editions**".

3.2 The copyright in the Contribution shall be vested in the name of the **Author**. The Author has asserted their right(s) to be identified as the originator of the Contribution in all editions and versions, published in all forms and media. The Author agrees that all editing, alterations or amendments to the Contribution made by or on behalf of the Publisher or its licensees for the purpose of fulfilling this Agreement or as otherwise allowed by the above rights shall not require the approval of the Author and will not infringe the Author's "moral rights" (or any equivalent rights). This includes changes made in the course of dealing with retractions or other legal issues.

**4. Self-Archiving and Reuse**

- 4.1 **Self-Archiving:** The Publisher permits the Rights Holder to archive the Contribution in accordance with the Publisher's guidelines, the current version of which is set out in the **Appendix "Author's Self-Archiving Guidelines"**.
- 4.2 **Reuse:** The Publisher permits the Author to copy, distribute or otherwise reuse the Contribution, without the requirement to seek specific prior written permission from the Publisher, in accordance with the Publisher's guidelines, the current version of which is set out in the **Appendix "Author's Reuse Rights"**.

**5. The Publisher's Responsibilities**

- 5.1 Subject always to the other provisions of this Clause below, the Publisher will undertake the production, publication and distribution of the Contribution and the Work in print and/or electronic form at its own expense and risk within a reasonable time after acceptance of the Work unless the Publisher is prevented from or delayed in doing so due to any circumstances beyond its reasonable control. The Publisher shall have the entire control of such production, publication and distribution determined in its sole discretion in relation to any and all editions and versions of the Contribution and the Work, including in respect of all the following matters:
- (a) distribution channels, including determination of markets;
  - (b) determination of the range and functions of electronic formats and/or the number of print copies produced;
  - (c) publication and distribution of the Contribution, the Work, or parts thereof as individual content elements, in accordance with market demand or other factors;
  - (d) determination of layout and style as well as the standards for production;
  - (e) setting or altering the list price, and allowing for deviations from the list price (if permitted under applicable jurisdiction);
  - (f) promotion and marketing as the Publisher considers most appropriate.
- 5.2 All rights, title and interest, including all intellectual property or related rights in the typography, design and/or look-and-feel of the Contribution shall remain the exclusive property of and are reserved to the Publisher. All illustrations and any other material or tangible or intangible property prepared at the expense of the Publisher including any marketing materials remain, as between the Parties, the exclusive property of the Publisher. The provisions of this subclause shall continue to apply notwithstanding any termination of, and/or any reversion of rights in the Contribution to the Author, under this Agreement.
- 5.3 Without prejudice to the Publisher's termination and other rights hereunder including under the Clause "**The Author's Responsibilities**", it is agreed and acknowledged by the Parties that nothing in this Agreement shall constitute an undertaking on the part of the Publisher to publish the Contribution unless and until: (i) any and all issues in relation to the Work (including all necessary revisions, consents and permissions) raised by the Publisher have been resolved to the Publisher's satisfaction, and (ii) the Publisher has given written notice of acceptance in writing of the final manuscript of the entire Work to the Editor. If following (i) and (ii) above the Publisher has not published the Contribution in any form within a reasonable period and the Author has given written notice to the Publisher requiring it to publish within a further reasonable period and the Publisher has failed to publish in any form, then the Author may terminate this Agreement by one month's written notice to the Publisher and all rights granted by the Author to the Publisher under this Agreement shall revert to the Author (subject to the provisions regarding any third party rights under any subsisting licence or sub-licence in accordance with the Clause "**Termination**"). The Author may also give such written notice requiring publication on the same terms as above if the Publisher has published the Contribution but subsequently ceases publishing the Contribution in all forms so that it is no longer available. This shall be the Author's sole right and remedy in relation to such non-publication and is subject always to the Author's continuing obligations hereunder including the Clause "**Warranty**".
- 6. The Author's Responsibilities**
- 6.1 **Delivery and Acceptance of the Manuscript**

- 6.1.1 The Author shall deliver the Contribution to the Editor (or, if requested by the Publisher, to the Publisher) on or before Delivery Date (the “**Delivery Date**”) electronically in the Publisher's standard requested format or in such other form as may be agreed in writing with the Publisher. The Author shall retain a duplicate copy of the Contribution. The Contribution shall be in a form acceptable to the Publisher (acting reasonably) and in line with the instructions contained in the Publisher's guidelines as provided to the Author by the Publisher. The Author shall provide at the same time, or earlier if the Publisher reasonably requests, any editorial, publicity or other information (and in such form or format) reasonably required by the Publisher. The Publisher may exercise such additional quality control of the manuscript as it may decide at its sole discretion including through the use of plagiarism checking systems and/or peer review by internal or external reviewers of its choice. If the Publisher decides at its sole discretion that the final manuscript does not conform in quality, content, structure, level or form to the stated requirements of the Publisher, the Publisher shall be entitled to terminate this Agreement in accordance with the provisions of this Clause.
- 6.1.2 The Author must inform the Publisher at the latest on the Delivery Date if the sequence of the naming of any co-authors entering into this Agreement shall be changed. If there are any changes in the authorship (e.g. a co-author joining or leaving), then the Publisher must be notified by the Author in writing immediately and the Parties will amend this Agreement accordingly. The Publisher shall have no obligation to consider publication under this Agreement in the absence of such agreed amendment.
- 6.1.3 If the Author fails to deliver the Contribution in accordance with the provisions of this Clause above by the Delivery Date (or within any extension period given by the Publisher at its sole discretion) or if the Author (or any co-author) dies or becomes incapacitated or otherwise incapable of performing the Author's obligations under this Agreement, the Publisher shall be entitled to either:  
(a) elect to continue to perform this Agreement in accordance with its terms and the Publisher may commission an appropriate and competent person (who, in the case of co-authors having entered into this Agreement, may be a co-author) to complete the Contribution; or  
(b) terminate this Agreement with immediate effect by written notice to the Author or the Author's successors, in which case all rights granted by the Author to the Publisher under this Agreement shall revert to the Author/Author's successors (subject to the provisions of the Clause “**Termination**”).
- 6.1.4 The Author agrees, at the request of the Publisher, to execute all documents and do all things reasonably required by the Publisher in order to confer to the Publisher all rights intended to be granted under this Agreement.
- 6.1.5 The Author warrants that the Contribution is original except for any excerpts from other works including pre-published illustrations, tables, animations, text quotations, photographs, diagrams, graphs or maps, and whether reproduced from print or electronic or other sources (“**Third Party Material**”) and that any such Third Party Material is in the public domain (or otherwise unprotected by copyright/other rights) or has been included with written permission from or on behalf of the rights holder (and if requested in a form prescribed or approved by the Publisher) at the Author's expense unless otherwise agreed in writing, or is otherwise used in accordance with applicable law. On request from the Publisher, the Author shall in writing indicate the precise sources of these excerpts and their location in the manuscript. The Author shall also retain the written permissions and make them available to the Publisher on request.
- 6.2 **Approval for Publishing**
- 6.2.1 The Author shall proofread the page proofs for the Contribution provided by or on behalf of the Publisher, including checking the illustrations as well as any media, social or functional enhancements and give approval for publishing, if and when requested by the Publisher. The Author's approval for publishing is deemed to have been given if the Author does not respond within a reasonable period of time (as determined by the

Publisher) after receiving the proofs nor contacts the Publisher within three days after receipt of the last of three reminders sent by the Publisher via email. The Publisher shall not be required to send a second set of corrected proofs unless specifically requested by the Author in writing but in any event no further amendments may be made or requested by the Author.

In the event of co-authors having entered into this Agreement the Publisher shall send the page proofs to the Corresponding Author only and all persons entering into this Agreement as Author agree that the Corresponding Author shall correct and approve the page proofs on their behalf.

- 6.2.2 If the Author makes changes other than correcting typographical errors, the Author shall bear all the Publisher's costs of such alterations to proofs including without limitation to alterations to pictorial illustrations. The Publisher shall have the right to charge and invoice these costs plus value added or similar taxes (if applicable) through its affiliated company Springer Nature Customer Service Center GmbH or Springer Nature Customer Service Center LLC, respectively, to the Author, payable within 14 days of receipt of the invoice.

6.3 **Cooperation**

Without prejudice to the warranties and representations given by the Author in this Agreement, the Author shall cooperate fully with the Editor and the Publisher in relation to any legal action that might arise from the publication or intended publication of the Contribution and the Author shall give the Publisher access at reasonable times to any relevant accounts, documents and records within the power or control of the Author.

7. **Warranty**

- 7.1 The Author warrants and represents that:
- (a) the Author has full right, power and authority to enter into and perform its obligations under this Agreement; and
  - (b) the Author is the sole legal owner of (and/or has been fully authorised by any additional rights owner to grant) the rights licensed in the Clause "**Rights Granted**" and use of the Contribution shall in no way whatever infringe or violate any intellectual property or related rights (including any copyright, database right, moral right or trademark right) or any other right or interest of any third party subject only to the provisions in the Clause "**The Author's Responsibilities**" regarding Third Party Material (as defined above); and
  - (c) the Contribution shall not contain anything that may cause religious or racial hatred or encourage terrorism or unlawful acts or be defamatory (or contain malicious falsehoods), or be otherwise actionable, including, but not limited to, any action related to any injury resulting from the use of any practice or formula disclosed in the Contribution and all of the purported facts contained in the Contribution are according to the current body of research and understanding true and accurate; and
  - (d) there is no obligation of confidentiality owed in respect of any contents of the Contribution to any third party and the Contribution shall not contain anything which infringes or violates any trade secret, right of privacy or publicity or any other personal or human right or the processing or publication of which could breach applicable data protection law and that informed consent to publish has been obtained for all research or other featured participants; and
  - (e) the Contribution has not been previously licensed, published or exploited and use of the Contribution shall not infringe or violate any contract, express or implied, to which the Author, or any co-author, who had entered into this Agreement, is a party and any academic institution, employer or other body in which work recorded in the Contribution was created or carried out has authorised and approved such work and its publication.
- 7.2 The Author warrants and represents that the Author, and each co-author who has entered into this Agreement, shall at all times comply in full with:
- (a) all applicable anti-bribery and corruption laws; and
  - (b) all applicable data protection and electronic privacy and marketing laws and regulations; and
  - (c) the Publisher's ethic rules (available at <https://www.springernature.com/gp/authors/book-authors-code-of-conduct>), as may be updated by the Publisher at any time in its sole discretion. The

Publisher shall notify the Author in the event of material changes by email or other written means (the "**Applicable Laws**").

If the Author is in material breach of any of the Applicable Laws or otherwise in material breach of accepted ethical standards in research and scholarship, or becomes the subject of any comprehensive or selective sanctions issued in any applicable jurisdiction (e.g. being subject to the OFAC sanctions list) or if, in the opinion of the Publisher, at any time any act, allegation or conduct of or about the Author prejudices the production or successful exploitation of the Contribution and the Work or brings the name and/or reputation of the Publisher or the Work into disrepute, or is likely to do so, then the Publisher may terminate this Agreement in accordance with the Clause "**Termination**".

- 7.3 The Publisher reserves the right to amend and/or require the Author to amend the Contribution at any time to remove any actual or potential breach of the above warranties and representations or otherwise unlawful part(s) which the Publisher or its internal or external legal advisers identify at any time. Any such amendment or removal shall not affect the warranties and representations given by the Author in this Agreement.

#### **8. Author's Discount and Electronic Access**

- 8.1 The Author, or each co-author, is entitled to purchase for their personal use the Work and other books published by the Publisher at a discount of 40% off the list price, for as long as there is a contractual arrangement between the Author and the Publisher and subject to any applicable book price law or regulation. The copies must be ordered from the affiliated entity of the Publisher (Springer Nature Customer Service Center GmbH or Springer Nature Customer Service Center LLC, respectively). Resale of such copies is not permitted.

- 8.2 The Publisher shall provide the electronic final published version of the Work to the Author, provided that the Author has included their e-mail address in the manuscript of the Contribution.

#### **9. Consideration**

- 9.1 The Parties agree that the Publisher's agreement to its contractual obligations in this Agreement in respect of its efforts in considering publishing and promoting the Contribution and the Work is good and valuable consideration for the rights granted and obligations undertaken by the Author under this Agreement, the receipt, validity and sufficiency of which is hereby acknowledged by the Author. The Parties expressly agree that no royalty, remuneration, licence fee, costs or other moneys whatsoever shall be payable to the Author.

- 9.2 The Publisher and the Author each have the right to authorise collective management organisations ("**CMOs**") of their choice to manage some of their rights. Reprographic and other collectively managed rights in the Contribution ("**Collective Rights**") have been or may be licensed on a non-exclusive basis by each of the Publisher and the Author to their respective CMOs to administer the Collective Rights under their reprographic and other collective licensing schemes ("**Collective Licences**"). Notwithstanding the other provisions of this Clause, the Publisher and the Author shall each receive and retain their share of revenue from use of the Contribution under Collective Licences from, and in accordance with, the distribution terms of their respective CMOs. To the fullest extent permitted by law, any such revenue is the sole property of the Publisher and the Author respectively and, if applicable, the registration and taxation of that revenue is the sole responsibility of the respective recipient party. The Publisher and the Author shall cooperate as necessary in the event of any change to the licensing arrangements set out in this Clause.

#### **10. New Editions**

- 10.1 The Publisher has the sole right to determine whether to publish any subsequent edition of the Work containing an updated version of the Contribution, but only after reasonable consultation with the Author. Once notified by the Publisher that an update of the Contribution is deemed necessary, the Author agrees to deliver an updated manuscript in accordance with the terms of the Clause "**The Author's Responsibilities**" and the other relevant provisions of this Agreement, together with the material for any new illustrations and any other supporting content including media enhancements, within a reasonable period of time (as determined by the Publisher) after such notification. Substantial changes in the nature or size of the Contribution require the written approval of the

Publisher at its sole discretion. The terms of this Agreement shall apply to any new edition of the Work that is published under this "**New Editions**" Clause.

- 10.2 If the Author, for whatever reason, is unwilling, unable or fails (including as a result of death or incapacity) to submit an updated manuscript that meets the terms of this Agreement within the above stated period, then the Publisher is entitled to revise, update and publish the content of the existing edition or to designate one or more individuals (which, where co-authors have entered into this Agreement, may be one or more of the co-authors) to prepare this and any future editions provided that the new editions shall not contain anything that is a derogatory use of the Author's work that demonstrably damages the Author's academic reputation. In such case, the Author shall not participate in preparing any subsequent editions. The Author agrees that the Publisher shall be entitled but not obliged to continue to use the name of the Author on any new editions of the Work together with the names of the person or persons who contributed to the new editions. Should the Author or the Author's successors object to such continuing use then they must notify the Publisher in writing when first contacted by the Publisher in connection with any new edition.

#### **11. Termination**

- 11.1 In addition to the specific rights of termination set out in the Clause "**The Publisher's Responsibilities**" and the Clause "**The Author's Responsibilities**", either Party shall be entitled to terminate this Agreement forthwith by notice in writing to the other Party if the other Party commits a material breach of the terms of the Agreement which cannot be remedied or, if such breach can be remedied, fails to remedy such breach within 45 days of being given written notice to do so.
- 11.2 Termination of this Agreement, howsoever caused, shall not affect:
- (a) any subsisting rights of any third party under any licence or sub-licence validly granted by the Publisher prior to termination and the Publisher shall be entitled to retain its share of any sum payable by any third party under any such licence or sub-licence;
  - (b) except where stated otherwise in this Agreement, any claim which either Party may have against the other for damages or otherwise in respect of any rights or liabilities arising prior to the date of termination;
  - (c) the Publisher's right to continue to sell any copies of the Work which are in its power, possession or control as at the date of expiry or termination of this Agreement for a period of six months on a non-exclusive basis.

#### **12. General Provisions**

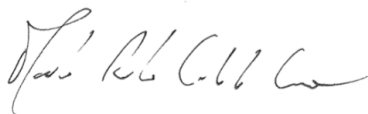
- 12.1 This Agreement, and the documents referred to within it, constitute the entire agreement between the Parties with respect to the subject matter hereof and supersede any previous agreements, warranties, representations, undertakings or understandings. Each Party acknowledges that it is not relying on, and shall have no remedies in respect of, any undertakings, representations, warranties, promises or assurances that are not set forth in this Agreement. Nothing in this Agreement shall exclude any liability for or remedy in respect of fraud, including fraudulent misrepresentation. This Agreement may be modified or amended only by agreement of the Parties in writing. For the purposes of modifying or amending this Agreement, "in writing" requires either a written document signed by both the Parties or an electronic confirmation by both the Parties with DocuSign or a similar e-signature solution. Any notice of termination and/or reversion and, where applicable, any preceding notices (including any requesting remediable action under the Clause "**Termination**") must be provided in writing and delivered by post, courier or personal delivery addressed to the physical address of the relevant Party as set out at the beginning of this Agreement or any replacement address notified to the other Party for this purpose. All such notices shall become effective upon receipt by the other Party. Receipt is deemed to have taken place five working days after the respective notice was sent by post or left at the address by courier or personal delivery. If the Publisher is the terminating Party the notice need only be provided to the address of the Corresponding Author. If the Author is the terminating Party a copy of the notice must also be sent to the Publisher's Legal Department located at Heidelberger Platz 3, 14197 Berlin, Germany.
- 12.2 Nothing contained in this Agreement shall constitute or shall be construed as constituting a partnership, joint venture or contract of employment between the Publisher and the Author. No

Party may assign this Agreement to third parties but the Publisher may assign this Agreement or the rights received hereunder to its affiliated companies. In this Agreement, any words following the terms "include", "including", "in particular", "for example", "e.g." or any similar expression shall be construed as illustrative and shall not limit the sense of the words preceding those terms.

- 12.3 If any difference shall arise between the Author and the Publisher concerning the meaning of this Agreement or the rights and liabilities of the Parties, the Parties shall engage in good faith discussions to attempt to seek a mutually satisfactory resolution of the dispute. This Agreement shall be governed by, and shall be construed in accordance with, the laws of Choose an item.. The courts of Choose an item. shall have the exclusive jurisdiction.
- 12.4 A person who is not a party to this Agreement (other than an affiliate of the Publisher) has no right to enforce any terms or conditions of this Agreement. This Agreement shall be binding upon and inure to the benefit of the successors and assigns of the Publisher. If one or more provisions of this Agreement are held to be unenforceable (in whole or in part) under applicable law, each such provision shall be deemed excluded from this Agreement and the balance of the Agreement shall remain valid and enforceable but shall be interpreted as if that provision were so excluded. If one or more provisions are so excluded under this Clause then the Parties shall negotiate in good faith to agree an enforceable replacement provision that, to the greatest extent possible under applicable law, achieves the Parties' original commercial intention.

The Corresponding Author signs this Agreement on behalf of any and all co-authors.

**Signature of Corresponding Author:**



.....

Marcelo Rudolfo Calvete Gaspar

Date: November, 17<sup>th</sup> 2021

*For internal use only:*

Order Number: 89143056

GPU/PD/PS: 3/32/454

ER\_Book\_Contributor\_CAL\_ST\_EN - Contract Express V.1.0 (12\_2020)

#### Appendix "Author's Self-Archiving Rights"

The Publisher acknowledges that the Author retains rights to archive the Contribution but only subject to and in accordance with the following provisions:

1. **Preprint:**

A "Preprint" is defined as the Author's version of the Contribution submitted to the Publisher but before any peer review or any other editorial work by or on behalf of the Publisher has taken place. The Author may make available the Preprint of the Contribution for personal and private reading purposes only on any of:

(a) the Author's own personal, self-maintained website over which the Author has sole operational control; and/or

(b) a legally compliant, non-commercial preprint server, such as but not limited to arXiv, bioRxiv and RePEc; provided always that once the "Version of Record" (as defined below) of the Contribution has been published by or on behalf of the Publisher, the Author shall immediately ensure that any Preprint made available above shall contain a link to the Version of Record and the following acknowledgement: *"This is a preprint of the following chapter: [author of the chapter], [chapter title], published in [book title], edited by [editor of the book], [year of publication], [publisher (as it appears on the cover of the book)] reproduced with permission of [publisher (as it appears on the copyright page of the book)]. The final authenticated version is available online at: [http://dx.doi.org/\[insert DOI\]](http://dx.doi.org/[insert DOI])".*

2. **Author's Accepted Manuscript:**

The "Author's Accepted Manuscript" ("AAM") is defined as the version of the Contribution following any peer review and acceptance, but prior to copy-editing and typesetting, by or on behalf of the Publisher.

The Author may make available the AAM of the Contribution on any of:

(a) the Author's own, personal, self-maintained website over which the Author has sole operational control; and/or

(b) the Author's employer's internal website or their academic institution or funder's repository; provided that in each case the respective part of the AAM is not made publicly available until after the Embargo Period.

The "**Embargo Period**" is a period ending twelve (12) months from the first publication of the "Version of Record" (as defined below) of the Contribution by or on behalf of the Publisher.

The Author must ensure that any part of the AAM made available contains the following:

*"Users may only view, print, copy, download and text- and data-mine the content, for the purposes of academic research. The content may not be (re-)published verbatim in whole or in part or used for commercial purposes. Users must ensure that the author's moral rights as well as any third parties' rights to the content or parts of the content are not compromised."*

These terms shall also be applicable to the Author.

Once the Version of Record (as defined below) of the Contribution has been published by or on behalf of the Publisher the Author shall immediately ensure that any part of the AAM made available shall contain a link to the Version of Record and the following acknowledgement:

*"This is an Author Accepted Manuscript version of the following chapter: [author of the chapter], [chapter title], published in [book title], edited by [editor of the book], [year of publication], [publisher (as it appears on the cover of the book)] reproduced with permission of [publisher (as it appears on the copyright page of the book)]. The final authenticated version is available online at: [http://dx.doi.org/\[insert DOI\]](http://dx.doi.org/[insert DOI])".*

3. **Version of Record:**

The "**Version of Record**" is defined as the final version of the Contribution as originally published, and as may be subsequently amended following publication in a contractually compliant manner, by or on behalf of the Publisher.

4. Any linking, collection or aggregation of self-archived Contributions from the same Work is strictly prohibited.



**Appendix "Author's Reuse Rights"**

1. The Publisher acknowledges that the Author retains the ability to copy, distribute or otherwise reuse the Contribution, without the requirement to seek specific prior written permission from the Publisher, ("**Reuse**") subject to and in accordance with the following provisions:
  - (a) Reuse of the Contribution or any part of it is permitted in a new edition of the Work or in a new monograph or new textbook written by the same Author provided that in each case the new work is published by the Publisher under a publishing agreement with the Publisher; and
  - (b) Reuse of the Version of Record (as defined below) of the Contribution or any part of it is permitted in a thesis written by the same Author, and the Author is entitled to make a copy of the thesis containing content of the Contribution available in a repository of the Author's awarding academic institution, or other repository required by the awarding institution; an acknowledgement should be included in the citation: "Reproduced with permission from Springer Nature"; and
  - (c) any other Reuse of the Contribution in a new book, book chapter, proceedings or journal article, whether published by the Publisher or by any third party, is limited to three figures (including tables) or a single text extract of less than 400 words; and
  - (d) any further Reuse of the Contribution is permitted only to the extent and in so far as is reasonably necessary: (i) to share the Contribution as a whole to no more than 10 research colleagues engaged by the same institution or employer as the Author for each colleague's personal and private use only; (ii) for classroom teaching use by the Author in their respective academic institution provided that the Contribution or any part of it is not included in course packs for sale or wider distribution to any students, institutions or other persons nor any other form of commercial or systematic exploitation; or (iii) for the Author to use all or parts of the Contribution in the further development of the Author's scientific and/or academic career, for private use and research or within a strictly limited circulation which does not allow the Contribution to become publicly accessible nor prejudice sales of, or the exploitation of the Publisher's rights in, the Contribution (e.g. attaching a copy of the Contribution to a job or grant application).
2. Any Reuse must be based on the Version of Record only, and the original source of publication must be cited according to current citation standards. The "**Version of Record**" is defined as the final version of the Contribution as originally published, and as may be subsequently amended following publication in a contractually compliant manner, by or on behalf of the Publisher.
3. In each case where the Author has Reuse rights or the Publisher grants specific use rights to the Author according to the above provisions, this shall be subject always to the Author obtaining at the Author's sole responsibility, cost and expense the prior consent of any co-author(s) and/or any relevant third party.
4. Any linking, collection or aggregation of reused Contributions from the same Work is strictly prohibited.

## Attachment 5

### Recycled Reinforced PLA as Ecodesign Solution for Customized Prostheses

Marcelo Gaspar<sup>1,3</sup> [0000-0003-3153-6468], Miguel Ferraz<sup>1</sup> [0000-0003-3748-3133],  
Armando Ramalho<sup>2,4</sup> [0000-0003-0500-0459], Joel Vasco<sup>1,5</sup> [0000-0001-8185-8145]  
and Carlos Capela<sup>1,4</sup> [0000-0003-3334-4945]

<sup>1</sup> School of Technology and Management, Polytechnic of Leiria, Leiria, Portugal

<sup>2</sup> Polytechnic Institute of Castelo Branco, Castelo Branco, Portugal

<sup>3</sup> Centre for Rapid and Sustainable Product Design, Polytechnic of Leiria, Leiria, Portugal

<sup>4</sup> Centre for Mechanical Engineering, Materials and Processes, University of Coimbra, Portugal

<sup>5</sup> Institute for Polymers and Composites, University of Minho, Guimarães, Portugal  
marcelo.gaspart@ipleiria.pt

**Abstract.** Additive manufacturing is a key technology for the digital production of customized prostheses and orthoses. Considering that such assistive devices can be designed to meet specific biomechanical needs based on the actual contours of the patients' limbs, the ability of those having physical disabilities being able to produce their custom prostheses and orthoses at home would be groundbreaking, by current standards. To such an end, this research aims at selecting sustainable biopolymers that can be used as filaments to produce customized prosthetic sockets using low-cost additive manufacturing technology. Special focus was put into characterizing the use of recycled PLA reinforced with short carbon fibers as filaments for additive manufacturing. Numerical simulation results showed the potential of this sustainable material combination as an ecodesign solution for customized prostheses and orthoses. Such a solution should allow for patients being able to successfully produce and assemble their own customized assistive devices using fused deposition modelling.

**Keywords:** Additive Manufacturing, Customization, Biomechanics, Ecodesign, Sustainability.

#### 1 Introduction

Additive manufacturing (AM) has been referred as an effective alternative to traditional fabrication processes to manufacture customized prosthesis and orthosis, as it is not as material-wasting, time-consuming or as labor-intensive, when compared with conventional manufacturing [1]. These direct digital technologies are advanced manufacturing processes which allow for mass customization to develop and produce dedicated products [2] which may be adapted to their users' requirements.

Considering the advantages of designing prosthesis and orthosis to meet specific biomechanical needs based on the actual contours of the patients' limbs, current research focuses on the ability of those having physical disabilities being able to produce

2

specific parts of their custom prostheses and orthoses at their homes using conventional low-cost AM devices. To improve the sustainability of such custom-made parts, the selection of dedicated eco-materials will be discussed to allow for their use in these AM processes.

### **1.1 Customization with Additive Manufacturing**

When compared with traditional manufacturing processes, AM presents several distinctive features [3], such as the ability of freeform manufacturing and the possibility to combine into a single component a whole assembly of parts. This latter feature is usually required by the need of breaking down a given product into separate parts to comply with the limits of conventional manufacturing. Both these AM characteristics allow for dedicated product customization with lower overall manufacturing costs [4] and with special focus on adapting the product performance to its user's specific needs.

AM customization does not rely solely on the final manufactured parts and/or product's features but is also referred to the ability to produce products and parts based on a wide range of material types and nature [5, 6]. These range from additive manufactured food products [7] to high performance aeronautic [8] and aerospace parts [9], with ever increasing new feedstock materials for AM [10].

When concerned to the AM of polymer-based products, the lower mechanical properties of this type of materials for structural applications usually require for alternative solutions to comply with the strength requisites required for their end-use. Thus, the recent ability to produce polymer-based composites by AM [7, 11, 12] allow for an increased range of applications, thus broadening the structural use of polymer-based components and parts.

One particularly promising field of use for AM is the possibility to design and produce dedicated prosthesis and devices adapted to their users' needs [13, 14]. To such an end, AM has been reported as particularly beneficial in dental applications [15], in customized airway prosthesis [16], in bio-inspired heart valves [17], in craniofacial soft tissue prostheses [18], in customized tracheal stents [19], among many other successful applications, in which AM allows to design and manufacture custom prostheses and orthoses to their final users' requirements.

### **1.2 Additive Manufacturing Environmental Sustainability through Recycling**

The current effort to promote circular economy solutions amongst manufacturing processes allows highlighting the environmental benefits of AM [20, 21]. When compared to traditional manufacturing, AM is usually referred as being an environmentally sustainable way to produce tangible goods [22] as it allows for reduced material waste, lower energy use, and lesser emissions than those of conventional processes [23].

Considering the whole life cycle of AM products, the reuse of both waste materials and end-of-life AM parts through recycling is also an environmentally sustainable solution as it contributes to lower the environmental impacts of these manufacturing processes. Metal-based AM parts can be recycled for a wide range of engineering alloys [24], whereas the polymer-based AM parts can also be recycled, particularly if they are

of a thermoplastic nature [25]. Cruz *et al.* [26] present an extensive literature review on the latter subject.

The use of natural fibers as reinforcement in AM engineering materials may also be perceived as an environmentally sustainable solution to incorporate biomaterials into AM composites to improve their mechanical, thermal, chemical, surface, and morphological properties [27]. However, as these AM composites are not mono-materials, increased challenges must be overcome to allow for their successful recyclability [28, 29].

## 2 Materials and Methods

Current research focuses on the use of recycled PLA biopolymers with, and without carbon fiber reinforcement. To discuss the usability of these eco-materials in custom prosthesis design and manufacturing, a brief discussion will be carried-out about the materials and methods used in this study.

### 2.1 Recycled Reinforced PLA for Additive Manufacturing

Due to its sustainable nature, minimal warping and ease of use, Polylactic Acid (PLA) is currently one of the highest biopolymers produced at a global scale [30]. The PLA filaments are also amongst the most popular materials used in open-source desktop 3D-printing [31] mainly due to its renewable resource nature. The increased adoption of virgin and recycled PLA in AM led to corresponding research efforts to characterize optimal process parameters, performance, and waste reuse [32–35].

The potential of PLA reinforced composite materials has been discussed and tested by different researchers to infer about its usability in many engineering fields, using mainly long natural and non-natural fibers [30, 36, 37]. In current research, PLA reinforced with carbon fibers was selected since these fibers are not significantly affected by the thermal cycles of the recycling process [38]. After shredding, the original end-of-life PLA parts and waste reinforced with long carbon fibers result in a homogeneous mix of short carbon reinforced particles with no preferential fiber alignment. The shredded particles will be used to create new filaments of rPLA with different percentages of carbon-fiber reinforcements. The mechanical properties of these rPLA-based eco-materials are based on the work carried-out by Farah *et al.* [39], Hu & Karki [40] and De Groot *et al.* [41].

### 2.2 Numerical Model

With the numerical simulation, it is intended to characterize the magnitude of stresses that occur at the socket-type prosthesis level to aid inferring about the mechanical properties of different sustainable materials to be used in such type of assistive devices.

The numerical model presented in **Fig. 1** was used to carry out different simulations based on the 2D axisymmetric approximation of the patient's residual limb contours and the prosthesis itself. This model, also used by the authors in previous research [42, 43], was adapted to support and discuss the results of current research. It consists of the

4

patient's residual limb femur and the evolving soft tissues, as well as the dedicated prosthesis and liner used to better accommodate the socket-type device.

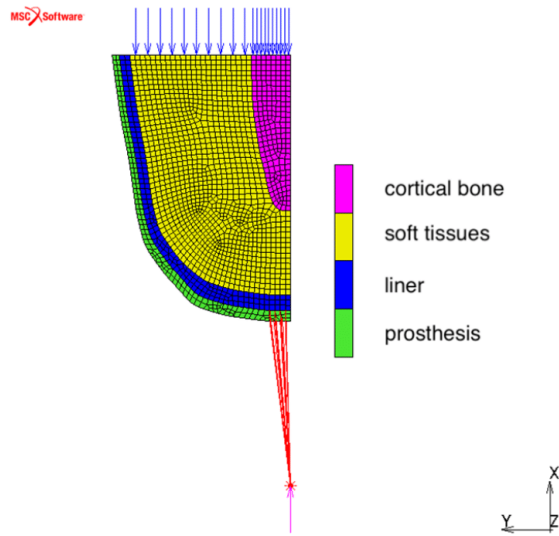


**Fig. 1.** Geometries, meshes and deformable bodies of the biomechanical model.

**Geometry and loading.** The data that enabled creating the geometry of this model's anthropometry and customized prosthesis was acquired through the patient's medical digital imaging. Such data was interpolated using cubic splines. The prosthesis was considered to support a load of 70 kgf, which corresponds to the total weight of the user during the static stance. Loading is imposed in quasi-static conditions [44], as illustrated in **Fig. 1**.

**Materials.** A conventional thermoplastic polymer (polypropylene) and five different eco-materials were considered for the composition of the socket-type prosthesis: an epoxy resin whose molecular structure is mostly of vegetable origin (SR GreenPoxy 56, produced by Sicomin [45]); a composite in which a SR GreenPoxy 56 resin matrix is reinforced with 40% natural jute fibers; a recycled PLA biopolymer, and two composites in which the recycled PLA biopolymer matrix is reinforced with 20% and 30% short carbon fibers.

**Finite Element Analysis (FEM).** Given the symmetry of the model (see **Fig. 1**), a 2D axisymmetric analysis was performed. The simulations with this model were made using the implicit module of MSC Marc Mentat 2018 [46].

A multifrontal direct sparse solver, the Paradiso solver, is used with a Newton-Raphson iterative procedure. For convergence testing, a relative force tolerance of 10% is used. An adaptive multicriteria stepping procedure is used for load increment was used for the initial time step (load increment) of  $1 \times 10^{-6}$ .

The numerical constrictions associated with the implicit method were overcome using a mesh adaptivity algorithm, the advancing front quadrilateral. An automatic algorithm was used for meshing, and linear quadrilateral axisymmetric solid elements with four nodes (Quad 10) were used.

The initial mesh dimensions of the elements were of 3 mm. This value was established in a previous iterative process and is considered an objective in the adaptive mesh algorithm. In this process, the mesh size may be reduced to a quarter of its initial value, depending on the strain change and the distortion that may take place in each element [42, 43]. In the structural analysis, large strain nonlinear procedures were used.

For the soft tissues' materials, the Neo-Hookean model presented in [47] was used, whereas, for the liner, Mooney-Rivlin behavior with three parameters [48] was considered.

On what concerns the hard materials – femur and socket – a linear elastic behavior was considered. The femur, the resin and thermoplastic materials were modeled as isotropic linear elastic. The reinforce fibers – jute and carbon – were modeled as orthotropic linear elastic materials. The composite materials are modeled as anisotropic linear elastic materials.

**Composite materials simulation.** For the composite materials numerical simulation, the Halpin-Tsai model for discontinuous fibers was used [49]. The composite material's elastic properties were computed in the MSC Patran 2019 software [50] considering the respective resin/fiber volume ratio. A 10 to 1 ratio was considered for the fibers' length vs diameter.

The fibers on the composite were later dispersed using a 2D short fiber model implemented in the MSC Patran 2019 software [50], with angles  $\alpha = 0^\circ$  and  $\phi = 45^\circ$ , a standard deviation of  $10^\circ$  through a random process, with zero correlation, using 1000 Monte Carlo iterations.

The composites were oriented so that axis 1 has, at each point, the direction of the tangent to the prosthesis profile shown in Fig. 1. Axis 2 has the direction of thickness and axis 3, the tangential direction [46].

### 3 Results and Discussion

The results section of current research starts with both the biomechanical system and the custom socket-type prosthesis simulation to analyze the local stress fields resulting

6

from the use of the prosthesis. In the end of this section, the results are discussed towards the usability of the rPLA biocomposite as a structural material in such custom assistive device.

### 3.1 Biomechanical system simulation

In the contact between the system's various components, a Coulomb's bilinear friction model was used, with an average friction coefficient between the cortical bone and the soft tissues of  $\mu = 0.3$  [51].

A friction coefficient of  $\mu = 0.5$  was considered for the contact between the socket type prosthesis and the liner. For the liner and the soft tissues contacts, a friction coefficient of  $\mu = 0.65$  was used [43].

In the numerical model, the contact between deformable bodies is modelled by the finite sliding segment-to-segment contact algorithm. The separation criteria are based upon stresses (Lagrange multipliers): separation threshold is treated as residual stress of negligible magnitude ( $0.9 \times 10^{-6}$  MPa) [43].

**Biological tissues.** The patient's soft tissues were modeled by a Neo-Hookean model for the muscle, with  $C_{10} = 4.25$  kPa and the volumetric behavior obtained only with the first term of the series,  $D_1 = 24.34$  MPa<sup>-1</sup>. The patient's femur was modelled as an isotropic, homogeneous, and linear elastic material. The cortical bone properties are considered along the longitudinal direction [52], with an elastic modulus,  $E = 11.5$  GPa, and Poisson's ratio,  $\nu = 0.31$  [43].

**Non-biological materials.** When modelling the biomechanical model liner (see Fig. 1) the TEC Pro 18 polyurethane was considered. This material is produced by TEC Interface Systems, Waite Park, Minnesota, modeled by a the second-order Mooney-Rivlin model, with the following parameters:  $C_{10} = 1.5152 \times 10^{-6}$  kPa;  $C_{01} = 41.365$  kPa;  $C_{11} = 9.4846 \times 10^{-7}$  kPa; and the bulk modulus of 413.65 MPa. Considering that six different materials were considered for the prosthesis, a dedicated section for the details of their numerical simulation will be presented next [43].

### 3.2 Socket-type prostheses simulation

To better visualize and quantify the stress field that occurs in the socket-type prosthesis, which is the main object of current research, the part of the model related to it was isolated from the rest of the numerical model components (see Fig. 1). As previously referred, a conventional thermoplastic polymer (polypropylene) and five different eco-materials were considered for the composition of the socket-type prosthesis. The simulation for each of these material types will be presented and discussed in this section.

**Polypropylene.** This thermoplastic material was modelled as homogeneous, isotropic, and linear elastic, with an elastic modulus ( $E$ ) of 1000 MPa and the Poisson's ratio  $\nu = 0.30$  [43]. Considering these parameters, a dedicated simulation for the polypropylene

material for the prosthetic socket was carried out and the stress fields on the socket are shown in Fig. 2. The mean normal stress field is presented in Fig. 2a), whereas Fig. 2b) illustrates the von Mises stress field. It can be observed that the higher stress levels are located at the lower end of the patient's prosthesis, in the connection between the socket and the pylon. In the surrounding contact area with the pylon, compression stresses are observed. On the opposite side of the socket thickness, tensile stresses are generated. In this simulation, the mean normal stresses varied between -32 and 24 MPa and the equivalent von Mises stresses varied up to 64 MPa.

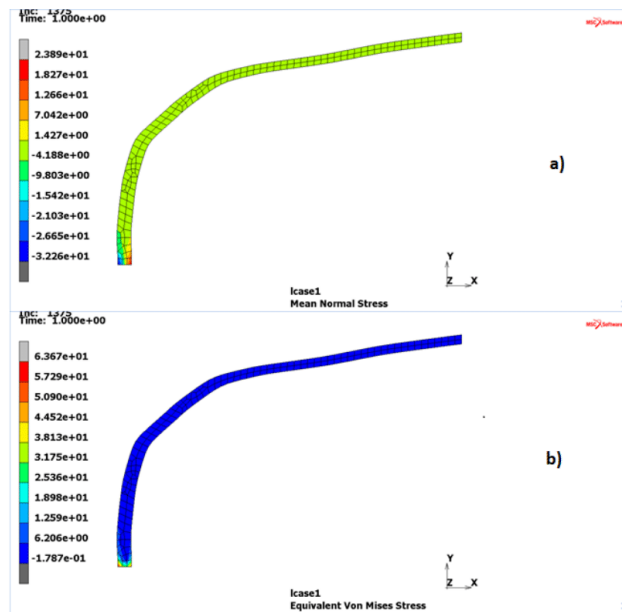


**Fig. 2.** Stress fields (in MPa) for the polypropylene socket-type prosthesis: a) Mean normal stress; b) Equivalent von Mises stress.

**SR GreenPoxi 56.** This biopolymer was modelled as homogeneous, isotropic, and linear elastic, with an elastic modulus ( $E$ ) of 3000 MPa, a Poisson's ratio  $\nu = 0.39$  and the specific mass  $\rho = 1180 \text{ kg/m}^3$  [43]. The contact stresses on the socket-type prosthesis, namely the mean normal stresses and the equivalent von Mises stresses are shown in the numerical simulation presented in Fig. 3. Considering these parameters, a dedicated simulation for the SR GreenPoxi 56 resin was carried out and the stress fields on the socket are presented in Fig. 3. Thus, Fig. 3a) illustrates the mean normal stress field and Fig. 3b) shows the von Mises stress field.



8

As what occurred for the polypropylene, it can be observed that the higher stress levels are located at the lower end of the patient's prosthesis. However, the stress levels are lower for the SR GreenPoxi 56 resin than those for the thermoplastic polymer. In the surrounding area of the contact with the pylon compression stresses take place and, on the other side of the socket thickness, tensile stresses are observed. In this simulation, the mean normal stresses varied between -28 and 21 MPa and the equivalent von Mises stresses varied up to 55 MPa.

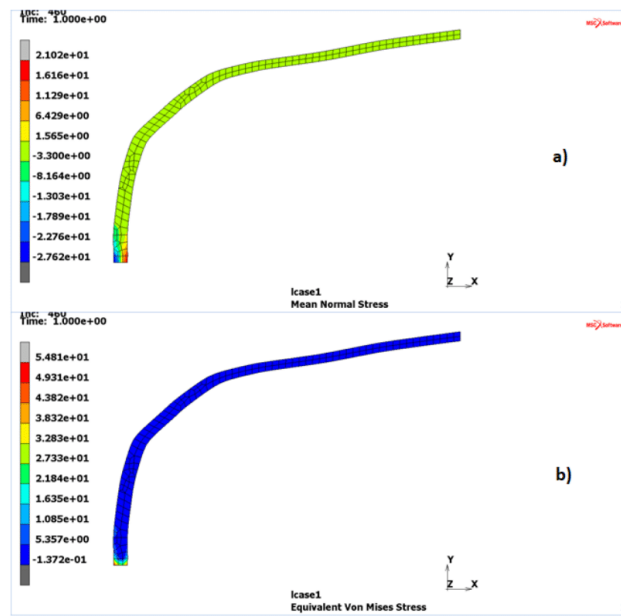


**Fig. 3.** Stress fields (in MPa) for the SR GreenPoxi 56 resin reinforced socket-type prosthesis: a) Mean normal stress; b) Equivalent von Mises stress.

**SR GreenPoxi 56 resin reinforced with 40% jute fibers.** This biopolymer-based composite reinforced with 40% jute fibers was modelled as following: the jute fibers were considered as homogeneous whilst the resulting composite was modelled as 2D orthotropic and linear elastic, with an elastic modulus  $E_1 = 23949$  MPa and  $E_2 = 978$  MPa, the Poisson's ratio  $\nu_{12} = 0.374$  and  $\nu_{21} = 0.014$ , the shear modulus  $G_{12} = 411$  MPa and the specific mass  $\rho = 1440$  kg/m<sup>3</sup> [43]. For this biocomposite, a 60 to 40% resin-to-fiber volume ratio was considered. From the simulation in MSC Patran 2019, using the Halpin-Tsai model [49], the resulting elasticity matrix for this composite is presented in equation (1).

$$[C_{ij}] = \begin{bmatrix} 1.30 \times 10^5 & 1.39 \times 10^5 & 1.26 \times 10^5 & 3.07 \times 10^1 \\ 1.39 \times 10^5 & 1.59 \times 10^5 & 1.40 \times 10^5 & 5.04 \times 10^1 \\ 1.26 \times 10^5 & 1.40 \times 10^5 & 1.31 \times 10^5 & 5.32 \times 10^1 \\ 3.07 \times 10^1 & 5.04 \times 10^1 & 5.32 \times 10^1 & 2.10 \times 10^3 \end{bmatrix} \text{ (MPa)} \quad (1)$$

The dedicated simulation with the SR GreenPoxi 56 composite reinforced with jute fibers was carried out and the stress field on the socket are available at Fig. 4. Again, as for previous simulations it can be observed that the higher stress levels are located at the lower end of the patient's prosthesis. The normal stress levels are lower for the SR GreenPoxi 56 resin than those for the GreenPoxi-Jute composite. However, the von Mises stresses have the opposite behavior. In the surrounding area of the contact with the pylon compression stresses take place, whereas on the other side of the socket thickness tensile stresses can be observed. In this simulation, the mean normal stresses varied between -57 and 59 MPa and the equivalent von Mises stresses varied up to 13 MPa.

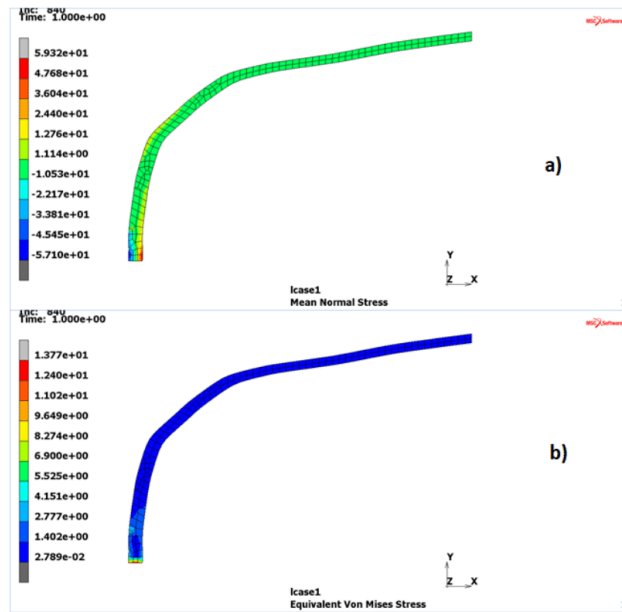
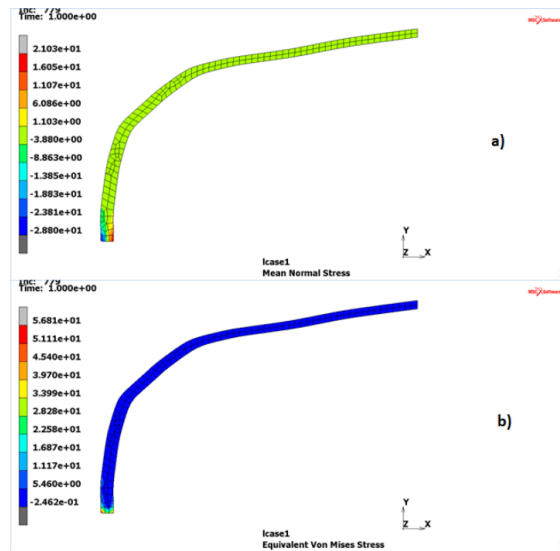


Fig. 4. Stress fields (in MPa) for the SR GreenPoxi 56 resin reinforced socket-type prosthesis with 40% jute fibers socket-type prosthesis: a) Mean normal stress; b) Equivalent von Mises stress.

**Recycled PLA biopolymer.** The research conducted by Anderson [53] shows that for a short number of recycling cycles the mechanical properties of rPLA are similar to those of the virgin PLA. Consequently, both PLA and rPLA biopolymers can be modelled as homogeneous, isotropic, and linear elastic, with an elastic modulus ( $E$ ) of 3500 MPa, a Poisson's ratio  $\nu = 0.36$  and the specific mass  $\rho = 1252 \text{ kg/m}^3$  [39]. Considering these parameters, a dedicated simulation for the rPLA biopolymer used in the prosthetic socket was carried out and the stress fields on the socket are presented in Fig. 5. It can be observed that the PLA/rPLA biopolymer has similar stress fields as those observed for the GreenPoxy 56 resin. In this simulation, the mean normal stresses varied between -29 and 21 MPa and the equivalent von Mises stresses varied up to 57 MPa.



**Fig. 5.** Stress fields (in MPa) for the PLA/rPLA biopolymer socket-type prosthesis: a) Mean normal stress; b) Equivalent von Mises stress.

**Recycled PLA biopolymer composite (20% carbon fiber).** For the rPLA+20% carbon composite, the properties presented above for the PLA/rPLA biopolymer were considered for this composite's matrix. As for the carbon fibers, these were modeled as homogeneous, 2D orthotropic and linear elastic, with elastic modulus  $E_1 = 250 \text{ GPa}$  and  $E_2 = 22.4 \text{ GPa}$ , the Poisson's ratio  $\nu_{12} = 0.35$  and  $\nu_{21} = 0.0024$ , the shear modulus  $G_{12} = 22.1 \text{ GPa}$  and the specific mass  $\rho = 1760 \text{ kg/m}^3$  [40, 41]. For the first PLA composite simulation, a rPLA\_0.2C with 80 to 20% resin-to-fiber volume ratio was considered. From the composite simulation in MSC Patran 2019 using the Halpin-Tsai model [49], the elasticity matrix was obtained for this composite as presented in equation (2).

$$[C_{ij}] = \begin{bmatrix} 1.86 \times 10^4 & 1.36 \times 10^4 & 1.42 \times 10^4 & 1.50 \times 10^1 \\ 1.36 \times 10^4 & 1.89 \times 10^4 & 1.36 \times 10^4 & 5.57 \times 10^0 \\ 1.42 \times 10^4 & 1.36 \times 10^4 & 1.86 \times 10^4 & 8.33 \times 10^0 \\ 1.50 \times 10^1 & 5.57 \times 10^0 & 8.33 \times 10^0 & 1.98 \times 10^3 \end{bmatrix} \text{ (MPa)} \quad (2)$$

Considering these parameters, a dedicated simulation for the Recycled PLA biopolymer composite with 20% carbon fiber was carried out and the main results are shown in **Fig. 6**. When compared with the rPLA biopolymer, a great increase in magnitude of the normal stress field can be observed, with a slight decrease of the von Mises stress field. In this simulation, the mean normal stresses varied between -48 and 44 MPa and the equivalent von Mises stresses varied up to 53 MPa.

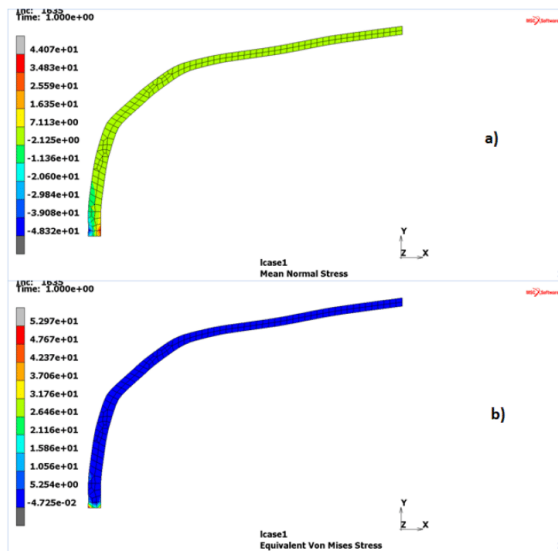


**Fig. 6.** Stress fields (in MPa) for the recycled PLA biopolymer reinforced with 20% short carbon fibers socket-type prosthesis: a) Mean normal stress; b) Equivalent von Mises stress.

**Recycled PLA biopolymer composite (30% carbon fiber).** For the second rPLA+30% carbon composite, the same properties for the recycled PLA matrix and carbon fiber were considered. However, a different PLA\_0.3C with 70 to 30% resin-to-fiber volume ratio was considered. From the composite simulation in MSC Patran 2019 using the Halpin-Tsai model [49], the elasticity matrix was obtained for this composite as presented in equation (3).

12

$$[C_{ij}] = \begin{bmatrix} 1.56 \times 10^5 & 1.76 \times 10^5 & 1.49 \times 10^5 & 3.68 \times 10^1 \\ 1.76 \times 10^5 & 2.16 \times 10^5 & 1.76 \times 10^5 & 1.15 \times 10^2 \\ 1.49 \times 10^5 & 1.76 \times 10^5 & 1.56 \times 10^5 & 1.25 \times 10^2 \\ 3.68 \times 10^1 & 1.15 \times 10^2 & 1.25 \times 10^2 & 2.83 \times 10^3 \end{bmatrix} (MPa). \quad (3)$$

Based on these parameters, a dedicated simulation for the rPLA biopolymer composite with 30% carbon fiber was carried out and the main results are illustrated in Fig. 7. When compared with the plain rPLA biopolymer results, a great increase in magnitude of the normal stress field has occurred and also a great decrease of the von Mises stress field took place. In this simulation, the mean normal stresses varied between -49 and 51 MPa and the equivalent von Mises stresses varied up to 17 MPa.

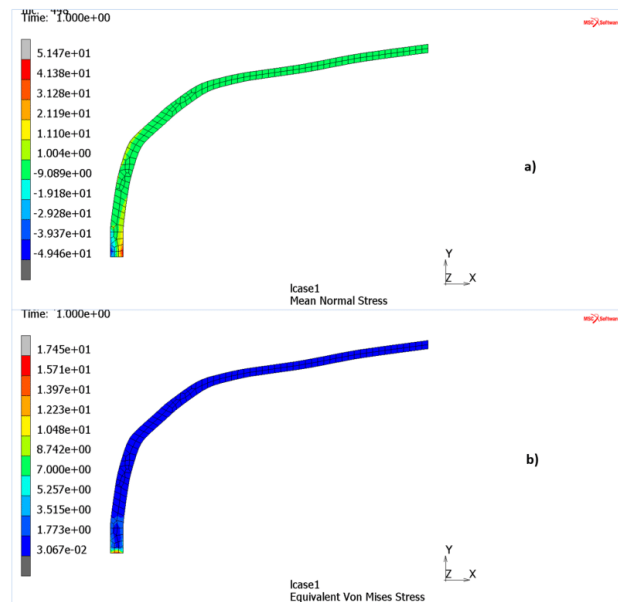


**Fig. 7.** Stress fields (in MPa) for the recycled PLA biopolymer reinforced with 30% short carbon fibers socket-type prosthesis: a) Mean normal stress; b) Equivalent von Mises stress.

**Contact stresses.** To assess the effect of increased stiffness and anisotropy of the prosthesis material on the patient's comfort using it, as well as to analyse the transmission of forces at the interfaces of the different components of the prosthesis, Fig. 8 and Fig. 9, show, respectively, the field of contact stresses developed in the system for the rPLA biopolymer socket and the rPLA+30% carbon composite.

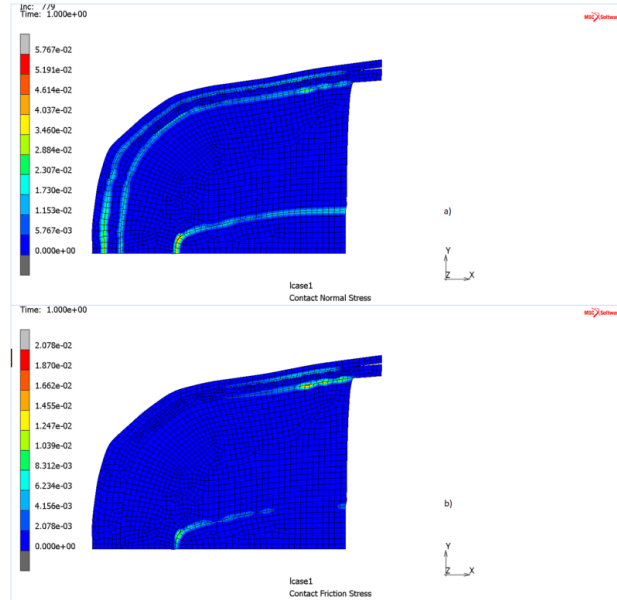


**Fig. 8.** Contact stress field (in MPa) developed in the system with rPLA biopolymer socket: a) Normal stress; b) Friction stress.

From the analysis of the results presented in both **Fig. 8** and **Fig. 9.**, it can be observed that the normal contact stresses in the polymer are significantly lower than for the composite, while the opposite occurs for the friction stresses.

14

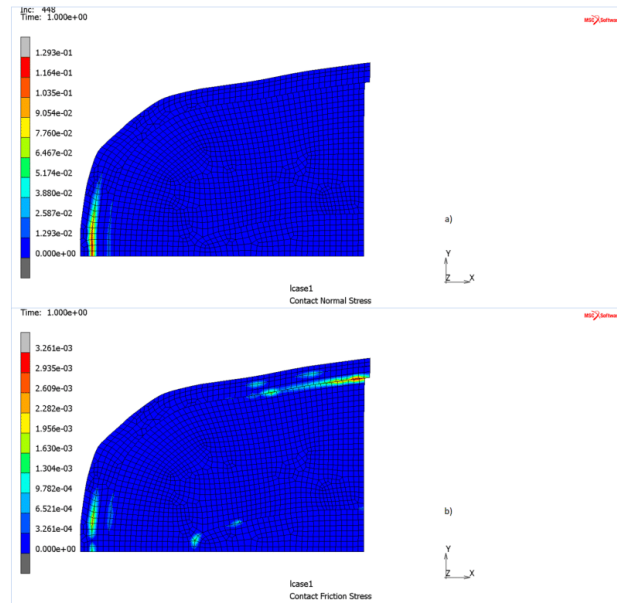


**Fig. 9.** Contact stress field (in MPa) developed in the system with the socket of rPLA biopolymer reinforced with 30% short carbon fibers: a) Normal stress; b) Friction stress.

**Components of stresses.** To assess the influence of the components of stresses in the mean normal stress and in the von Mises stress fields, **Fig. 10** and **Fig. 11** show, respectively, the field of components of stresses developed in the socket of rPLA biopolymer and the rPLA+30% carbon composite.

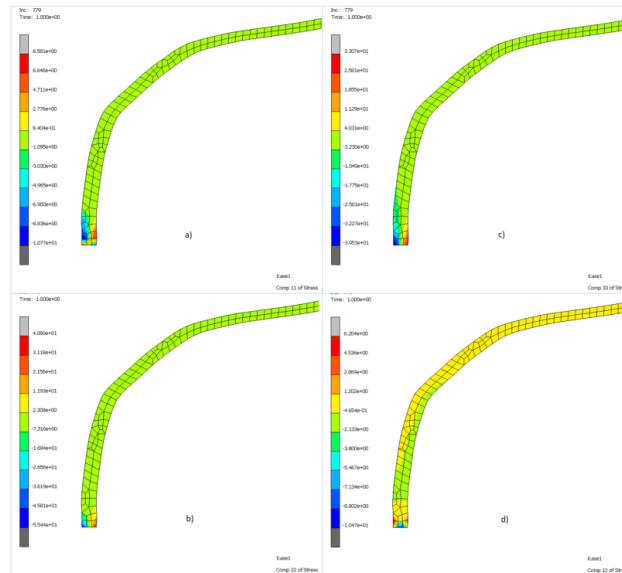


**Fig. 10.** Components stress fields (in MPa) developed in PLA biopolymer socket: a) Axial stress; b) Radial stress; c) Normal stress in tangential direction; d) Shear stress.

From the analysis of the results presented in both **Fig. 10** and **Fig. 11**, it can be observed that all the components of normal stresses in the composite have similar magnitudes, which result in lower von Mises stresses and increased mean normal stresses.



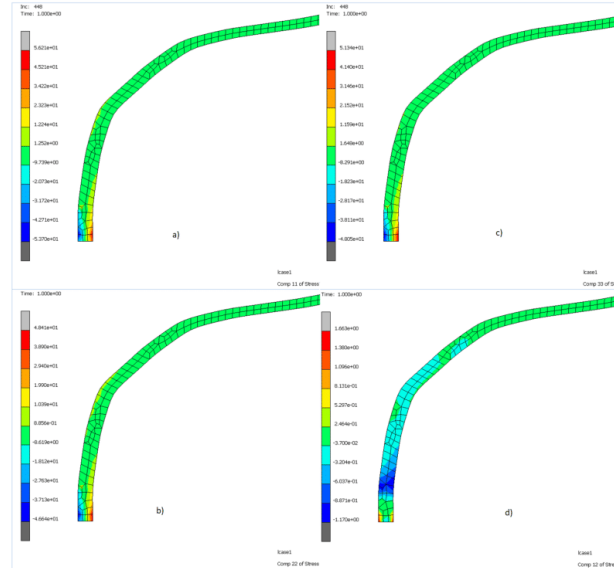


**Fig. 11.** Components stress fields (in MPa) developed in socket of recycled PLA reinforced with 30% short carbon fibers: a) Axial stress; b) Radial stress; c) Normal stress in tangential direction; d) Shear stress.

### 3.3 Discussion

The recycled PLA biopolymer composite reinforced with short carbon fibers has special relevance for the current customized prosthesis development scenario. Particularly, the 70 to 30% resin-to-fiber volume ratio presents the most promising results. Thus, although the GreenPoxy composite may include more environmentally friendly materials, this latter biocomposite cannot be transformed into an extrudable filament and, therefore, cannot be used in low-cost fused deposit modelling additive processes.

To compare the proposed rPLA biocomposite with other alternative materials for the customized socket-type prosthesis, various numerical simulations were carried-out towards inferring about the suitability of use to satisfy the requirements for the application under research. The results of these simulations were shown in **Fig. 2** to **Fig. 7**, in which it was observed that the highest stress levels were located at the lower end of the prosthesis geometry. **Fig. 12** shows the nodes of the numerical model located on such critical area.

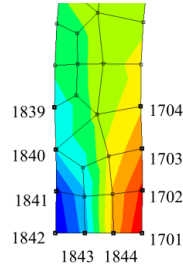


**Fig. 12.** Identification of nodes located at the critical zone of all the numerical model simulations.

**Raghava-Caddell-Atkins equivalent stresses.** Considering that solely the von Mises plasticity criterion would not present satisfactory results when applied to polymeric materials, as it did not include the dependence of the hydrostatic pressure and assumed equal values of yield stress to compression and tension Raghava *et al.* [54], proposed a new plasticity criterion adapting the von Mises model to include the effect of the hydrostatic pressure.

Later, Caddell *et al.* [55] confirmed the validity of the modified criterion to be used as the yield criteria for polymeric materials. The elasticity limit function  $F(\sigma_{ij})$  according to the Raghava-Caddell-Atkins criterion can be expressed as follows:

$$F(\sigma_{ij}) = (\sigma_1 - \sigma_2)^2 + (\sigma_1 - \sigma_3)^2 + (\sigma_2 - \sigma_3)^2 + 2(\sigma_1 + \sigma_2 + \sigma_3)(C - T) = 2CT \quad (4)$$

in which  $C$  and  $T$  refer to the absolute values of the yield stress, respectively in compression and traction.

Groot *et al.* [41], mentioned the modified von Mises criteria to be efficient when considering the effect of hydrostatic pressure to assess the yield of reinforced resins. Conversely, in current research, the Raghava-Caddell-Atkins criterion was used to assess the yield stresses on the socket-type prosthesis when applied to different materials. When analyzing the mechanical behavior of the polymer-based composites, it was considered that the yield occurs in the matrix.

**Summary of the results.** For the polymers and resins considered, the respective yield strengths to compression and tension were obtained according to the **Table 1**.

**Table 1.** Yield strengths to compression and tension for the considered polymers and resins.

	Polypropylene	GreenPoxy	PLA/rPLA
<b>Compressive strength</b>	40 MPa	79 MPa	13600 psi = 93,79 MPa 68 MPa
<b>Tensile strength</b>	20 MPa	50 MPa	9531 psi = 65,73 MPa 40 MPa
<b>C-T</b>	20 MPa	29 MPa	28,06 MPa
<b>References</b>	[56, 57]	[58]	[53, 59]

**Table 2** and **Table 3** present the results for the von Mises equivalent stresses ( $\sigma_{\text{von Mises}}$ ), the hydrostatic stresses ( $\sigma_{kk}$ ) and the Raghava-Caddell-Atkins equivalent stresses ( $\sigma_{\text{RCA}}$ ) at the nodes on the critical zone (see **Fig. 8**), for the various materials. For the various polymers and resins, these values are compared with the respective yield strength and the reference stress for the Raghava-Caddell-Atkins criterion.

**Table 2.** Summary of all the simulation results for the Polipropylene, GreenPoxy and Composite GreenPoxy +40% jute materials.

NODE	Polipropylene			GreenPoxy			GreenPoxy+40% jute composite		
	$\sigma_{\text{vonMises}}$	$\sigma_{kk}$	$\sigma_{\text{RCA}}$	$\sigma_{\text{vonMises}}$	$\sigma_{kk}$	$\sigma_{\text{RCA}}$	$\sigma_{\text{vonMises}}$	$\sigma_{kk}$	$\sigma_{\text{RCA}}$
1839	10,48	-7,67	16,22	6,60	-9,37	17,76	2,40	-25,90	27,51
1840	14,01	-10,13	19,97	8,88	-12,58	21,06	3,23	-34,83	31,94
1841	34,75	-25,28	41,39	24,16	-24,65	36,03	3,62	-57,10	40,85
1842	63,67	-32,26	<b>68,55</b>	54,81	-27,62	<b>61,68</b>	11,09	-41,04	36,24
1843	35,98	-17,84	40,63	33,04	-15,89	39,40	13,25	-22,48	28,77
1844	30,69	10,28	33,87	27,09	8,47	31,30	13,77	14,34	24,61
1701	53,86	23,89	58,13	46,91	21,02	53,01	9,32	56,08	41,39
1702	25,28	17,25	31,37	18,02	17,60	28,90	3,10	59,32	<b>41,59</b>
1703	12,13	8,42	17,77	8,01	10,72	19,36	3,26	35,06	32,05
1704	7,71	4,39	12,13	5,13	5,73	13,88	2,10	22,59	25,68
Strength [MPa]			<b>28,28</b>			<b>62,80</b>			<b>62,80</b>

**Table 3.** Summary of all the simulation results for the Recycled PLA, rPLA+20% carbon composite and rPLA+30% carbon composite materials.

NODE	Recycled PLA			rPLA +20% carbon composite			rPLA +30% carbon composite		
	$\sigma_{\text{vonMises}}$	$\sigma_{kk}$	$\sigma_{\text{RCA}}$	$\sigma_{\text{vonMises}}$	$\sigma_{kk}$	$\sigma_{\text{RCA}}$	$\sigma_{\text{vonMises}}$	$\sigma_{kk}$	$\sigma_{\text{RCA}}$
1839	7,58	-8,31	17,05	4,41	-14,41	20,59	3,27	-21,60	24,83
1840	10,20	-11,18	20,44	5,93	-19,40	24,08	4,39	-29,04	28,88
1841	26,68	-24,00	37,21	15,32	-48,32	39,88	4,07	-49,46	<b>37,48</b>
1842	56,81	-28,80	<b>63,53</b>	52,97	-21,08	<b>58,28</b>	11,32	-32,23	32,13
1843	34,28	-16,74	40,56	29,71	-13,12	35,37	16,58	-17,36	27,60
1844	27,08	8,21	31,04	19,87	7,21	24,44	17,45	10,74	24,62
1701	47,40	21,03	53,26	46,12	28,16	54,01	9,25	44,87	36,67
1702	19,66	16,60	29,20	12,04	44,07	37,17	3,81	51,47	38,19
1703	9,01	9,18	18,40	5,52	18,04	23,17	4,47	29,55	29,14
1704	5,77	4,89	13,06	3,54	11,58	18,37	2,88	19,04	23,30
Strength [MPa]			<b>52</b>			<b>52</b>			<b>52</b>

On what concerns to the normal stresses, it can be observed that, in general, the highest stresses take place on the most distal part of the socket-type prosthesis, at the interface between the socket and the liner. Conversely, considering the equivalent von Mises stresses, it can also be observed that the higher stresses occur on the most distal part of the socket-type prosthesis.

By observing the summarized results presented in **Table 2** and **Table 3** it is possible to verify that only the composites of SR GreenPoxy 56 resin reinforced with 40% jute fibers and of recycled PLA biopolymer reinforced with 30% short carbon fibers meet, with a safety margin, the requirements to support the loads necessary to this application. These are very positive results in that it opens the possibility to build a socket-type

prosthesis through additive manufacturing, such as with the Fused Deposition Modeling (FDM) technology. Nonetheless, the resulting mechanical properties shall also be assessed and validated using an experimental setup.

Analyzing the results presented in **Fig. 4** and **Fig. 7**, it can be observed that both the GreenPoxy+40% jute and the rPLA+30% carbon composites have similar behaviors. When compared, the GreenPoxy-jute composite has slightly lower normal stresses than the rPLA-carbon composite, whereas when considering the von Mises stresses, these are slightly higher for the GreenPoxy-jute composite than for the rPLA-carbon composite. As previously mentioned, for current case-study, the rPLA biopolymer composite is preferred towards the GreenPoxy due to its applicability in additive manufacturing. Thus, further analysis will be restricted to the recycled PLA biopolymer reinforced with 30% carbon fibers.

Considering the stress fields presented in both **Fig. 10** and **Fig. 11**, it can be observed that the increased mechanical behavior of the rPLA composite, when compared to the rPLA biopolymer, is due to the higher stiffness of the composite in the axial direction (**Fig. 10a** and **Fig. 11a**), which is the thickness direction of the critical zone. The stiffness increase derives from the dispersion of short carbon fibers in the direction of the socket thickness. Thus, a particular attention must be paid to this fact during the manufacturing of the prosthesis, as such increase in stiffness leads to the transmission of efforts to the soft tissues in a more uniform way, resulting in better comfort for the patient, as can be observed from the results presented in **Fig. 9** and **Fig. 10**. In fact, as the shear stresses are amongst the main causes for diseases produced by prosthesis in lower limb amputations [42], these are significantly lower for the rPLA+30% carbon composite, which further supports the preferred selection of this material for the current case-study's socket-type prosthesis.

#### 4 Summary and Conclusions

This study analysed the use of recycled reinforced PLA as feedstock material for additive manufacturing to produce customized socket-type prostheses.

Based on the actual anatomical contour of the patients' residual limb, numerical simulations were carried out both at the biomechanical system and the custom socket-type prosthesis to analyze the local stress fields resulting from the use of the prosthesis.

These numerical analyses were carried out considering a conventional thermoplastic polymer (polypropylene) and five different eco-materials, namely a bioepoxy resin SR GreenPoxy 56 with, and without natural jute fibers reinforcement and recycled PLA biopolymer with, and without short carbon fibers as reinforcement.

Analyzing the results, for the given custom geometry of the prosthesis, only the GreenPoxy-jute composite with 40% reinforcement fibers and the rPLA biopolymer reinforced with 30% carbon fibers met the design criteria to be used on such assistive device. However, for the current case-study, the rPLA biopolymer composite is preferred towards the GreenPoxy composite due to its applicability as filaments for additive manufacturing.

In conclusion, the numerical simulation results showed the potential of the the rPLA biopolymer reinforced with 30% carbon fibers as an ecodesign solution for customized prostheses and orthoses. This recycled feedstock material should allow for patients being able to successfully produce and assemble their own customized assistive devices using fused deposition modelling.

### References

1. Wang Y, Tan Q, Pu F, et al (2020) A Review of the Application of Additive Manufacturing in Prosthetic and Orthotic Clinics from a Biomechanical Perspective. *Engineering* 6:1258–1266
2. Mahamood RM, Akinlabi ET (2016) Achieving Mass Customization Through Additive Manufacturing. In: Schlick C, Trzcieliński S (eds) *Advances in Ergonomics of Manufacturing: Managing the Enterprise of the Future*. Springer International Publishing, Cham, pp 385–390
3. Thompson MK, Moroni G, Vaneker T, et al (2016) Design for Additive Manufacturing: Trends, opportunities, considerations, and constraints. *CIRP Annals* 65:737–760. <https://doi.org/10.1016/j.cirp.2016.05.004>
4. Ko H, Moon SK, Hwang J (2015) Design for additive manufacturing in customized products. *International Journal of Precision Engineering and Manufacturing* 16:2369–2375. <https://doi.org/10.1007/s12541-015-0305-9>
5. Bhatia A, Sehgal AK (2021) Additive manufacturing materials, methods and applications: A review. *Materials Today: Proceedings*. <https://doi.org/10.1016/j.matpr.2021.04.379>
6. Pajonk A, Prieto A, Blum U, Knaack U (2022) Multi-material additive manufacturing in architecture and construction: A review. *Journal of Building Engineering* 45:103603. <https://doi.org/10.1016/j.jobbe.2021.103603>
7. Siacor FDC, Chen Q, Zhao JY, et al (2021) On the additive manufacturing (3D printing) of viscoelastic materials and flow behavior: From composites to food manufacturing. *Additive Manufacturing* 45:102043. <https://doi.org/10.1016/j.addma.2021.102043>
8. Blanco D, Rubio EM, Marín MM, Davim JP (2021) Advanced materials and multi-materials applied in aeronautical and automotive fields: a systematic review approach. *Procedia CIRP* 99:196–201. <https://doi.org/10.1016/j.procir.2021.03.027>
9. Blakey-Milner B, Gradl P, Snedden G, et al (2021) Metal additive manufacturing in aerospace: A review. *Materials & Design* 209:110008. <https://doi.org/10.1016/j.matdes.2021.110008>

10. Praveena BA, Lokesh N, Abdulrajak B, et al (2021) A comprehensive review of emerging additive manufacturing (3D printing technology): Methods, materials, applications, challenges, trends and future potential. *Materials Today: Proceedings*. <https://doi.org/10.1016/j.matpr.2021.11.059>
11. Liu G, Xiong Y, Zhou L (2021) Additive manufacturing of continuous fiber reinforced polymer composites: Design opportunities and novel applications. *Composites Communications* 27:100907. <https://doi.org/10.1016/j.coco.2021.100907>
12. Yuan S, Li S, Zhu J, Tang Y (2021) Additive manufacturing of polymeric composites from material processing to structural design. *Composites Part B: Engineering* 219:108903. <https://doi.org/10.1016/j.compositesb.2021.108903>
13. Chen RK, Jin Y an, Wensman J, Shih A (2016) Additive manufacturing of custom orthoses and prostheses-A review. *Additive Manufacturing* 12:77–89
14. Wang Y, Tan Q, Pu F, et al (2020) A Review of the Application of Additive Manufacturing in Prosthetic and Orthotic Clinics from a Biomechanical Perspective. *Engineering* 6:1258–1266. <https://doi.org/10.1016/j.eng.2020.07.019>
15. Revilla-León M, Fountain J, Piedra-Cascón W, et al (2021) Workflow of a fiber-reinforced composite fixed dental prosthesis by using a 4-piece additive manufactured silicone index: A dental technique. *The Journal of Prosthetic Dentistry* 125:569–575. <https://doi.org/10.1016/j.prosdent.2020.02.030>
16. Schweiger T, Moscato F, Hoetzenecker K (2021) Commentary: Three-dimensional-printed, customized airway prosthesis—is it justified to walk the extra mile? *JTCVS Techniques*. <https://doi.org/10.1016/j.xjtc.2021.09.025>
17. Coulter FB, Schaffner M, Faber JA, et al (2019) Bioinspired Heart Valve Prosthesis Made by Silicone Additive Manufacturing. *Matter* 1:266–279. <https://doi.org/10.1016/j.matt.2019.05.013>
18. Miechowicz S, Wojnarowska W, Majkut S, et al (2021) Method of designing and manufacturing craniofacial soft tissue prostheses using Additive Manufacturing: A case study. *Bio cybernetics and Biomedical Engineering* 41:854–865. <https://doi.org/10.1016/j.bbe.2021.05.008>
19. Colpani A, Fiorentino A, Ceretti E (2020) Design and Fabrication of Customized Tracheal Stents by Additive Manufacturing. *Procedia Manufacturing* 47:1029–1035. <https://doi.org/10.1016/j.promfg.2020.04.318>
20. Diegel O, Singamneni S, Reay S, Withell A (2010) Tools for Sustainable Product Design: Additive Manufacturing. *Journal of Sustainable Development* 3:

21. Javaid M, Haleem A, Singh RP, et al (2021) Role of additive manufacturing applications towards environmental sustainability. *Advanced Industrial and Engineering Polymer Research* 4:312–322. <https://doi.org/10.1016/j.aiepr.2021.07.005>
22. Siva Rama Krishna L, Srikanth PJ (2021) Evaluation of environmental impact of additive and subtractive manufacturing processes for sustainable manufacturing. *Materials Today: Proceedings* 45:3054–3060. <https://doi.org/10.1016/j.matpr.2020.12.060>
23. Javaid M, Haleem A, Singh RP, et al (2021) Role of additive manufacturing applications towards environmental sustainability. *Advanced Industrial and Engineering Polymer Research* 4:312–322. <https://doi.org/10.1016/j.aiepr.2021.07.005>
24. Moghimian P, Poirié T, Habibnejad-Korayem M, et al (2021) Metal powders in additive manufacturing: A review on reusability and recyclability of common titanium, nickel and aluminum alloys. *Additive Manufacturing* 43:102017. <https://doi.org/10.1016/j.addma.2021.102017>
25. Zander NE (2019) Recycled Polymer Feedstocks for Material Extrusion Additive Manufacturing. pp 37–51
26. Cruz Sanchez FA, Boudaoud H, Camargo M, Pearce JM (2020) Plastic recycling in additive manufacturing: A systematic literature review and opportunities for the circular economy. *Journal of Cleaner Production* 264:121602. <https://doi.org/10.1016/j.jclepro.2020.121602>
27. Tonk R (2021) Natural fibers for sustainable additive manufacturing: A state of the art review. *Materials Today: Proceedings* 37:3087–3090. <https://doi.org/10.1016/j.matpr.2020.09.017>
28. Sauerwein M, Doubrovski E, Balkenende R, Bakker C (2019) Exploring the potential of additive manufacturing for product design in a circular economy. *Journal of Cleaner Production* 226:1138–1149. <https://doi.org/10.1016/j.jclepro.2019.04.108>
29. Bernatas R, Dagneou S, Despax-Ferreres A, Barasinski A (2021) Recycling of fiber reinforced composites with a focus on thermoplastic composites. *Cleaner Engineering and Technology* 5:100272. <https://doi.org/10.1016/j.clet.2021.100272>
30. Ilyas RA, Sapuan SM, Harussani MM, et al (2021) Polylactic Acid (PLA) Biocomposite: Processing, Additive Manufacturing and Advanced Applications. *Polymers* 13:1326. <https://doi.org/10.3390/polym13081326>
31. Kuznetsov V, Solonin A, Urzhumtsev O, et al (2018) Strength of PLA Components Fabricated with Fused Deposition Technology Using a Desktop 3D Printer as a Function of Geometrical Parameters of the Process. *Polymers* 10:313. <https://doi.org/10.3390/polym10030313>

32. Beltrán FR, Arrieta MP, Moreno E, et al (2021) Evaluation of the Technical Viability of Distributed Mechanical Recycling of PLA 3D Printing Wastes. *Polymers* 13:1247. <https://doi.org/10.3390/polym13081247>
33. Chacón JM, Caminero MA, García-Plaza E, Núñez PJ (2017) Additive manufacturing of PLA structures using fused deposition modelling: Effect of process parameters on mechanical properties and their optimal selection. *Materials & Design* 124:143–157. <https://doi.org/10.1016/j.matdes.2017.03.065>
34. Anderson I (2017) Mechanical Properties of Specimens 3D Printed with Virgin and Recycled Polylactic Acid. *3D Printing and Additive Manufacturing* 4:110–115. <https://doi.org/10.1089/3dp.2016.0054>
35. Cicala G, Giordano D, Tosto C, et al (2018) Polylactide (PLA) Filaments a Biobased Solution for Additive Manufacturing: Correlating Rheology and Thermomechanical Properties with Printing Quality. *Materials* 11:1191. <https://doi.org/10.3390/ma11071191>
36. Lee CH, Padzil FNBM, Lee SH, et al (2021) Potential for Natural Fiber Reinforcement in PLA Polymer Filaments for Fused Deposition Modeling (FDM) Additive Manufacturing: A Review. *Polymers* 13:1407. <https://doi.org/10.3390/polym13091407>
37. Maqsood N, Rimašauskas M (2021) Delamination observation occurred during the flexural bending in additively manufactured PLA-short carbon fiber filament reinforced with continuous carbon fiber composite. *Results in Engineering* 11:100246. <https://doi.org/10.1016/j.rineng.2021.100246>
38. Liu W, Huang H, Zhu L, Liu Z (2021) Integrating carbon fiber reclamation and additive manufacturing for recycling CFRP waste. *Composites Part B: Engineering* 215:. <https://doi.org/10.1016/j.compositesb.2021.108808>
39. Farah S, Anderson DG, Langer R (2016) Physical and mechanical properties of PLA, and their functions in widespread applications — A comprehensive review. *Advanced Drug Delivery Reviews* 107:367–392
40. Hu Z, Karki R (2015) Prediction of mechanical properties of three-dimensional fabric composites reinforced by transversely isotropic carbon fibers. *Journal of Composite Materials* 49:1513–1524. <https://doi.org/10.1177/0021998314535960>
41. de Groot R, Peters MCRB, de Haan' YM, et al (1987) Failure Stress Criteria for Composite Resin
42. Ramalho A, Ferraz M, Gaspar M, Capela C (2020) Development of a preliminary finite element model to assess the effects



- of friction on the residual limb of a transfemoral amputee. *Materials Today: Proceedings* 33:1859–1863. <https://doi.org/https://doi.org/10.1016/j.matpr.2020.05.199>
43. Ramalho A, Ferraz M, Gaspar M, Capela C (2022) Influence of Materials and their Constitutive Laws on the Stress Fields produced in the Residual Limb of a Transfemoral Amputation. *Lecture Notes in Mechanical Engineering* - In Press
  44. Lin C-C, Chang C-H, Wu C-L, et al (2004) Effects of liner stiffness for trans-tibial prosthesis: a finite element contact model. *Medical Engineering & Physics* 26:1–9. [https://doi.org/10.1016/S1350-4533\(03\)00127-9](https://doi.org/10.1016/S1350-4533(03)00127-9)
  45. Sicomin (2015) SR GreenPoxy 56 Technical Datasheet
  46. MSC Software Corporation (2018) Marc 2018.0 Theory and User Information. Newport Beach, CA 92660 USA:
  47. Portnoy S, Siev-Ner I, Shabshin N, Gefen A (2011) Effects of sitting postures on risks for deep tissue injury in the residuum of a transtibial prosthetic-user: a biomechanical case study. *Computer Methods in Biomechanics and Biomedical Engineering* 14:1009–1019. <https://doi.org/10.1080/10255842.2010.504719>
  48. Łagan S, Liber-Kneć A (2018) The determination of mechanical properties of prosthetic liners through experimental and constitutive modelling approaches. *Czasopismo Techniczne* 3:197–209. <https://doi.org/10.4467/2353737XCT.18.048.8343>
  49. Shokrieh MM, Moshrefzadeh-Sani H (2016) On the constant parameters of Halpin-Tsai equation. *Polymer* 106:14–20. <https://doi.org/10.1016/j.polymer.2016.10.049>
  50. MSC Patran (2008) Materials Application - Theory - Composite Materials. In: Patran 2008 r1, Reference Manual Part 4: Functional Assignments. Santa Ana, CA 92707 USA, pp 88–160
  51. Shacham S, Castel D, Gefen A (2010) Measurements of the Static Friction Coefficient Between Bone and Muscle Tissues. *Journal of Biomechanical Engineering* 132:1–4. <https://doi.org/10.1115/1.4001893>
  52. Ivarsson B, Crandall J, Hall G (2004) Biomechanics. In: F. Kreith (ed) *Handbook of Mechanical Engineering*, 2nd ed. CRC Press, Boca Raton
  53. Anderson I (2017) Mechanical Properties of Specimens 3D Printed with Virgin and Recycled Polylactic Acid. *3D Printing and Additive Manufacturing* 4:110–115. <https://doi.org/10.1089/3dp.2016.0054>
  54. Raghava S, Caddell RM, Yeh G S Y (1973) The macroscopic yield behaviour of polymers. *Journal of Materials Science*

- 8:225–232.  
<https://doi.org/https://doi.org/10.1007/BF00550671>
55. Caddell RM, Raghava RS, Atkins AG (1974) Pressure dependent yield criteria for polymers. *Materials Science and Engineering* 13:113–120. [https://doi.org/https://doi.org/10.1016/0025-5416\(74\)90179-7](https://doi.org/https://doi.org/10.1016/0025-5416(74)90179-7)
56. matweb.com (2021) <http://www.matweb.com/reference/compressivestrength.aspx>
57. polymerdatabase.com (2021) <http://polymerdatabase.com/Commercial%20Polymers/PP.html>
58. Perrier A (2016) Influence du vieillissement hydrique sur le comportement mécanique de l'interface fil/matrice dans les composites chanvre/époxy. *Chanvre/Époxy*. L'École Nationale Supérieure de Méca-nique et D' Aérotechnique
59. makerbot.com (2021) [https://downloads.makerbot.com/legal/MakerBot\\_R\\_\\_PLA\\_and\\_ABS\\_Strength\\_Data.pdf](https://downloads.makerbot.com/legal/MakerBot_R__PLA_and_ABS_Strength_Data.pdf)